CEREBELLAR PURKINJE CELL DEATH IN THE P/Q-TYPE

VOLTAGE-GATED CALCIUM ION CHANNEL MUTANT MOUSE,

LEANER

A Dissertation

by

TAMY CATHERINE FRANK-CANNON

Submitted to the Office of Graduate Studies of
Texas A&M University
in partial fulfillment of the requirements for the degree of

DOCTOR OF PHILOSOPHY

December 2005

Major Subject: Veterinary Anatomy

CEREBELLAR PURKINJE CELL DEATH IN THE P/Q-TYPE

VOLTAGE-GATED CALCIUM ION CHANNEL MUTANT MOUSE,

LEANER

A Dissertation

by

TAMY CATHERINE FRANK-CANNON

Submitted to the Office of Graduate Studies of
Texas A&M University
in partial fulfillment of the requirements for the degree of

DOCTOR OF PHILOSOPHY

Approved by:

Chair of Committee,   Louise C. Abbott
Committee Members, Robert C. Burghardt
                              Rajesh C. Miranda
                              C. Jane Welsh
                              Evelyn Tiffany-Castiglioni
Head of Department, Evelyn Tiffany-Castiglioni

December 2005

Major Subject: Veterinary Anatomy

ABSTRACT

Cerebellar Purkinje Cell Death in the P/Q-Type Voltage-Gated Calcium Ion Channel

Mutant Mouse, Leaner. (December 2005)

Tamy Catherine Frank-Cannon, B.S.; B.S.; DVM, Texas A&M University

Chair of Advisory Committee: Dr. Louise C. Abbott

Mutations of the α_{1A} subunit of P/Q-type voltage-gated calcium channels are responsible for several inherited disorders affecting humans, including familial hemiplegic migraine, episodic ataxia type 2 and spinocerebellar ataxia type 6. These disorders include phenotypes such as a progressive cerebellar atrophy and ataxia. The leaner mouse also carries a mutation in the α_{1A} subunit of P/Q-type voltage-gated calcium channels, which results in a severe cerebellar atrophy and ataxia. The leaner mutation causes reduced calcium ion influx upon activation of P/Q-type voltage-gated calcium channels. This disrupts calcium homeostasis and leads to a loss of cerebellar neurons, including cerebellar Purkinje cells. Because of its similarities with human P/Q-type voltage-gated calcium channel mutations, leaner mouse has served as a model for these disorders to aid our understanding of calcium channel function and neurodegeneration associated with calcium channel dysfunction. The aims of this dissertation were: (1) to precisely define the timing and spatial pattern of leaner Purkinje cell death and (2) to assess the role of caspases and specifically of caspase 3 in directing leaner Purkinje cell death.

We used the mechanism independent marker for cell death Fluoro-Jade and demonstrated the leaner Purkinje cell death begins around postnatal day 25 and peaks at postnatal day 40 to 50. Based on this temporal pattern of Purkinje cell death we then investigated the role of caspases in leaner Purkinje cell death. These studies showed that caspase 3 is specifically activated in dying leaner cerebellar Purkinje cells. In addition, *in vitro* inhibition of caspase 3 activity partially rescued leaner Purkinje cells. Further investigation revealed that caspase 3 activation may be working together with or in response to macroautophagy. This study also indicated a potential role for mitochondrial signaling, demonstrated by the loss of mitochondrial membrane potential in leaner cerebellar Purkinje cells. However, our study revealed that if the loss of mitochondrial membrane potential is associated with leaner Purkinje cell death, this process is not mediated by the mitochondrial protein cytochrome C.

ACKNOWLEDGMENTS

I am deeply grateful to all those who have offered me their support, advice, encouragement and patience in this accomplishment. While I will only acknowledge a few of you here, for those I fail to mention, please forgive the omission and take heart that without everyone who has been there for me over the last few years I could never have made it to this day.

First, I would like to thank Drs. Louise Abbott, Robert Burghardt, Rajesh Miranda, Jane Welsh and Evelyn Tiffany-Castiglioni for their guidance and for always asking the challenging questions during my graduate studies. I am forever grateful for the generosity of Mr. Charles Plum, whose gift allowed me to complete my education at a time when financial concerns threatened to prevent it. Special thanks also go to Drs. Anton Hoffman and Mary Herron for their mentoring and leading by example, which gave me the strength and courage to follow my dreams in spite of the short term hardships.

To my parents, my brother Mark, his wife Denise and their three beautiful daughters Catherine, Ashleigh and Makayla, I cannot thank you enough for all you have done for me over the years. I am also deeply appreciative for the support, love, and encouragement from Doris Rush, my parents by marriage Linda and Jerry, their daughter Kaylyn and all of my friends, colleagues and family.

I am most grateful to my husband, Bill, who has endured many long nights of work and countless hours of frustration, doubt, tears and hair pulling with patience,

grace, and an undying love. Words alone cannot express how truly thankful I am to him

or how much his patience and love have enabled me to accomplish this feat.

NOMENCLATURE

$\Delta\Psi_m$	Mitochondrial membrane potential
AIF	Apoptosis inducing factor
ANOVA	Analysis of variance
Apaf 1	Apoptosis associated factor 1
BH	Bcl-2 homology domain
Ca^{2+}	Calcium ion
CICR	Calcium induced calcium release
CNS	Central nervous system
DAB	Diaminobenzadine
DMSO	Dimethylsulfoxide
DNA	Deoxyribonucleic acid
E	Embryonic day
EA-2	Episodic ataxia type 2
ER	Endoplasmic reticulum
FHM	Familial hemiplegic migraine
Fisher's LSD	Fisher's least significant difference
IAP	Inhibitor of apoptosis protein
IDV	Integrated density value
IHC	Immunohistochemistry
K^+	Potassium ion

MDC   Monodansylcadaverine

Neu N   Neuronal nuclei protein

P   Postnatal day

Na^+ Sodium ion

PI3-K   Phosphoinositide-3 kinase

SCA-6   Spinocerebellar ataxia type 6

SMAC   Second mitochondrial activator of caspase

TH   Tyrosine hydroxylase

Tukey's HSD   Tukey's honest significant difference

TUNEL   Terminal deoxyuridine nick end labeling

VGCC   Voltage-gated calcium ion channel

TABLE OF CONTENTS

LIST OF FIGURES

LIST OF TABLES

CHAPTER I

INTRODUCTION

CEREBELLAR ANATOMY AND FUNCTION

The cerebellum is part of the central nervous system (CNS) responsible for coordination of motor function and balance. The cerebellum does not initiate motor actions. Instead, it receives sensory input from the body, head, eyes and ears as well as intention of planned movements from the cerebral motor cortex in order to control rate, range and force of motion (Nolte, 1999). The cerebellum is situated caudal to the cerebral hemispheres and dorsal to the 4th ventricle, metencephalon and myelencephalon of the brain stem. Grossly, the cerebellum can be divided into three regions: a central vermis, paired lateral hemispheres and flocculi (Figure I-1). The vermis is primarily responsible for spinocerebellar or somatosensory functions, while the hemispheres function in motor planning to coordinate motor function in the limbs and motor learning (Nolte, 1999). The flocculi are part of the floculonodular lobe of the cerebellum, which is responsible for balance and equilibrium (Nolte, 1999).

_____

This dissertation follows the style of Neuroscience.
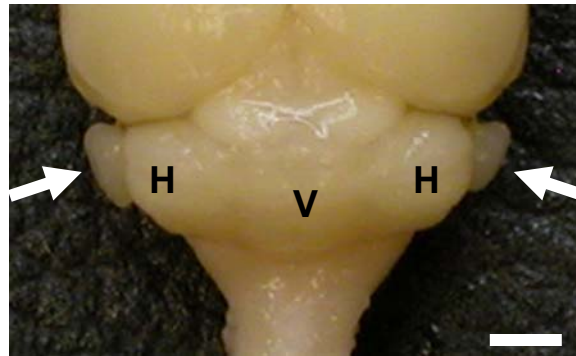
Figure I-1: Dorsal view of the adult mouse cerebellum. V indicates vermis, H indicates hemispheres and arrows indicate flocculi. Scale bar is 2 mm. Image provided by Kerry A. Thuett.

The cerebellum can be divided into rostral (or anterior) and caudal (or posterior) parts separated by the primary fissure and a flocculonodular lobe which is separated from the remaining cerebellum by the posterolateral fissure (Marani and Voogd, 1979; Altman and Bayer, 1997). The cerebellum is a highly lobulated structure. By convention, there are 10 distinct lobules or folia within the cerebellum (Altman and Bayer, 1997; Voogd and Glickstein, 1998). Different nomenclature for these lobules is used between human and other mammalian species (Table I-1). In the mouse cerebellar vermis (Figure I-2), lobules I and II are fused as are lobules IV and V, while lobule III remains separate (Marani and Voogd, 1979).

Table I-1: Nomenclature of cerebellar lobules.

Vermis		Hemispheres	
Human	**Other Mammals**	**Human**	**Other Mammals**
Lingual	Lobule I	Vincingulum lingulae	Anterior lobule
Central	Lobule II & III	Ala lobulus centralis	Anterior lobule
Culmen	Lobule IV & V	Anterior quadrangulate lob.	Anterior lobule
Declive	Lobule IV	Posterior quandrangulate lob.	Lobule simplex
Folium	Lobule VIIA	Superior semilunar lobule	Ansiform lob. Crus I
Tuber	Lobule VIIB	Inf. semilunar & gracile lob.	Ansiform lob. Crus II
Pyramis	Lobule VIII	Biventral lobule	Paramedian lobule
Uvula	Lobule IX	Tonsilla	Dorsal paraflocculus
Nodulus	Lobule X	Accessory paraflocculus	Ventral paraflocculus
		Flocculus	Flocculus

Lob. = lobule; Inf. = inferior (Altman and Bayer, 1997; Voogd and Glickstein, 1998)

Microscopically, the cerebellar cortex is arranged into three layers: molecular layer, Purkinje cell layer, and granule cell layer (Figure I-2). The molecular layer consists of interneurons (stellate and basket cells), the dendritic processes of Purkinje cells and the axons of granule cells (parallel fibers) and inferior olive neurons (climbing fibers). The Purkinje cell layer consists of the cell bodies of Purkinje neurons, and the granule cell layer includes granule cell neurons, unipolar brush cell interneurons and Golgi cell interneurons.
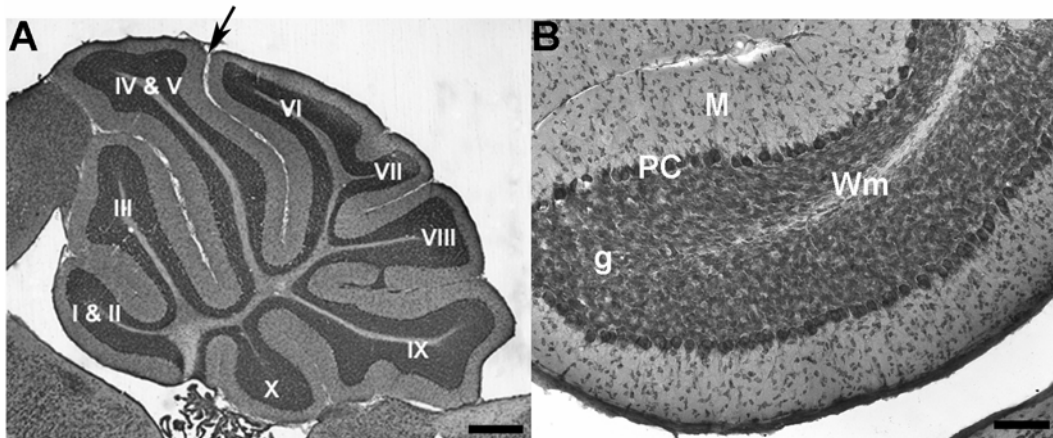
Figure I-2: Microscopic anatomy of the adult mouse cerebellum. A sagittal view of a mouse cerebellar vermis, identifying of lobules I - X (A). Arrow indicates primary fissure. A high magnification view of a cerebellar lobule I & II (B). A and B are paraformaldehyde fixed, frozen sections stained with 1% thionin. M represents molecular layer, PC is Purkinje cell layer, g is granule cell layer and Wm is white matter. Scale bar in A is 500 μm. Scale bar in B is 100 μm.

Communication between the different neurons in the cerebellar cortex is summarized in Figure I-3. The cerebellum receives afferent inputs from climbing fibers and mossy fibers. Climbing fibers originate from neurons in the inferior olive and relay information from the spinal cord, red nucleus and cerebral motor cortex through the caudal (or inferior) cerebellar peduncles to cerebellar Purkinje cells as well as sending collateral innervation to deep cerebellar nuclei neurons (O'Leary, et al., 1970; Altman and Bayer, 1997). Mossy fibers originate from neurons in the brain stem, pontine nuclei and spinal cord to relay information from the cerebral motor cortex (pontine nuclei) and body (spinal cord and brain stem) through the middle and caudal cerebellar peduncles to cerebellar granule cells, unipolar brush cells, and collateral innervation to the deep cerebellar nuclei neurons (Chan-Palay, et al., 1977; Olschowka and Vijayan, 1980;

Altman and Bayer, 1997; Morin, et al., 2001). Somatosensory information from spinal cord and brain stem is projected to the cerebellar vermis while information from the cerebral motor cortex is projected to the cerebellar hemispheres (Nolte, 1999). Cerebellar granule cells in the granule cell layer project into the molecular layer via parallel fibers to modulate cerebellar Purkinje cells, stellate cells, and basket cells (Eccles, et al., 1967; Palkovits, et al., 1971).

Granule cell parallel fiber innervation and climbing fiber innervation of Purkinje cells is excitatory (Altman and Bayer, 1997; Voogd and Glickstein, 1998). Granule cell parallel fibers will innervate several Purkinje cells, while climbing fibers are strictly limited to a single Purkinje cell (Larramendi and Victor, 1967). The molecular layer interneurons, stellate cells and basket cells, are inhibitory to cerebellar Purkinje cells (Altman and Bayer, 1997; Voogd and Glickstein, 1998). The combined innervation of climbing fibers, parallel fibers, stellate cells and basket cells modulate Purkinje cell activity. In addition, Purkinje cells send inhibitory collateral innervation to the granule cell layer interneuron, Golgi cells (Eccles, et al., 1967). Since Golgi cells are inhibitory to cerebellar granule cells, this provides a negative feedback loop for Purkinje cell excitability and further modulates Purkinje cell activity. In contrast, unipolar brush cells, which receive excitatory input from mossy fibers, are excitatory to cerebellar granule cells providing a positive feedback loop for Purkinje cell excitability (Dino, et al., 2000).
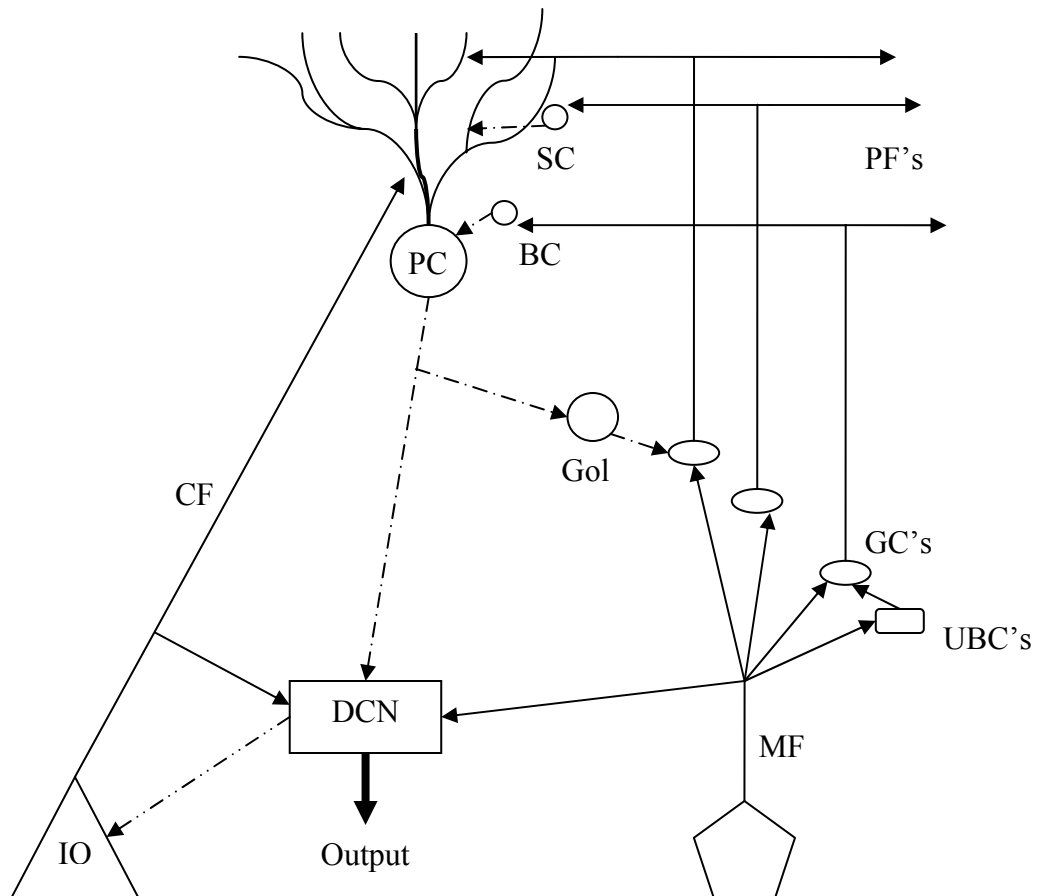
Figure I-3: Overview of cerebellar circuitry. IO is inferior olive, DCN is deep cerebellar nuclei, MF are mossy fibers, CF are climbing fibers, UBC's are unipolar brush cells, GC's are granule cells, Gol are Golgi cells, PC are Purkinje cells, BC are basket cells, SC are stellate cells, and PF's are parallel fibers. Solid lines represent excitatory innervation. Dashed lines represent inhibitory innervation.

Cerebellar Purkinje cells are the only efferent axons from the cerebellar cortex. They project to and inhibit neurons in the deep cerebellar nuclei and vestibular nuclei. The flocculonodular lobe or vestibulocerebellum includes lobules IX, X and the flocculi, and Purkinje cell axons of flocculonodular lobe project directly to the vestibular nuclei

to influence equilibrium and balance (De Zeeuw, et al., 1994). The remaining Purkinje cells axons project to the deep cerebellar nuclei, which occur in bilateral pairs and include the fastigial, interpositus and dentate nuclei (Marani and Voogd, 1979). In humans, the interpositus nucleus is often further subdivided into globus and emboliformis parts (Chan-Palay, et al., 1977). The fastigial nuclei receive axons from the cerebellar vermis, while the interpositus and dentate nuclei receive axons from the paravermis and hemispheres respectively (Nolte, 1999). The deep cerebellar nuclei project through the rostral (or superior) cerebellar peduncle to various regions of the brain stem including, vestibular nuclei, red nuclei and thalamus (Altman and Bayer, 1997; Nolte, 1999). The fastigial and interpositus nuclei are responsible for modulating motor activity, while the dentate nuclei relay information to the motor and premotor cerebral cortex to influence motor function and planning (Nolte, 1999). A summary of neurotransmission associated with cerebellar innervation is found in Table I-2.

Table I-2: Summary of neurotransmission in cerebellar circuits.

Synapse	Neurotransmitter	Effect
Climbing fiber→Purkinje cell	Corticotropin releasing factor, aspartate	Excitatory
Climbing fiber→deep cerebellar n.	Corticotropin releasing factor	Excitatory
Mossy fiber→granule cell	Glutamate, acetylcholine	Excitatory
Mossy fiber→unipolar brush cell	Glutamate	Excitatory
Unipolar brush cell→granule cell	Glutamate*	Excitatory
Granule cell→Purkinje cell	Glutamate	Excitatory
Granule cell→stellate cell	Glutamate	Excitatory
Granule cell→basket cell	Glutamate	Excitatory
Stellate cell→Purkinje cell	γ-amino butyric acid (GABA), taurine	Inhibitory
Basket cell→Purkinje cell	GABA	Inhibitory
Golgi cell→granule cell	GABA, glycine	Inhibitory
Purkinje cell→Golgi cell	GABA	Inhibitory
Purkinje cell→deep cerebellar n.	GABA	Inhibitory

(Altman and Bayer, 1997; Voogd and Glickstein, 1998) *(Dino, et al., 2000; Billups, et al., 2002)

Cerebellar afferents, climbing fibers and mossy fibers, are segregated along the parasagittal bands and functionally divide the cerebellum along these lines (Oberdick, et al., 1998). In addition to the compartmentalization determined by afferent innervation, the expression of certain genes within the cerebellum is also restricted to parasagittal

bands (Hawkes and Herrup, 1995; Herrup and Kuemerle, 1997; Ozol, et al., 1999). One of the most recognized is that of Zebrin II labeling of cerebellar Purkinje cells. Zebrin II staining, which labels the glycolytic enzyme aldolase C, is restricted to alternating parasagittal bands of Purkinje cells throughout development and adulthood (Leclerc, et al., 1992; Hawkes and Herrup, 1995). Other genes, such as tyrosine hydroxylase (TH) and calbindin are developmentally expressed in parasagittal banded patterns (Herrup and Kuemerle, 1997). While the expression of TH is transient and not present in the adult cerebellum, the expression of calbindin becomes uniform throughout the adult cerebellum (Herrup and Kuemerle, 1997). These examples of the partitioning of the cerebellum into compartments demonstrate an important fundamental aspect of the cerebellum. This complex organization and patterning of the cerebellum often results in the patterned dysfunction or loss of neurons in seen in many neuropathology of diseases and disorders affecting the cerebellum.

EARLY CEREBELLAR DEVELOPMENT

The cerebellum is derived from the alar (dorsal) plate of the neural tube at the mesencephalon-metencephalon junction shortly after neural tube closure at embryonic day (E) 8.5 in rats and mice (McMahon and Bradley, 1990; Herrup and Kuemerle, 1997; Goldwitz and Hamre, 1998). Initially the cerebellum develops as two bilaterally symmetrical bulges in the roof of the 4th ventricle (Hallonet, et al., 1990; Hallonet and Le Douarin, 1993). Over the course of development these two bilateral anlages preferentially proliferate on the medial surface and fuse on midline to form the

precursors of the central cerebellar vermis and bilaterally paired cerebellar hemispheres by E16.5 in mice (Sgaier, et al., 2005). Beginning in late embryogenesis there is an overall outward, radial expansion of the cerebellum accompanied by folding that produces lobules (Herrup and Kuemerle, 1997; Goldwitz and Hamre, 1998). In the mouse, cerebellar development is complete by about postnatal day (P) 20.

The cells in the cerebellum arise from two germinal zones. The initial germinal matrix consists of a rostral neuroepithelial ventricular zone (derived from mesencephalon and metencephalon) and a more caudal rhombic lip (derived only from metencephalon) (Goldwitz and Hamre, 1998). The ventricular zone gives rise to the first germinal matrix and most of the neurons in the cerebellum from E7 – 13 in rats and mice (Goldwitz and Hamre, 1998). Neurons of the deep cerebellar nuclei develop first followed by Purkinje cells (Altman and Bayer, 1978; Altman and Bayer, 1985a; Altman and Bayer, 1985b). Golgi cells are born last in the diminishing ventricular zone (Altman and Bayer, 1978; Altman and Bayer, 1985a; Altman and Bayer, 1985b). At approximately E13, which is the time that deep cerebellar nuclear neurons and Purkinje cells stop dividing in the ventricular zone (Miale and Sidman, 1961), the secondary germinal matrix, derived from the rhombic lip, gives rise to the external granule cell layer (Goldwitz and Hamre, 1998). The secondary germinal matrix migrates over the cerebellar surface to a position immediately beneath the pia mater. Unipolar brush cell interneurons develop around E14, migrate to the internal or adult granule cell layer by P2 to P9 where the complete their differentiation and maturation by P20 (Abbott and Jacobowitz, 1995; Morin, et al., 2001). During early postnatal development in the

mouse, molecular layer interneurons (stellate and basket cells) are generated deep in the white matter of the cerebellum (Zhang and Goldman, 1996). Basket cells migrate into the molecular layer at P6 – 7 and complete their differentiation from P10 to P14, while stellate cells move into the molecular layer at P8 – 11 and complete differentiation by P20 (Zhang and Goldman, 1996; Collin, et al., 2005). The external granule cell layer gives rise to granule cell neuroblasts that migrate inward guided by Bergmann glial radial fibers past cerebellar Purkinje cells to their adult location in the internal or adult granule cell layer by P20 (Fujita, et al., 1966).

DEVELOPMENT OF CEREBELLAR PURKINJE CELLS

Cerebellar Purkinje cells are derived from precursors in the ventricular zone, beginning about E8. Initially the parasagittal banding pattern, typical of Zebrin II staining (zebrin phenotype) and compartmentalization of the adult cerebellum, is not detectible (Hawkes, et al., 1998). However, by the time Purkinje cells undergo their terminal mitosis at E10 – 13 they are committed to their zebrin phenotype as the cerebellum initiates compartmentalization (Miale and Sidman, 1961; Leclerc, et al., 1988). Purkinje cells migrate from the ventricular zone at E11 – 13 into the cerebellar anlage forming a temporary multiple cell layered plate-like structure (Edwards, et al., 1990; Goldwitz and Hamre, 1998). At approximately E14 climbing fiber and mossy fiber afferents begin to enter the cerebellum and make initial contacts with specific Purkinje cell groups. The earliest detected molecular banding pattern, first becomes evident beginning at E14.5 (Arsenio Nunes and Sotelo, 1985; Grishkat and Eisenman,

1995). Around the time of birth, Purkinje cells disperse rostrocaudally into a monolayer committed to specific parasagittal bands or zones (Goldwitz and Hamre, 1998).

Postnatal development of mouse cerebellar Purkinje cells consists primarily of the formation and elaboration of dendritic arbors and their synaptic contacts. Following formation of the monolayer of cerebellar Purkinje cell bodies beneath the external granule cell layer, Purkinje cells become oriented in a translobular plan (Altman and Bayer, 1997). Dendritic development begins at P3 as apical swellings which then form main stem dendrites by P10 – 12 (Altman and Bayer, 1997). Branching of the main stem dendrite begins immediately and the Purkinje cell dendritic arbor is further elaborated and dendritic spines develop from P12 – 20 (Altman and Bayer, 1997). During this time, Purkinje cells form synapses at dendritic spines with granule cell parallel fibers (Larramendi and Victor, 1967). Most of the development and elaboration of the dendritic arbor is dependent on the synaptic contacts between granule cells and Purkinje cells (Schrenk, et al., 2002; Adcock, et al., 2004). Also during this time, Purkinje cells limit synaptic contacts between its dendritic shafts and climbing fibers to achieve a 1:1 association between Purkinje cells and inferior olive neurons (Mason and Gregory, 1984; Mason, et al., 1990). At P20 cerebellar Purkinje cells have settled into their adult location and become their distinctive adult shape with its elaborate dendritic arbors that is flattened and oriented in a translobular plan (Altman and Bayer, 1997).

PROGRAMMED CELL DEATH

Overview

Cell death is an integral part of the nervous system, playing roles in both neurodevelopment and in many neurodegenerative diseases. Cell death can be divided into two broad categories: necrosis and programmed cell death (Kerr, et al., 1972; Schweichel and Merker, 1973). The morphologic features of cell death are summarized in Table I-3. Necrosis is characterized by energy independent cellular swelling and lysis that leads to inflammation (Leist, et al., 1997). Necrosis is seen in some neurodegenerative disorders including ischemic brain injuries (stroke) and excitotoxicity (Yuan and Yankner, 2000; Yuan, et al., 2003). Programmed cell death is an energy dependent, highly regulated process that allows for controlled breakdown of a cell without inducing an inflammatory response in the tissue surrounding the affected cell (Sastry and Rao, 2000; Yuan and Yankner, 2000; Yuan, et al., 2003). Programmed cell death is an essential requirement for normal neurodevelopment and a key component of many neurodegenerative disorders including spinocerebellar ataxias, Alzheimer's disease, Parkinson's disease, Huntington's disease and stroke (Oppenheim, et al., 2001; Benn and Woolf, 2004).

Table I-3: Morphologic features of different mechanisms of cell death.

	Necrosis	Programmed Cell Death	
		Macroautophagy	Apoptosis
ATP Synthesis	Lost	Maintained	Maintained
Mitochondrial morphology	Swelling	Some swelling #'s decreased Some normal	Normal
ER/Golgi	Swelling	Some swelling Some normal	Normal
Cytoplasm	Empty spaces (nonlysosomal)	Autophagic vacuoles Loss of density	Condensation
Plasma membrane	Fragmentation	Minor blebbing late in process	Blebbing into apoptotic bodies
Nucleus	Fragmentation +/– swelling	Some pyknosis late in process	Pyknosis
Chromatin/DNA	Release in loss of nuclear integrity	+/– Fragmentation late in process	Condensation Fragmentation
Final Clean Up	Loss of membrane integrity & lysis; Removed by phagocytosis with inflammation	Remaining cell removed by phagocytosis without inflammation	Membrane bound apoptotic bodies removed by phagocytosis without inflammation

(Bursch, 2001; Yuan, et al., 2003)

Programmed cell death can be further divided into macroautophagy and apoptosis based on its morphologic features, see Table I-3. Both types of programmed cell death are highly conserved signaling pathways found from yeast to vertebrates (Bursch, 2001; Yuan, et al., 2003). Macroautophagy represents a normal homeostatic

process of a cell that when, triggered in excess, leads to cell death (Shintani and Klionsky, 2004). Macroautophagy shares features with both necrosis and apoptosis. For example, while some mitochondrial swelling is observed and there is a decrease in mitochondrial numbers, enough normal mitochondria are retained to maintain ATP synthesis and complete a controlled break down of the cell (Bursch, 2001). Macroautophagy tends to be activated when there is a demand for elimination of larger cells, requiring the removal bulk cytoplasm before nuclear breakdown (Bursch, 2001). Apoptosis is a highly regulated process by which specific proteases are activated and execute the degradation of the cytosolic and nuclear contents (Yuan and Yankner, 2000; Hengartner, 2000). Both types of programmed cell death are essential for normal neurodevelopment and both are found in neurodegenerative disorders. While these processes are distinct, they are not necessarily mutually exclusive events (Nitatori, et al., 1995; Xue, et al., 1999). Additionally, if the initiating stimulus is too severe or other factors interfere with the death program, both types of cell death are able to abort their programs, resulting in necrotic cell death (Leist, et al., 1997; Vercammen, et al., 1998).

Apoptosis

Apoptotic machinery consists of two basic components, mitochondrial signaling and caspase proteases, which may work in concert with one another or independently to execute cell death (Hengartner, 2000; Yuan, et al., 2003). Many different cellular signals are able to trigger apoptosis. Certain cell surface death receptors, including Fas receptors, TNF receptors, TRAIL receptors activate apoptotic cell death upon binding

their specific ligands and forming a trimeric complex of three ligands and three receptors (Vercammen, et al., 1998; Ashkenazi and Dixit, 1998; Werner, et al., 2002). Other signals such as growth factor withdrawal, altered intracellular calcium (Ca^{2+}) signaling, or reactive oxygen species (ROS) are also able to initiate apoptosis (Yuan and Yankner, 2000; Benn and Woolf, 2004). These signals use numerous pathways, such as mitogen activated protein kinases (MAPK) (Kharbanda, et al., 2000), ceramide signaling (De Maria, et al., 1997), lysosomal proteases (Hishita, et al., 2001) or direct activation of caspases or mitochondrial signaling, to carry out cell death.

Mitochondrial mediated apoptosis is regulated by the Bcl-2 family of proteins. The Bcl-2 family of proteins are a group of proteins that share a conserved Bcl-2 homology (BH) domain (Cory and Adams, 2002). This family of proteins can be divided into three functional groups, one that is anti-apoptotic and two that are pro-apoptotic. The Bcl-2 subfamily of proteins, including Bcl-2, Bcl-x_L, and Bcl-w, have BH domains 1 – 4 and are anti-apoptotic (Cory and Adams, 2002). The Bax subfamily proteins have BH domains 1 – 3, are pro-apoptotic, and include proteins such as Bax, Bak, and Bok (Cory and Adams, 2002). The second group of pro-apoptotic proteins contain only the BH 3 domain and are refer to as BH3 proteins (Cory and Adams, 2002). BH3 proteins include members such as Bid and Bad.

Bax proteins execute mitochondrial death signals by oligomerizing and either forming a pore or triggering opening of the mitochondrial permeability transition pore causing the release of key death signaling factors from the mitochondrial intermembrane space (Desagher, et al., 1999; Eskes, et al., 2000; Letai, et al., 2002). Bcl-2-like proteins

prevent apoptosis by binding Bax proteins, preventing oligomerization (Luo, et al., 1998; Letai, et al., 2002). BH3 proteins promote apoptosis by sequestering Bcl-2, preventing its inhibition of Bax proteins (Letai, et al., 2002). Apoptotic initiating signals interact with the Bcl-2 family of proteins in numerous ways. Some directly activate BH3 proteins, others phosphorylate Bcl-2-like proteins to prevent their function, and yet others alter the relative gene expression of the various subfamily members to favor apoptosis (Cory and Adams, 2002). Once released from mitochondria, proteins such as cytochrome C and second mitochondrial activator of caspase (SMAC), activate caspase proteases, which carry out degradation of the cell (Liu, et al., 1996; Du, et al., 2000). Cytochrome C forms a protein complex which activates caspases directly (Li, et al., 1997). SMAC, alternatively blocks the action of inhibitor of apoptosis proteins (IAP) to free caspases for activation (Du, et al., 2000). Other proteins such as apoptosis inducing factor (AIF) act independent of caspases to breakdown the cell (Susin, et al., 1999; Joza, et al., 2001).

Caspases are proteases responsible for many of the morphologic features of apoptosis (Earnshaw, et al., 1999; Hengartner, 2000; Yuan, et al., 2003). They possess an active site cysteine residue and cleave their substrates following an aspartate residue (Thornberry, et al., 1997). Caspases are produced as inactive zymogens, which must be cleaved in order to become proteolytically active (Earnshaw, et al., 1999). Caspases may be activated directly through death receptor signaling or other cell signaling pathways, or their activation may be mediated through mitochondrial apoptotic pathways (Earnshaw, et al., 1999; Hengartner, 2000). Caspases are divided into two groups. The

first are initiator caspases, which include caspases 2, 8, 9, 10 and 12 (Slee, et al., 1999; Earnshaw, et al., 1999; Hengartner, 2000). These caspases cleave other caspases to initiate or maintain caspase activity. The second group of caspases are effector caspases, such caspases 3, 6, and 7, which are responsible for carrying out degradation of the cell (Slee, et al., 1999; Earnshaw, et al., 1999; Hengartner, 2000). Their targets are cytoplasmic and nuclear proteins, including the activation of DNases responsible for breaking DNA into fragments and additional effector and initiator caspases to maintain their activity (Earnshaw, et al., 1999). Some caspases such as caspases 8 and 12, when active, are able to cleave and activate effector caspase 3 directly (Vercammen, et al., 1998; Ashkenazi and Dixit, 1998; Hitomi, et al., 2004). Other initiator caspases form a protein complex which then activates an effector caspase. For example, caspase 9, forms a protein complex with Apaf-1 and the mitochondrial protein cytochrome C, activating caspase 9 which in turn activates caspases 3 and 7 (Li, et al., 1997; Slee, et al., 1999). Initiator caspases also play a dual role in effector caspase activation. For example, in addition to direct activation of caspase 3, caspase 8 is also able to activate the BH3 protein, Bid, triggering mitochondrial release of cytochrome C and subsequent caspase 3 activation (Luo, et al., 1998).

Cell survival or apoptotic death is the result of an intricate balance of anti- and pro-apoptotic signaling pathways. The complexity of mitochondrial signaling and caspase signaling are indicative of the safeguards used by the cell to precisely control when and where the apoptotic program of cell death is activated. While apoptosis is an

essential process for normal neurodevelopment, it may also be triggered in response to an insult to the cell in neurodegenerative diseases.

Macroautophagy

Macroautophagy is part of a normal cellular system of autophagy responsible for lysosomal mediated removal of unwanted or damaged proteins and organelles, allowing recycling of their basic components (Bursch, 2001; Klionsky, 2005). Chaperone-mediated autophagy uses chaperone proteins and receptors to directly transport proteins into lysosomes for degradation (Klionsky, 2005). Microautophagy sequesters cytoplasm (proteins and organelles) by invagination of the lysosomal membrane (Klionsky, 2005). Macroautophagy involves the formation of double membrane vesicles derived from either the smooth ER or Golgi apparatus that sequester portions of the cytoplasm (proteins and organelles), called an autophagosome (Bursch, 2001; Klionsky, 2005). The autophagosome fuses with a lysosome delivering an inner vesicle or autophagic body to the lysosome that is subsequently degraded by lysosomal proteases (Bursch, 2001; Klionsky, 2005). Macroautophagy normally occurs at low levels as part of the routine turn over of cellular components (Shintani and Klionsky, 2004). However, it can also be induced to higher levels that cause cell death by certain environmental changes in development and differentiation for tissue remodeling or disease states such as cancer, neurodegeneration, and infection (Shintani and Klionsky, 2004).

The induction of macroautophagy can be mediated through two mechanisms. One uses class III phosphoinositide-3 kinase (PI3-K) activity to trigger macroautophagy.

Class III PI3-K and macroautophagic membrane dynamics are partly regulated by the Bcl-2 interacting protein, beclin-1(Blommaart, et al., 1997; Petiot, et al., 2000; Kihara, et al., 2001a; Kihara, et al., 2001b). The second mechanism involves inhibition of autophagy in response to growth factor stimulation such as insulin-like growth factors and neurotrophins. In this mechanism class, I PI3-K through phosphtidylinositol 3,4 diphosphate and 3,4,5 triphosphate, activates phosphoinositide-dependent kinase 1 and Akt (protein kinase B) (Arico, et al., 2001; Melendez, et al., 2003). Akt subsequently activates Tor (Target for rapamycin), preventing macroautophagy by inhibiting an Atg gene product activator of macroautophagy (Blommaart, et al., 1995; Noda and Ohsumi, 1998; Kamada, et al., 2000). The intricacies of the class I PI3-K signaling allow homeostatic levels of macroautophagy for normal recycling of cell components, yet induction of macroautophagic cell death upon events such as growth factor withdrawal.

Like some apoptotic pathways, macroautophagy often causes cell death independent of caspase activation or in the absence of caspase proteases (Bursch, 2001; Florez-McClure, et al., 2004). However, it has also been shown to interact with and activate portions of the apoptotic cell death pathway (Chi, et al., 1999; Kitanaka and Kuchino, 1999). Macroautophagy is able to activate caspases downstream of macroautophagic induction, where cell death cannot be prevented by the inhibition of caspase activity (Xue, et al., 1999). In other circumstances, macroautophagy can be dependent on caspase activity in order to cause cell death (Canu, et al., 2005). And, while macroautophagy and apoptosis can occur independent of one and other, they can

also be found to work together either in the same tissue or within the same cells in order to execute cell death (Bursch, 2001; Klionsky, 2005).

NEURONAL CALCIUM SIGNALING

Overview of calcium signaling

Calcium (Ca^{2+}) signaling is a diverse intracellular signaling system that regulates many different cellular processes and functions. In neurons these include neurotransmitter release, excitability, neurite outgrowth, synaptogenesis, activity dependent gene expression, differentiation, plasticity, cell death and survival (Pietrobon, 2002). Ca^{2+} concentration gradients between various cellular compartments are particularly important for these neuronal functions. Extracellular Ca^{2+} concentrations are high, about 1mM, compared to those inside the cells (Berridge, et al., 2000). Intracellular Ca^{2+} concentrations can be divided between the cytosolic compartment and Ca^{2+} storage sites such as the endoplasmic reticulum (ER). Resting intracellular Ca^{2+} concentrations are low, about 100nM, but rise to about 1μM during calcium signaling events (Berridge, et al., 2000; Bootman, et al., 2001). Within the ER, Ca^{2+} concentrations are in the 100μM range (Berridge, et al., 2000; Bootman, et al., 2001). Several proteins, including Ca^{2+} exchangers, Ca^{2+} transporters, voltage-gated calcium channels (VGCC), ligand-gated calcium channels, store-operated calcium channels and calcium binding proteins work in concert to maintain the Ca^{2+} concentrations and gradients that are essential for normal Ca^{2+} signaling (Berridge, et al., 2000; Bootman, et al., 2001).

During depolarization of a neuron, sodium (Na^+) channels open allowing Na^+ influx and depolarization of the plasma membrane (Koester and Siegelbaum, 2000). This depolarization activates and opens VGCC allowing Ca^{2+} to move down its concentration gradient from the extracellular space into the neuron. Following depolarization, voltage-gated potassium (K^+) channels open, K^+ exits the cell repolarizing the membrane and closing the VGCC (Koester and Siegelbaum, 2000). In addition, during synaptic transmission, ligand-gated calcium channels, such as the *N*-methyl-D-aspartate (NMDA) receptor, open a cation channel permeable to Ca^{2+} in response to neurotransmitter binding (Kandel and Siegelbaum, 2000). The Ca^{2+} influx associated with these events is able to trigger numerous signaling events. The diverse roles of Ca^{2+} signaling are regulated by the amplitude, frequency and duration of Ca^{2+} influx.

Following Ca^{2+} influx, rapid calcium buffering is accomplished mainly through calcium binding proteins (Thayer, et al., 2002). Many of these proteins share a common Ca^{2+} binding motif, called the EF-hand (Bastianelli, 2003). In addition to buffering the influx of Ca^{2+}, these calcium binding proteins are key components of several second messenger signaling pathways and control diverse cellular functions (Berridge, et al., 2000). Key calcium binding proteins in the mouse cerebellum are listed in Table I-4. Ca^{2+} influx and a particular calcium signal can be further modulated by Ca^{2+} induced Ca^{2+} release (CICR). Two ligand-gated calcium channels on the ER, inositol triphosphate (IP_3) receptors and ryanodine receptors, are primarily responsible for CICR (Berridge, et al., 2000; Ashby and Tepikin, 2001). Ca^{2+} dependent activation of these

receptors trigger calcium release from the ER. Depending on the number of receptors activated, the nature of the calcium signal is altered. For example, if only a few receptors are activated, a small amount of Ca^{2+} is released called a "blip" or "quark" (Berridge, et al., 2000). When several receptors are activated, more Ca^{2+} is release producing "puffs", "sparks" or "spirals" (Berridge, et al., 2000). When enough receptors are activated that the subsequent Ca^{2+} release is able to activate additional receptors, an intracellular calcium wave and CICR is triggered (Berridge, et al., 2000). These variations in calcium signaling are able to establish either microdomains of specific calcium signaling or more global, cell-wide changes (Blackstone and Sheng, 2002).

Table I-4: Distribution of key calcium binding proteins in the adult mouse cerebellum.

	Purkinje Cells	Granule cells	Golgi cells	Basket & Stellate cells
Calmodulin	++	+	?	+
Calbindin	+++	–	++	–
Parvalbumin	++	–	+/–	+++
Calretinin	+/–	+++	+	+/–

+ is present in small amounts, ++ is present in moderate amounts, and +++ is present in large amounts. – indicates protein is not present, +/– may be present in extremely small amounts, and ? indicates presence or absence is unknown (Bastianelli, 2003).

Neurons also employ numerous mechanisms to return cytosolic Ca^{2+} concentrations to resting levels and further regulate the nature of a Ca^{2+} signal. Plasma membrane Na^{+}/Ca^{2+} exchangers are Ca^{2+} ATPase pumps that remove Ca^{2+} from the cytosol, returning it to the extracellular space (Berridge, et al., 2000; Thayer, et al., 2002). Sarco-endoplasmic reticulum Ca^{2+} ATPases pump cytosolic Ca^{2+} into the ER

(Berridge, et al., 2000; Thayer, et al., 2002). Additionally, if the ER Ca^{2+} concentrations drop sufficiently, store-operated calcium channels are activated, which transport Ca^{2+} from the extracellular space into the ER further replenishing Ca^{2+} ER stores (Berridge, et al., 2000; Thayer, et al., 2002). Ca^{2+} also enters the mitochondria through a uniporter, which transports Ca^{2+} down a charge (pH) gradient into the mitochondrial matrix (Ichas and Mazat, 1998; Duchen, 1999). After the initial influx of Ca^{2+} into the mitochondria, a mitochondrial Na^{+}/ Ca^{2+} exchanger slowly returns Ca^{2+} to the cytosol, reestablishing the mitochondrial matrix pH (Ichas and Mazat, 1998; Duchen, 1999). Mitochondrial Ca^{2+} influx can trigger a temporary opening of the permeability transition pore, also returning Ca^{2+} to the cytosol (Ichas and Mazat, 1998; Duchen, 1999). These mitochondrial events have several important roles. They are able to modulate ATP synthesis, as well as local or microdomain Ca^{2+} signals in addition to protecting the cell from excessive, potentially lethal levels of cytosolic Ca^{2+} (Blackstone and Sheng, 2002). Ca^{2+} influx and efflux mechanisms together with calcium binding proteins create an intricate signaling mechanism to regulate functions as diverse as cell proliferation, differentiation, neurotransmission, and cell death or survival.

Voltage-gated calcium channels

Voltage-gated calcium channels (VGCC) mediate Ca^{2+} entry into a cell in response to membrane depolarization, transducing an electrical signal into a chemical one (Catterall, 2000). VGCCs are a multisubunit structure consisting of a pore forming subunit (α_1) and auxiliary subunits β, γ, and $\alpha_2\delta$, which modulate the biophysical

properties of the pore subunit (Westenbroek, et al., 1995; Koester and Siegelbaum, 2000). There are at least 10 genes for the pore forming subunit that encode five current types of VGCCs (Catterall, 2000; Pietrobon, 2002). The genes are summarized in Table I-5. The current types of VGCCs include the high voltage activated channels N-, R-, P/Q- and L-types and the low voltage activated channel, T-type. The high voltage activated channels are differentiated by their sensitivity to specific inhibitors (Koester and Siegelbaum, 2000; Catterall, 2000). N-type channels are sensitive to ω-conotoxin, P/Q-type channels to ω-agatoxin and L-type channels to dihydropyridine, while R-type channels are resistant to these inhibitors. There are eight genes that encode γ subunits, four for β subunits and three for $\alpha_2\delta$ subunits. In addition, both pore and auxiliary subunit genes have multiple splice variants, as well as differential expression in various neuronal populations and differential localization within a neuron. This allows for an enormous diversity of function and specificity of signaling throughout the nervous system.

Table I-5: Voltage-gated calcium channel pore forming subunit genes.

Ca^{2+} channel	α_1 subunit	Current type	Primary location	Primary function
Ca$_v$1.1	α_{1S}	L	Skeletal muscle	Initiate contraction, calcium homeostasis, gene regulation
Ca$_v$1.2	α_{1C}	L	Cardiac muscle Endocrine cells Neurons	Initiate contraction Initiate hormone secretion Gene expression
Ca$_v$1.3	α_{1D}	L	Endocrine cells Neurons	Initiate hormone secretion Gene expression
Ca$_v$1.4	α_{1F}	L	Retina	Tonic neurotransmitter release
Ca$_v$2.1	α_{1A}	P/Q	Nerve terminals Nerve dendrites	Neurotransmitter release Ca^{2+} transients
Ca$_v$2.2	α_{1B}	N	Nerve terminals Nerve dendrites	Neurotransmitter release Ca^{2+} transients
Ca$_v$2.3	α_{1E}	R	Nerve soma Nerve terminals Nerve dendrites	Ca^{2+} dependent action potential Neurotransmitter release Ca^{2+} transients
Ca$_v$3.1	α_{1G}	T	Cardiac muscle Skeletal muscle Neurons	Control repetitive firing patterns Control repetitive firing patterns Control repetitive firing patterns
Ca$_v$3.2	α_{1H}	T	Cardiac muscle Neurons	Control repetitive firing patterns Control repetitive firing patterns
Ca$_v$3.3	α_{1I}	T	Neurons	Control repetitive firing patterns

(Catterall, 2000; Pietrobon, 2002)

Pore forming subunits of VGCCs share a common structure (Figures I-4 and I-5) (Westenbroek, et al., 1995; Catterall, 2000; Pietrobon, 2002). Each α_1 subunit is

composed of four domains and cytoplasmic amino (N) terminal and carboxy (C) terminal tails. Each domain is composed of six transmembrane segments. The fourth transmembrane segment in each domain acts as the voltage sensor for the channel. The extracellular loop connecting transmembrane segments five and six of each domain fold into the membrane close to the mouth of the pore and acts as the ion selectivity filter. In addition to the auxiliary subunits, the pore forming subunit is modulated by phosphorylation (Li, et al., 2005), Ca^{2+} and calmodulin (a calcium binding protein) binding and synaptic vesicle proteins (Lee, et al., 1999). P/Q-, N- and R-type channels can also be regulated by G proteins (Herlitze, et al., 1996; Zhou, et al., 2003).
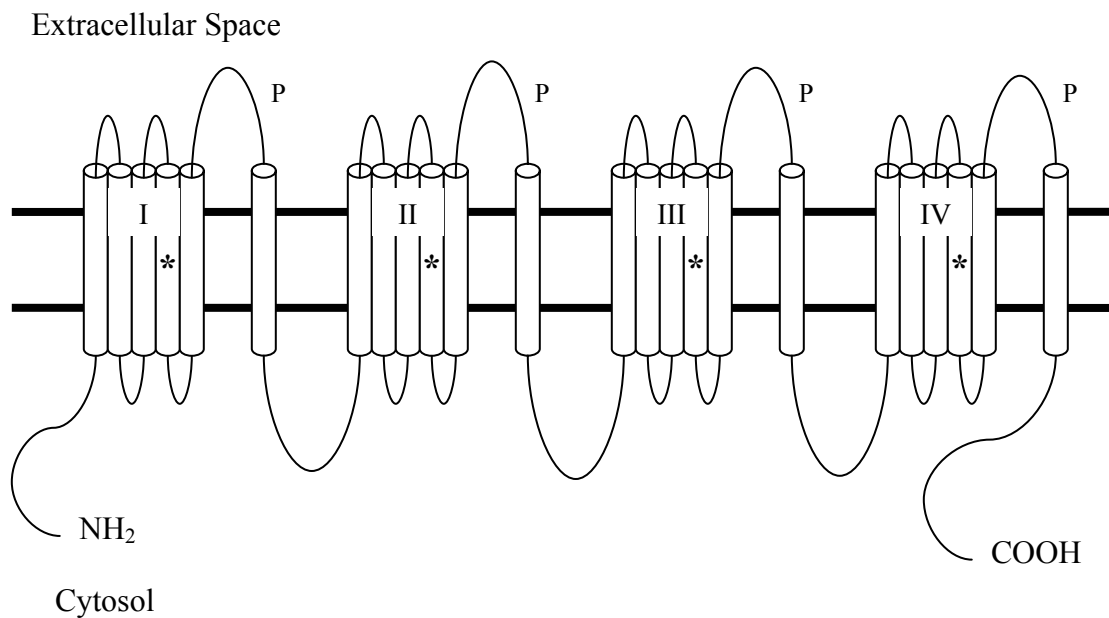
Figure I-4: Detailed structure of α_1 subunit of voltage-gated calcium channels. Roman numerals indicate domains. NH_2 represents the N-terminus of the α_1 protein and COOH represent the C-terminus. P is the P-loop of each domain. * indicates the voltage sensing transmembrane segment. (Westenbroek, et al., 1995; Catterall, 2000; Pietrobon, 2002)
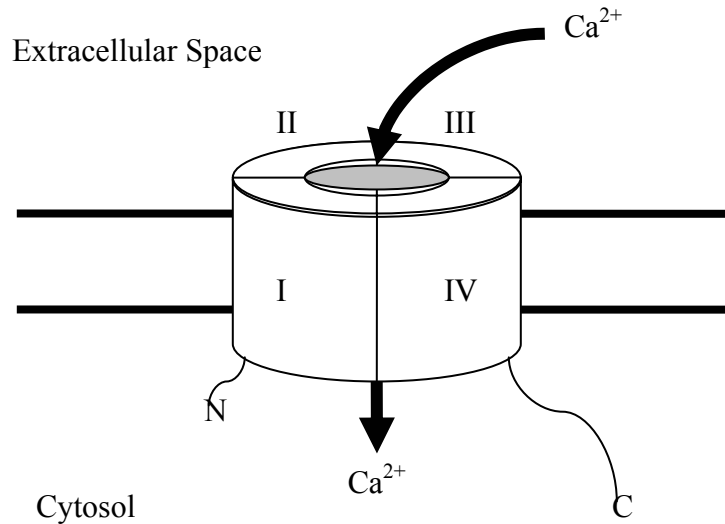
Figure I-5: Representation of folded α_1 subunit of a voltage-gated calcium channel within the membrane. Roman numerals indicate domains. N represents the N-terminus of the α_1 protein and C represents the C-terminus. (Westenbroek, et al., 1995; Catterall, 2000; Pietrobon, 2002)

Mutations in P/Q-type voltage-gated calcium channels

P/Q-type VGCCs are highly expressed in the dentate gyrus and CA fields of the hippocampus, the cerebellar cortex, pontine nucleus, olfactory bulb and cerebral cortex layers II and VI (Stea, et al., 1994). Moderate levels are also found in the striatum, hypothalamus, substania nigra, red nucleus, lateral reticular nucleus and inferior olive (Stea, et al., 1994). While N-, L-, and R-type channels can be found in the cerebellum, the majority of VGCCs in the cerebellum are P/Q-type VGCCs (Westenbroek, et al., 1995). P/Q-type VGCCs are most prominently expressed by Purkinje cells, are found throughout the dendritic arbor and at the cell body(Westenbroek, et al., 1995). These

channels are expressed to a lesser extent by cerebellar granule cells (Westenbroek, et al., 1995). In addition, molecular layer interneurons express P/Q-type VGCC at their presynaptic terminals on cerebellar Purkinje cells(Westenbroek, et al., 1995).

Calcium ion channel mutations are responsible for several inherited neurological disorders. Mutations in the α_{1A} or pore forming subunit of P/Q-type VGCC's have been linked to several human disorders including familial hemiplegic migraine (FHM), episodic ataxia type 2 (EA-2) and spinocerebellar ataxia type 6 (SCA-6) (Ophoff, et al., 1996; Klockgether and Evert, 1998; Ducros, et al., 1999; Pietrobon, 2002). FHM is associated with 12 different mutations in the α_{1A} gene that cause migraine accompanied by intermittent weakness or paralysis (Ophoff, et al., 1996; Klockgether and Evert, 1998; Pietrobon, 2002). These mutations are found in various domains in the voltage sensor, P-loop and in transmembrane segments five and six (Pietrobon, 2002). Approximately half of the FHM mutations cause a slowly progressive cerebellar ataxia and atrophy (Ducros, et al., 1999). The most common mutation for FHM with progressive cerebellar atrophy is T666M in the P-loop of domain II of the α_{1A} subunit (Pietrobon, 2002). EA-2 has been linked to 15 different mutations in the α_{1A} gene. Most of these mutations disrupt the open reading frame resulting in either truncation, intron inclusion or exon skipping of the α_{1A} subunit (Ophoff, et al., 1996; Klockgether and Evert, 1998; Pietrobon, 2002). These changes cause episodes of ataxia that may be progressive and cerebellar atrophy localized to the anterior vermis (Klockgether and Evert, 1998; Pietrobon, 2002). SCA-6 is caused by polyglutamine repeats in the carboxy-terminus of the α_{1A} subunit that result in a slowly progressive cerebellar ataxia with marked

cerebellar atrophy (Pietrobon, 2002). SCA-6 cerebellar atrophy is concentrated in the anterior cerebellar vermis and includes a severe loss of cerebellar Purkinje cells and granule cells (Pietrobon, 2002).

There are several mutations of the α_{1A} gene found in mice in which the phenotype or clinical signs closely resemble those in humans and have therefore been used as animal models to investigate the cellular and molecular consequences of α_{1A} mutations in FHM, EA-2 and SCA-6 (Fletcher, et al., 1996). Naturally occurring mutations include leaner, tottering, rocker, Nagoya rolling, and possibly pogo (Hyun, et al., 2001; Zwingman, et al., 2001). A genetic knockout of the α_{1A} gene (P/Q null) has also been created (Jun, et al., 1999).

The leaner mouse (tg^{la} or Cacna1a^{tg-la}) has a nucleotide substitution at an intron-exon junction causing an aberrant splicing event in the carboxy tail resulting in a severe cerebellar ataxia with a loss of both granule cells and Purkinje cells that is more severe in the rostral cerebellum (Fletcher, et al., 1996). The tottering (tg or Cacna1a^{tg}) mouse mutation results in an amino acid substitution (leucine for proline) in the P-loop of domain II of the α_{1A} protein, which is located about 20 amino acids away from T666M mutation of FHM (Fletcher, et al., 1996; Ducros, et al., 1999; Pietrobon, 2002). The tottering phenotype is characterized by an intermittent dyskinesia and a mild to moderate cerebellar ataxia without a significant loss of cerebellar neurons (Green and Sidman, 1962; Isaacs and Abbott, 1992; Klionsky, 2005). The rocker (tg^{rkr} or Cacna1a^{rkr}) mutation results in an amino acid substitution (lysine for threonine) in the P-loop of domain III (Zwingman, et al., 2001). The rocker phenotype is also characterized by a

mild to moderate cerebellar ataxia without a loss of cerebellar neurons (Zwingman, et al., 2001). The Nagoya rolling (tg^{rol} or Cacnala^{tg-rol}) mouse mutation is a glycine for arginine substitution in the voltage sensor of domain III (Oda, 1981). The rolling mouse phenotype is a moderate to severe ataxia with a minor loss of granule cells in the rostral cerebellum (Suh, et al., 2002). The pogo (*pogo/pogo*) mouse mutation has been mapped to an area of chromosome 8 that includes the α_{1A} gene (Hyun, et al., 2001). Even though the mapped area also includes a chloride channel, phenotypically the pogo mouse resembles other P/Q-type VGCC mutations. The phenotype of the pogo mouse includes a severe cerebellar ataxia, intermittent dyskinesia, and a loss of cerebellar Purkinje cells concentrated in the rostral vermis (Jeong, et al., 2000). The P/Q knockout or null mouse (Cacnala^{Fctm1}) most closely resembles the leaner mouse and its phenotype includes a severe cerebellar ataxia a loss of cerebellar granule cells and Purkinje cells (Jun, et al., 1999; Fletcher, et al., 2001). See Table I-6 for a summary and comparison of mouse P/Q-type VGCC mutations.

Table I-6: Comparison of α_{1A} mutations in the mouse

	Tottering	Rocker	Rolling	Leaner	P/Q null*	Pogo**
Ataxia	Mild	Mild	Moderate	Severe	Severe	Severe
Onset of ataxia	P24 – 26	P21 – 28	P10 – 14	P10 – 12	P10	P14
Neuronal loss	None	None	GC	PC, GC	PC, GC	PC
Ectopic TH expression	+	–	+	+	–	+
Abnormal PC synapses	+	?	+	+	?	+
PC dendritic arbor	Ectopic spines	Weeping dendritic arbor	Ectopic spines	Ectopic spines	?	–
Axonal torpedoes	+	–	+	+	+	+

PC is Purkinje cell, GC is granule cell, and TH is tyrosine hydroxylase. + indicates feature is present, – indicates feature is absent, and ? indicates presence or absence is unknown. Pogo may not be a due to a α_{1A} mutation. In all mutants where Purkinje cell death occurs, it is most prominent in the rostral cerebellum and occurs in parasagittal zones. Leaner, P/Q null and pogo mice also experience decrease survival rates during postnatal development. Adapted from (Zwingman, et al., 2001); *(Jun, et al., 1999; Fletcher, et al., 2001); **(Jeong and Hyun, 2000; Jeong, et al., 2000; Jeong, et al., 2001)

Mutations in the α_{1A} gene in both humans and mice share many features. Phenotypically, these mutations cause a cerebellar ataxia that is variable in severity. A common feature in many of these mutations is cerebellar atrophy with loss of cerebellar neurons. In addition to ataxia, both human and mouse mutations frequently produce an intermittent movement disorder and mice often exhibit absence seizures. The variability in various features of each mutation in the mouse mirrors the variability observed with the human mutations of FHM, EA-2 and SCA-6. Studies that investigate the nature of each mouse mutation as well as those that compare and contrast differences between them will provide key insights to our understanding of the diverse nature of these human disorders and the functions of P/Q-type VGCCs.

THE LEANER MOUSE

The leaner mouse (tg^{la}/tg^{la} or Cacna1a^{tg-la}) carries a naturally occurring autosomal recessive mutation. The leaner mouse was named for its motor dysfunction, which caused the mouse to "lean" against a wall to prevent it from falling while walking (Sidman, et al., 1965). Two independent studies demonstrated that the leaner mutation localized to the α_{1A} gene on mouse chromosome 8 (Fletcher, et al., 1996; Doyle, et al., 1997). The α_{1A} gene encodes the pore forming subunit of P/Q-type VGCCs (Westenbroek, et al., 1995; Gillard, et al., 1997; Dove, et al., 1998; Wakamori, et al., 1998; Lorenzon, et al., 1998). The leaner mutation is the result of a base substitution of guanine by adenine at the 5′ end of an intron at the carboxy terminal end of the α_{1A} gene (Fletcher, et al., 1996; Doyle, et al., 1997). The mutation alters intron – exon splicing at

this location, producing one of two products, an intron inclusion or exon skipped (truncated) α_{1A} protein at the carboxy-terminus (Fletcher, et al., 1996; Doyle, et al., 1997).

Severe cerebellar ataxia is the most notable phenotype of the leaner mouse. Ataxia first becomes apparent at P10 and becomes progressively worse until stabilizing at about P40 to P50 (Sidman, et al., 1965). During postnatal development leaner mice experience a reduced survivability, with death occurring in about three-quarters of the mice by P21 due to their inability to move about their environment (Sidman, et al., 1965; Meier, et al., 2000). However, when special care is given to support leaner mice through this critical period, they have a normal life expectancy (Abbott and Jacobowitz, 1999; Lau, et al., 2004).

Leaner mice also exhibit absence seizures and an intermittent dyskinesia (Sidman, et al., 1965; Levitt, 1988; Hess and Wilson, 1991). Generalized absence seizures begin as early as P14 and are similar to those in the tottering mouse, consisting of 6 – 7Hz spike wave discharges at a rate of 40 to 60 bursts an hour (Noebels, 1984; Klionsky, 2005). The intermittent dyskinesia, referred to most appropriately as paroxysmal dyskinesia since it is a sudden burst of involuntary activity that disrupts voluntary motion, has also been termed an intermittent movement disorder, focal motor seizures or myoclonus (Green and Sidman, 1962; Levitt, 1988; Hess and Wilson, 1991; Rhyu, et al., 1999). While this disorder is most prominent in tottering mutant mouse, the leaner mouse experiences it transiently, subsiding by P50.

In spite of the mutation, mRNA and protein expression of the leaner α_{1A} subunit is not altered (Wakamori, et al., 1998; Lau, et al., 1998). The leaner mutation does alter the function of P/Q-type VGCCs. The main effect of the mutation is a 60% decrease in Ca^{2+} currents, beginning as early as P7 – 9, just prior to the onset of ataxia (Dove, et al., 1998; Lorenzon, et al., 1998; Wakamori, et al., 1998). Voltage dependent gating, mean channel open time and Ca^{2+} conductance through the channel are unaffected (Dove, et al., 1998; Lorenzon, et al., 1998; Wakamori, et al., 1998). The leaner mutation causes a threefold lower probability of channel opening, reducing the frequency of opening and thus the amount of Ca^{2+} able to enter the cell following depolarization (Dove, et al., 1998; Lorenzon, et al., 1998; Wakamori, et al., 1998).

The C-terminal cytoplasmic tail of the α_{1A} subunit, which is altered by the leaner mutation, includes regulatory sites which are important in modulating P/Q-type VGCC properties (Catterall, 2000). These regulatory sites include interaction and modulation of P/Q-type VGCC function by G-protein coupled receptor $G\beta\gamma$ subunits (Hille, 1994; Herlitze, et al., 1996; Qin, et al., 1997; Ikeda and Dunlap, 1999) and a site for Ca^{2+}-calmodulin binding (Lee, et al., 1999). $G\beta\gamma$ subunits modulate gating properties while Ca^{2+}-calmodulin enhances P/Q-type channel recovery from inactivation, facilitating Ca^{2+} entry. The leaner mutation likely alters these or other regulatory functions such as phosphorylation sites in the C-terminal tail, to modify P/Q-type Ca^{2+} current.

Many cellular functions are regulated by Ca^{2+}, and in the CNS, VGCCs are the primary source of Ca^{2+} influx for Ca^{2+} signaling (Catterall, 2000; Berridge, et al., 2000; Bootman, et al., 2001). Since the leaner mutation dramatically alters P/Q-type Ca^{2+}

current, it also has a profound effect on various Ca^{2+} dependent cell signaling systems. For example, one important function of P/Q-type VGCCs is the presynaptic release of neurotransmitters. In the leaner cerebral cortex it has been demonstrated that glutamate neurotransmitter release is impaired (Ayata, et al., 2000; Qian and Noebels, 2001). P/Q-type VGCCs are prominently expressed in the cerebellum and thus have a significant role in the nature of Ca^{2+} signaling in cerebellar neurons. Leaner cerebellar Purkinje cells are able to maintain normal resting cytosolic concentrations of Ca^{2+} (Dove, et al., 2000; Murchison, et al., 2002). This is primarily achieved through compensatory mechanisms that reduce leaner Ca^{2+} buffering capacity. The leaner cerebellar Purkinje cell has reduced ER buffering as well as a decrease in the calcium binding proteins, parvalbumin and calbindin (Dove, et al., 2000). However, CICR remains intact in the leaner ER, suggesting the ER itself is not dysfunctional, but rather that Ca^{2+} concentrations are maintained closer to the functional capacity of the ER, reducing its ability to buffer additional Ca^{2+} (Murchison, et al., 2002). Thus, despite diminished Ca^{2+} entry, leaner cerebellar Purkinje cells are able to maintain Ca^{2+} transient amplitudes for a given stimulation (Dove, et al., 2000). Similar events also may be true for cerebellar granule cells since they show a decrease in their primary calcium binding protein, calretinin (Nahm, et al., 2002). In contrast to leaner Purkinje cells, leaner granule cells have decreased resting Ca^{2+} concentration (Lau, 1999). In addition, T-type VGCCs are increased in leaner cerebellar Purkinje cells and decreased in leaner granule cells (Nahm, et al., 2005). The differences between leaner Purkinje cells and granule cells, likely

represent different adaptive or compensatory processes within each cell type attempting to preserve cell function in presence of reduced Ca^{2+} currents.

These changes in calcium signaling in the leaner cerebellum have numerous down stream effects. Besides changes in T-type VGCC expression, there are many genes, whose expressions are dependent on Ca^{2+}, and calcium signaling pathways, which are altered in the leaner cerebellum (Austin, et al., 1992; Nahm, 2002). One example is that of tyrosine hydroxylase (TH) expression in cerebellar Purkinje cells. TH, which converts tyrosine to L-DOPA, is the rate limiting enzyme in the synthesis of the neurotransmitter dopamine. TH is transiently expressed in cerebellar Purkinje cells between the third and fifth postnatal weeks (Hess and Wilson, 1991; Austin, et al., 1992). However, in leaner cerebellar Purkinje cells, TH expression persists into adulthood (Hess and Wilson, 1991; Austin, et al., 1992). Studies in the tottering mouse have shown that this aberrant TH expression is regulated by Purkinje cell excitability and L-type VGCCs, which are upregulated in the tottering cerebellum in response to decreased P/Q-type Ca^{2+} currents (Fureman, et al., 1999; Fureman, et al., 2003).

Other changes in the leaner cerebellum include decreased numbers of cerebellar granule cell parallel fiber – Purkinje cell dendritic spine synapses as well as increased numbers of multiple synaptic contacts per parallel fiber varicosity in the leaner cerebellum (Rhyu, et al., 1999). Leaner Purkinje cells also have ectopic dendritic spines and abnormal axonal swellings or torpedoes (Rhyu, et al., 1999). However, the most notable phenotype and consequence of altered calcium signaling in the leaner cerebellum is neurodegeneration. Even though the overall cytoarchitecture of the cerebellum is

maintained, leaner cerebellar granule cells, Purkinje cells and Golgi cells die during postnatal development (Herrup and Wilczynski, 1982). Leaner cerebellar granule cells begin to die at P10 – 12 and peak granule cell death occurs at P20 (Herrup and Wilczynski, 1982; Lau, et al., 2004). Leaner cerebellar granule cell death remains noticeable until about P40, becoming infrequent by 4 months of age (Herrup and Wilczynski, 1982). Leaner cerebellar granules cells die via an apoptotic cell death process that includes activation of caspase 3 (Lau, et al., 2004). While it has been demonstrated that leaner cerebellar Purkinje cells die, it has been more difficult to determine both the precise timing and cellular mechanism of Purkinje cell death (Herrup and Wilczynski, 1982; Heckroth and Abbott, 1994). Herrup and Wilczynki's 1982 study found that dying leaner Purkinje cells were not reliably identifiable, so they used counts of surviving Purkinje cells to determine the timing of Purkinje cell death. Their study found that Purkinje cells begin dying after P26, with approximately half of the Purkinje cells lost by P60 and death continuing at lower levels until at least 1 year of age (Herrup and Wilczynski, 1982). Additional studies demonstrated that leaner cerebellar Purkinje cell death occurred in distinct parasagittal zones (Heckroth and Abbott, 1994). Further investigation showed that the parasagittal zones of surviving leaner Purkinje cells co-localized with zebrin II and aberrant, persistent expression of tyrosine hydroxylase zones (Hess and Wilson, 1991; Abbott, et al., 1996). However, it is not clear what impact the parasagittal zonation of the cerebellum or the aberrant TH expression has on Purkinje cell death and survival. While leaner cerebellar Purkinje cell

death does not appear to be a necrotic process, the specific mechanism of leaner Purkinje cell death remains uncertain.

OBJECTIVE OF THIS DISSERTATION

The objective of this dissertation was to increase our understanding of the key signaling factors resulting from decreased P/Q-type VGCC Ca^{2+} currents that direct leaner cerebellar Purkinje cell death. The long term goal of this research endeavor is to understand the process of cerebellar atrophy that plays such a significant role in human diseases such as familial hemiplegic migraine (FHM), episodic ataxia type 2 (EA-2) and spinocerebellar ataxia type 6 (SCA-6).

Gene expression studies have demonstrated that there several potential cell death signaling pathways that may be important in directing leaner Purkinje cell death (Nahm, 2002). The central hypothesis of this dissertation is that leaner cerebellar Purkinje cell death is mediated through activation of a caspase cascade. To evaluate this hypothesis, this dissertation investigated two specific aims:

1) Establish the temporospatial pattern of leaner cerebellar Purkinje cell death, and

2) Determine the role of caspase 3 activation in leaner cerebellar Purkinje cell death.

The objective of Specific Aim 1 (Chapter II) was to specifically determine the pattern of leaner Purkinje cell death. The first part of Specific Aim 1 confirmed the validity of the relative new cell death stain, Fluoro-Jade, in labeling dying leaner cerebellar neurons. The second part of Specific Aim 1 utilized Fluoro-Jade to determine the precise timing and pattern of leaner Purkinje cell death.

Changes in Ca^{2+} buffering suggest mitochondria are potentially stressed, which could result in the release of mitochondrial factors and trigger either caspase dependent or caspase independent programmed cell death (Dove, et al., 2000; Murchison, et al., 2002). Furthermore, apoptotic gene array data suggest there are changes in Bcl-2 family gene expression, namely an increase in Bad and Bak, which could cause Purkinje cells to be more susceptible to programmed cell death (Nahm, 2002). Gene array data however, also indicate there is an increase in cathepsin D, a lysosomal protease, suggesting the possibility of a lysosomal role in either direct caspase activation or macroautophagy (Nahm, 2002). Macroautophagy is able to trigger cell death through either activation of caspase 3 or by caspase independent means. The cell death signal pathways suggested by these studies indicate that determining the role of caspases is a key question that must be answered in order to elucidate the mechanism of leaner cerebellar Purkinje cell death.

In Specific Aim 2, the hypothesis that caspase 3 is specifically activated and essential to leaner cerebellar Purkinje cell death was tested. The first part of Specific Aim 2 (Chapter III) evaluated the pattern of caspase 3 activation in comparison to that of leaner cerebellar Purkinje cell death and the dependence of leaner Purkinje cell death on caspase 3 activation. The second part of Specific Aim 2 (Chapter IV) investigated potential mechanisms of caspase 3 activation.

CHAPTER II

FLUORO-JADE IDENTIFICATION OF CEREBELLAR GRANULE CELL AND PURKINJE CELL DEATH IN THE α_{1A} CALCIUM ION CHANNEL MUTANT MOUSE, LEANER*

SUMMARY

Cell death is a critical component of normal nervous system development, too little or too much results in abnormal development and function of the nervous system. The leaner mouse exhibits excessive, abnormal cerebellar granule cell and Purkinje cell death during postnatal development, which is a consequence of a mutated calcium ion channel subunit, α_{1A}. Previous studies have shown that leaner cerebellar Purkinje cells die in a specific pattern that appears to be influenced by functional and anatomical boundaries of the cerebellum. However, the mechanism of Purkinje cell death and the specific timing of the spatial pattern of cell death remain unclear. By double labeling both leaner and wild type cerebella with Fluoro-Jade and TUNEL or Fluoro-Jade and tyrosine hydroxylase immunohistochemistry we demonstrated that the relatively new stain, Fluoro-Jade, will label neurons that are dying secondary to a genetic mutation. Then, by staining leaner and wild type cerebella between postnatal days 20 to 80 with Fluoro-Jade, we were able to show that Purkinje cell death begins at approximately

postnatal day (P) 25, peaks in the vermis about P40 and in the hemispheres at P50 and persists at a low level at P80. In addition, we showed that there is a significant difference in the amount of cerebellar Purkinje cell death between rostral and caudal divisions of the leaner cerebellum, and that there is little to no Purkinje cell death in the wild type cerebellum at the ages we examined.

This is the first report of the use of Fluoro-Jade to identify dying neurons in a genetic model for neuronal cell death. By using Fluoro-Jade, we have specifically defined the temporospatial pattern of postnatal Purkinje cell death in the leaner mouse. This information can be used to gain insight into the dynamic mechanisms controlling Purkinje cell death in the leaner cerebellum.

INTRODUCTION

Many studies now demonstrate that factors determining which cells will die and when are not simple, direct mechanisms. Instead, a large number of proteins and signaling molecules from several cell signaling pathways are involved in complex interactions, which influence the balance between cell survival and cell death (Raff, 1998; Sastry and Rao, 2000; Yuan and Yankner, 2000). Not only is the presence or absence of trophic factors involved, but other pro- and anti-apoptotic factors have key determining roles (Giehl, et al., 2001; Krajewska, et al., 2002). Many pro- and anti-apoptotic factors are modulated by calcium signaling or calcium homeostatic changes (Berridge, et al., 2000). The leaner mouse has both altered calcium signaling and homeostasis which result in its specific temporospatial pattern of abnormal postnatal

Purkinje cell death in the cerebellum (Herrup and Wilczynski, 1982; Heckroth and Abbott, 1994; Dove, et al., 1998; Dove, et al., 2000). Thus, studies into the mechanisms of cerebellar Purkinje cell death and survival in the leaner mouse may provide key information about the complex interactions of calcium signaling, anatomical and functional determinants, and gene or protein expression variability that lead to cell death in some neurons, but not others.

Both leaner cerebellar granule cells and Purkinje cells die during postnatal development (Herrup and Wilczynski, 1982). However, unlike leaner granule cells, definitively determining the timing of Purkinje cell death has been more difficult (Herrup and Wilczynski, 1982; Heckroth and Abbott, 1994). Herrup and Wilczynski (1982) found it difficult to consistently identify dying leaner cerebellar Purkinje cells and instead evaluated surviving Purkinje cells at a variety of ages in order to establish a temporal pattern of cell death. This has provided an excellent framework to study the various aspects of the neurologic disorders exhibited by leaner mice. But now, as research focuses on uncovering the molecular mechanisms that direct and modulate the events that we see morphologically and phenotypically, a more detailed study of the temporal pattern of cerebellar Purkinje cell death is needed.

Fluoro-Jade is an anionic fluorescent dye that was introduced in 1997 to label degenerating neurons (Schmued, et al., 1997). Since its introduction, it has been used to identify dying neurons in a variety of situations including toxic insults (Freyaldenhoven, et al., 1997; Bowyer, et al., 1998; Hopkins, et al., 2000; Bishop and Robinson, 2001), traumatic injuries (Allen, et al., 2000; Zwienenberg, et al., 2001), ischemia models

(Kokaia, et al., 1998; Pennypacker, et al., 2000; Larsson, et al., 2001), seizure models (Poirier, et al., 2000; Kubova, et al., 2001), cell culture systems (Noraberg, et al., 1999; Kristensen, et al., 1999; Savaskan, et al., 2000), and recently in a transmissible spongiform encephalopathy infection (Ye, et al., 2001). But, Fluoro-Jade has yet to be tested in a genetic model of neuronal cell death.

The goals of this study are two fold. Since Fluoro-Jade is untested in a genetic model of neuronal cell death, the first objective was to validate the use of Fluoro-Jade in identifying known populations of dying cerebellar granule cells and Purkinje cells in the leaner cerebellum. The second, subsequent objective of this study was then to use Fluoro-Jade to more precisely define the temporospatial pattern of Purkinje cell death in the leaner mouse. With the information gained from this study, more detailed studies into the molecular mechanisms and interactions that produce the specific pattern of Purkinje cell death in the leaner cerebellum can be conducted.

EXPERIMENTAL PROCEDURES

Animals

Wild type and homozygous leaner mice on the C57BL/6J background between postnatal days (P) 20 to 80 were used. The mice were bred and housed at the Laboratory Animal Research and Resource facility at Texas A&M University. They were kept at a constant room temperature (70 - 72°C), exposed to a 12-hour light/dark cycle, and given access to food and water ad *libitum*. All mice were weaned between P30 and 40. All experimental procedures were carried out in accordance with National Institute of Health

Guide for Care and Use of Laboratory Animals (NIH publication No. 85-23, revised, 1996). Minimal numbers of animals necessary for each experiment were used.

Male and female heterozygous leaner mice were bred to produce homozygous offspring. Starting at P20, homozygous leaner mice could easily be distinguished from their heterozygous littermates by their ataxic phenotype. Homozygous leaner pups often die at P18 – 25 due to their severe ataxia, epileptiform seizures, and paroxysmal dyskinesia, which limit their ability to move about the cage. Therefore, homozygous leaner mice were kept alive by fostering newborn pups to lactating Swiss White Webster female mice, which are better able to nurture the pups, as they reach the critical age of P18 – 25. In addition, moistened rodent chow was placed in their cages, beginning at 2.5 weeks of age and changed daily. Leaner mice were weaned at P40, but the diet of dry rodent chow and water *ad libitum*, continued to be supplemented with moistened rodent chow.

Tissue collection

All mice were anesthetized intraperitoneally with 150 mg/kg ketamine and 15 mg/kg xylazine. Once anesthetized, the mice were perfused intracardially with 50 mL of Tyrode's Saline, followed by 500 mL of 4% paraformaldehyde in 0.12 M phosphate buffer (pH 7.4). For the Fluoro-Jade and TUNEL experiment, the brains were collected and embedded in paraffin. Sequential sagittal sections, 5 μm thick, were cut on an A/O microtome and mounted on plus coated ultraslick slides (VWR, West Chester, PA, USA). For the Fluoro-Jade and tyrosine hydroxylase experiment and the Fluoro-Jade

staining for the leaner Purkinje cell death pattern experiment, the brains were collected, cryoprotected in 20% sucrose in 0.1M phosphate buffered saline, frozen with powdered dry ice and stored at -70°C until sectioning on a cryostat. Throughout these experiments the rostral cerebellum is defined as lobules I through V, and the caudal cerebellum was defined as lobules VI through X.

Fluoro-Jade and TUNEL double labeling

Seven leaner mice, three males and four females, at P20 were used. Three to five slides, with three to four sections per slide, from the vermis of each cerebellum were double labeled with terminal deoxynucleotide transferase mediated, deoxyuridine triphosphate nick end labeling (TUNEL) and Fluoro-Jade. The slides were deparaffinized in a graded series of xylenes and ethanols. They were then TUNEL stained with the Apop-Tag kit (Intergen, Purchase, NY, USA) following the Intergen protocol for peroxidase staining of paraffin embedded tissues. The stain was developed with 0.024% 3,3 diaminobenzidine (Sigma, St. Louis, MO, USA) in 0.006% hydrogen peroxide and 0.05 M Tris-HCl buffer (pH 7.6) for five minutes. The reaction was stopped by three brief washes in 0.05 M Tris-HCl buffer (pH 7.6). Instead of counterstaining, the slides were taken directly into the Fluoro-Jade staining procedure.

Following TUNEL, the slides were rinsed in three, one minute washes in deionized water. The slides were then stained with Fluoro-Jade using a protocol previously described with the initial steps of drying the sections and 100% and 70% ethanol washes being omitted (Schmued, et al., 1997). The slides were instead, taken

directly into the 0.06% potassium permanganate solution for 15 minutes, washed in deionized water, and incubated in 0.001% Fluoro-Jade (Histochem, Jefferson, AR, USA) in 0.1% acetic acid for 30 minutes. Once staining was complete, the slides were washed in three, one minute rinses of deionized water, thoroughly dried with a hot air gun, immersed in xylene and coverslipped using DPX mounting media (EMS, Fort Washington, PA, USA). Sections of testes were included with each staining as a positive control for both TUNEL and Fluoro-Jade staining. Negative controls for TUNEL were also run by the omission of TdT enzyme from the TUNEL staining procedure. As a technical note, the double labeling procedure appears to decrease the durability and permanence of the diaminobenzadine reaction over the course of several months.

The slides were evaluated under bright field and fluorescence (fluorescein filter) microscopy. Digital images using a Zeiss Axioplot 2 Research Microscope and a 3-chip Hamamatsu video camera were captured from a rostral and a caudal region from sections on two different slides for each animal. The same field of view was captured with bright field illumination, for TUNEL staining, and fluorescein fluorescence illumination, for Fluoro-Jade staining, by alternating the light source without moving the stage. Images were alternately captured as pairs of images with either the TUNEL image first or the Fluoro-Jade image first, for a total of four image pairs for each light source per individual. The images were used to count positive cerebellar granule cells for each stain and determine which granule cells were labeled for both TUNEL and Fluoro-Jade. Two independent counts of the same images were completed and averaged. Two types

of comparisons were of interest in this experiment. The first was the evaluation overlap of TUNEL and Fluoro-Jade staining of granule cells for each individual. Specifically, were there significantly more double labeled granule cells than for either stain alone? This was evaluated using Fisher's protected least significant difference (Fisher's LSD) test at $\alpha = 0.05$. The second type of comparison was that of the stains over the entire population of leaner cerebellar granule cells. In other words, was there a significant difference between the populations of leaner cerebellar granule cells positive for one stain compared the granule cells positive for the other stain. For this comparison, counts were normalized as a percentage of total positive cells per image and an analysis of variance (ANOVA) was used to test for differences between individuals (a between factor) for each stain (a within factor) at $\alpha = 0.05$. However, even if the ANOVA analysis indicates a significant difference between the two stains, the variance calculation does not account for a random number of positive granule cells being counted in each image. Leslie Kish's formula for variance of unequal clusters (Kish, 1965), which accounts for this type of grouping is given below, and a z test were also used to more adequately evaluate and compare TUNEL and Fluoro-Jade staining granule cell populations at $\alpha = 0.05$ for significance.

Kish's Equation:

$$\operatorname{var}(r) = \left(\frac{1-f}{x^2}\right)\left(\frac{a}{a-1}\right)\left[\left(\sum y^2 - \frac{y^2}{a}\right) + r^2\left(\sum x^2 - \frac{x^2}{a}\right) - 2r\left(yx - \frac{yx}{a}\right)\right]$$

Where y = total number of y (cells per stain), x = total number or n, a = primary number of sampling units (individuals, 7), and f = sampling fraction (0).

Fluoro-Jade staining and tyrosine hydroxylase immunohistochemistry

Three leaner mice at P30 and three mice at P50 (males and females included in both groups) were selected and used based on preliminary staining trials, which showed numerous Fluoro-Jade positive Purkinje cells at these ages. When stained separately both tyrosine hydroxylase (TH) immunopositive Purkinje cells and Fluoro-Jade positive Purkinje cells could be identified, and as indicated in a previous study (Freyaldenhoven, et al., 1997) when double labeling was attempted, no Fluoro-Jade positive Purkinje cells could be detected. We expected to see little to no overlap between Fluoro-Jade staining and TH immunopositive Purkinje cells since Fluoro-Jade should label dying Purkinje cells while surviving Purkinje cells express TH. But upon evaluation of the double labeled sections, it appeared that TH immunopositive Purkinje cells failed pick up even the background level of Fluoro-Jade fluorescence (data not shown). This caused some concern that the immunostaining protocol might interfere with the ability of Fluoro-Jade to label dying cells under these conditions. In order to eliminate this potential problem, we utilized the parasagittal banding or zoned pattern of TH immunoreactivity in the leaner cerebellum, and compared serially paired coronal and frontal cerebellar sections, staining one slide for TH immunoreactivity and an adjacent slide for Fluoro-Jade. This allowed us to evaluate immediately adjacent sections for each stain. Based on the established staining pattern, a region of TH immunoreactivity in one section could be assumed to carry over into the adjacent section. For two individuals in each age group, 25 μm coronal sections of the cerebellum were cut on a cryostat as serial pairs and mounted on 0.3% gelatin-coated slides. Sets of paired slides evenly distributed from

rostral to caudal regions of the cerebellum of each individual were stained and evaluated. For the third individual in each age group, 25 μm frontal sections of the cerebellum were cut as serial pairs and mounted on 0.3% gelatin-coated slides. Paired slides, evenly distributed from dorsal to ventral positions within the cerebellum, were stained and evaluated. In each pair, one slide was stained with Fluoro-Jade, while the other was stained for tyrosine hydroxylase (TH) immunohistochemistry.

For TH immunohistochemistry, a standard protocol was used (Abbott and Jacobowitz, 1995). Briefly, slide mounted sections were permeablized in 0.3% Triton X – 100 for one hour and endogenous peroxidases were quenched with five minute incubation in 3.0% hydrogen peroxide in 0.1M phosphate buffered saline. The sections were blocked in 5.0% normal goat serum and incubated overnight at 4°C in rabbit polyclonal TH antibody (Protos Biotech Corporation, New York, NY, USA or Chemicon international, Temecula, CA, USA) at a 1:2,500 dilution. The sections were incubated in biotinylated goat anti-rabbit (Vector Laboratories, Burlingame, CA, USA) at a 1:400 dilution followed by peroxidase-labeled streptavidin (Kirkegaard & Perry Laboratories, Gaithersburg, MD, USA) at a 1:5,000 dilution, each for two hours at room temperature. The immunohistochemical reaction was developed with 0.024% 3,3 diaminobenzidine in 0.006% hydrogen peroxide and 0.05M Tris-HCl buffer (pH 7.6) for 20 minutes either with or without nickel intensification. The reaction was stopped by three brief washes in 0.05M Tris-HCl buffer (pH 7.6). The slides were thoroughly dried with a hot air gun, immersed in two changes of xylene, and coverslipped with DPX mounting media.

For Fluoro-Jade labeling, the appropriate paired slides to the tyrosine hydroxylase stained slides were stained following a previously described protocol with a slight modification (Schmued, et al., 1997). Frozen, slide mounted sections were thawed, dried in an oven at 54°C for two hours, and cooled to room temperature before staining. Then, as per the protocol described by Schmued, et al. (1997), the slides were washed in 100% ethanol, then 70% ethanol followed by deionized water; incubated in 0.06% potassium permanganate for 15 minutes, rinsed in deionized water then incubated in 0.001% Fluoro-Jade in 0.1% acetic acid for 30 minutes. The slides were rinsed in three, one minute washes of deionized water, thoroughly dried with a hot air gun, immersed in two changes of xylene, and coverslipped with DPX mounting media. Two slides with 25 μm testes sections were included with each staining as a positive staining control.

In order to evaluate the slides for overlapping regions of positively labeled cerebellar Purkinje cells, digital images were captured and compared. In the coronal sections, six evenly distributed (rostral to caudal) image pairs were captured per individual. In the frontal sections, two sets (one rostral and one caudal) of six evenly distributed (dorsal to ventral) image pairs were captured per individual. Half the image pairs per individual were captured by finding an area of tyrosine hydroxylase positive Purkinje cells under bright field microscopy and capturing the image without knowing the results of Fluoro-Jade staining in the adjacent sections. Then in an immediately adjacent Fluoro-Jade stained section, under fluorescence microscopy, the same specific area was identified, and its image was captured. The other half of the image pairs per

individual were captured in the opposite fashion, i.e. Fluoro-Jade positive Purkinje cells were identified and captured first, followed by images of tyrosine hydroxylase stained sections. The images were then compared for overlapping zones of Fluoro-Jade and tyrosine hydroxylase staining.

Fluoro-Jade staining for cerebellar Purkinje cell death pattern

The following ages were tested: postnatal days (P) 20, 25, 30, 40, 50, 60, 70, and 80. At P20, P30, P60, P70, and P80, four leaner and four wild type mice, two males, two females of each genotype were used. Based on the initial data, a Power Analysis at $\alpha = 0.05$ indicated an n = 6 would help clarify peaks in the data over the time course evaluated. At P25, P40, and P50, six leaner (three males, three females) and four wild type mice (two males, two females) were used. For each individual the entire cerebellum was cut on a cryostat as 25 μm sequential, sagittal sections. Every other slide from each individual was stained with Fluoro-Jade. To control for staining variability, the individuals were placed into staining groups containing one male and one female of each genotype at the same age per group. Testes sections were included as a positive staining control. The staining procedure was the same as that described in the Fluoro-Jade Staining and Tyrosine Hydroxylase Immunohistochemistry section except that after thawing, the slides were dried in a 54°C oven for three and a half to four hours and then cooled to room temperature before proceeding with the staining.

Prior to cutting the frozen brains, slides for individual mice were placed in their staining groups and given an identification number that lacked any indication of

genotype or gender. In this way, the remainder of the experiment was carried out blind to these factors. To evaluate cerebellar Purkinje cell death, the number of Fluoro-Jade positive Purkinje cells in each stained section was counted. When counting each individual, hemispheres were differentiated from vermis by the medial lack of the cerebellar peduncles to indicate a vermal section. In addition, the counts for the vermis were further divided into rostral (lobules I – V) and caudal (lobules VI – X) regions. Two independent counts were carried out for each individual using the following criteria: 1) only Purkinje cell bodies were counted, 2) the same cell body was not counted more than once (i.e. adjacent sections), 3) Purkinje cell dendrites alone were not counted. Total cerebellar counts for the two independent counters were averaged. Purkinje cell death comparisons included wild type (control) and leaner cerebella as well as anatomic locations (whole vermis, pooled hemispheres, rostral vermis and caudal vermis).

Since the data for P25 individuals was examined strictly for identification of initiation of Purkinje cell death, it was excluded from the following analyses in order simplify statistical calculations. ANOVA was used to test for differences based on gender, genotype, anatomic location, and age with significance indicated by $p < 0.05$. Trend analysis was used to compare time course data with significance indicated by $p < 0.0007$, for an $\alpha = 0.05$. Tukey's Honest Significant Difference (HSD) posthoc test was used to evaluate peaks with each time course examined at $\alpha = 0.05$ for significance.

RESULTS

Fluoro-Jade and TUNEL double labeling

In order to evaluate the use of Fluoro-Jade in the leaner mouse, whose genetic mutation results in neuronal death, we examined the staining of cerebellar granule cells, since this population of cells has been well studied. We utilized the known peak of leaner cerebellar granule cell death, P20, which was previously established by evaluating fragmented DNA associated with apoptosis using TUNEL labeling, comparing granule cell death indicated by TUNEL to that indicated by Fluoro-Jade (Herrup and Wilczynski, 1982; Lau, et al., 2004). Cerebellar sections from P20 leaner mice were double labeled with TUNEL and Fluoro-Jade. Figure II-1A and II-1B show a representative pair of captured images of double labeled sections. From 7 individuals, a total of 796 cerebellar granule cells were evaluated. Figure II-2 shows the average number of positive granule cells per individual for each stain. While some granule cells were positive only for Fluoro-Jade (17.5%) and others were positive only for TUNEL (29.5%), there were significantly more double-labeled (53%) granule cells (Fisher's protected Least Significant Difference: ANOVA $F_{2,21} = 14.2$, $p < 0.05$, Fischer's LSD $p < 0.05$).
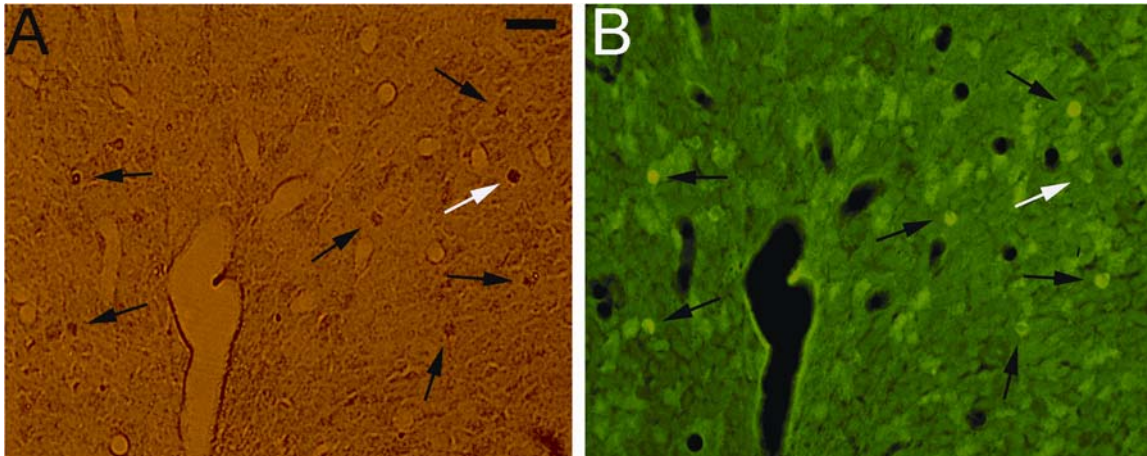
Figure II-1: Representative images of TUNEL and Fluoro-Jade labeling. A representative image pair of the granule cell layer from TUNEL (A) and Fluoro-Jade (B) double labeling is shown. A and B are the same field of view captured under different light sources, bright field for TUNEL (A) and FITC fluorescence for Fluoro-Jade (B). Scale bar in A indicates 20 μm. Black arrows indicate cerebellar granule cells positive for both stains. White arrow indicates granule cell positive for only one stain, TUNEL. Images were adjusted for brightness and contrast using Adobe Photoshop 5.0.

Of the 796 granule cells positive for at least one of the two stains, 82.5% were positive for TUNEL and 69.5% were positive for Fluoro-Jade. ANOVA analysis indicated no significant difference between individuals and no significant interaction between individuals and stain, but there was a significant effect of stain ($F_{1,6} = 64.38$, $p < 0.05$). Since it was necessary to change the light source to view double-labeled cells, it was not possible to count a predetermined number of cells in any one individual or field of view without biasing the data toward one stain or the other. Hence, in the images captured, all the positive cells were counted for each stain, meaning that in any given pair of images the total number of granule cells counted was a random number. Since there was no significant effect due to the individuals and no interaction between the

individuals and the staining procedure we grouped the individuals into a single data set of cerebellar granule cells rather than the individuals, with n = 796 for an alternate, more adequate comparison of the stains. Leslie Kish's formula for variance (indicated in the methods section), which accounts for this type of clustering of individuals and data, was used in a z test analysis of the TUNEL and Fluoro-Jade populations of granule cells(Kish, 1965). The z test indicated that there is a significant difference (z = -4.79, p < 0.01) between the TUNEL positive and the Fluoro-Jade positive populations of granule cells.
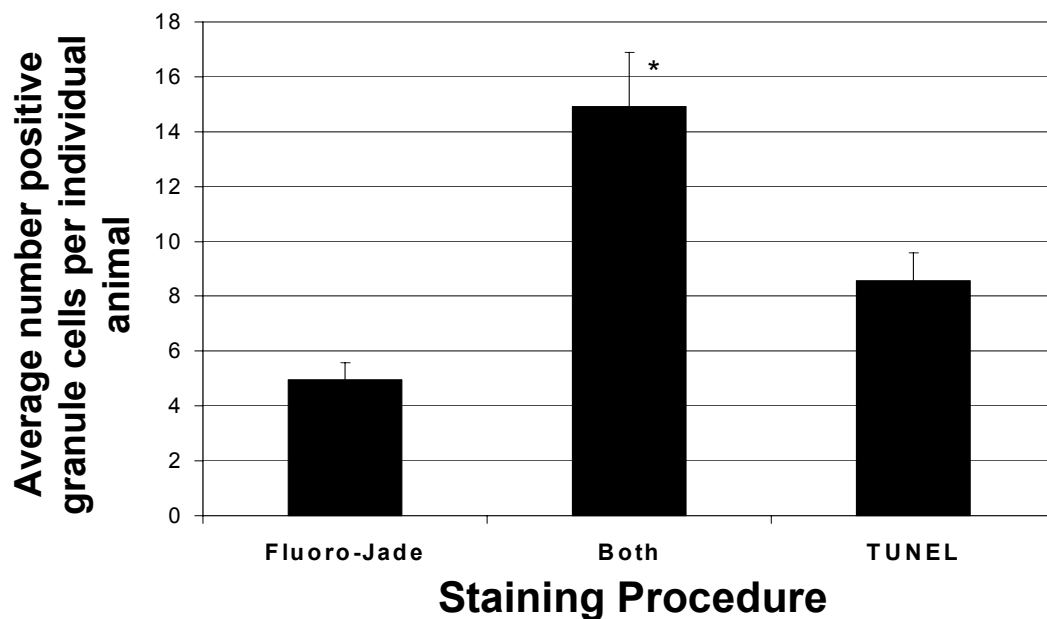
Figure II-2: Comparison of TUNEL and Fluoro-Jade double labeling in leaner cerebellar granule cells. Double labeling of TUNEL and Fluoro-Jade positive cerebellar granule cells from seven P20 leaner mice. For each category, TUNEL, Fluoro-Jade or Both (double labeled), the results per individual were averaged. The error bars represent standard error of the mean. Double labeled granule cells were significantly different from either Fluoro-Jade only labeling or TUNEL only labeling (indicated by an asterisk, *), but Fluoro-Jade only granule cells were not significantly different from TUNEL only granule cells.

Fluoro-Jade staining and tyrosine hydroxylase immunohistochemistry

In order to further test the use of Fluoro-Jade in identifying dying leaner neurons, and to specifically evaluate its use on dying cerebellar Purkinje cells, we utilized previously established patterns of Purkinje cell survival and death in these mice. Specifically, it has been shown, that surviving leaner cerebellar Purkinje cells abnormally express tyrosine hydroxylase (TH) in an rostrocaudal striped or mediolateral zoned pattern (Hess and Wilson, 1991; Austin, et al., 1992; Abbott, et al., 1996), and Purkinje cell death also occurs in a rostrocaudal striped pattern (Heckroth and Abbott, 1994). Figure II-3 shows two representative staining image pairs. 48 pairs of images (12 coronal and 12 frontal for each age group) were compared and results are shown in Table II-1. We found only one area where a single Fluoro-Jade positive Purkinje cell appeared to be located in an area of TH immunoreactivity.
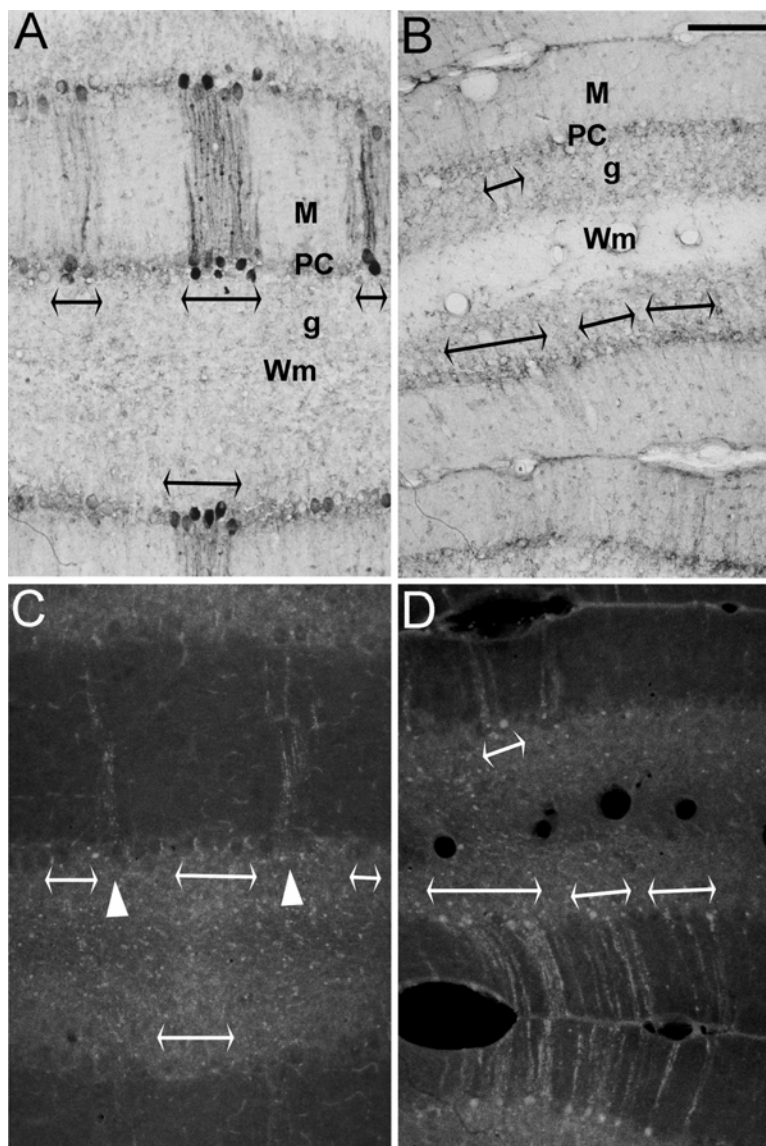
Figure II-3: Representative images of tyrosine hydroxylase and Fluoro-jade labeling. A - D are representative images of serially paired sections stained for tyrosine hydroxylase (A and B) and Fluoro-Jade (C and D) from a P30 leaner cerebellum. A and C are images where tyrosine hydroxylase positive Purkinje cells were found first. B and D are images where Fluoro-Jade positive Purkinje cells were found first. The double headed arrows in A and D indicate regions of positive Purkinje cells, which correspond to the regions lacking positive staining Purkinje cells indicated with double headed arrows in B and C. The arrowheads in C indicate Fluoro-jade positive Purkinje cell dendrites, located next to but not overlapping with tyrosine hydroxylase immunoreactivity. Scale bar in B indicates 100 μm for A - D. Images were adjusted for brightness and contrast using Adobe Photoshop 5.0.

Table II-1: Comparison of overlapping regions of tyrosine hydroxylase (TH) immunohistochemistry and Fluoro-Jade staining.

Overlap	Age and section type			
	P30, coronal	P50, coronal	P30, frontal	P50, frontal
No regions	11	12	12	12
One region	1	0	0	0
More than one region	0	0	0	0

Fluoro-Jade staining for cerebellar Purkinje cell death pattern

Based on cerebellar Purkinje cell survival in the leaner mouse, Purkinje cell death has been estimated to begin after P26, peak at P40 and a continued slow loss of Purkinje cells through at least one year of age with most of the Purkinje cell death occurring between P40 and P68 (Herrup and Wilczynski, 1982). In order to more clearly define the Purkinje cell death pattern in leaner mice, we evaluated the following age groups: P20, P30, P40, P50, P60, P70, and P80, so that the time frame evaluated would begin prior to the initiation of Purkinje cell death and include the most robust period of Purkinje cell death. Figure II-4 shows representative pictures of Fluoro-Jade staining from key time points. Once the initial data were evaluated, an age group at P25 was added in order to clarify the timing of initiation of Purkinje cell death. ANOVA analysis indicated that while gender was not significant, genotype ($F_{1,69} = 170.23$, $p < 0.05$), anatomic location ($F_{4,69} = 23.89$, $p < 0.05$) within the cerebellum and age ($F_{6,69} = 16.04$, $p < 0.05$) were significant.
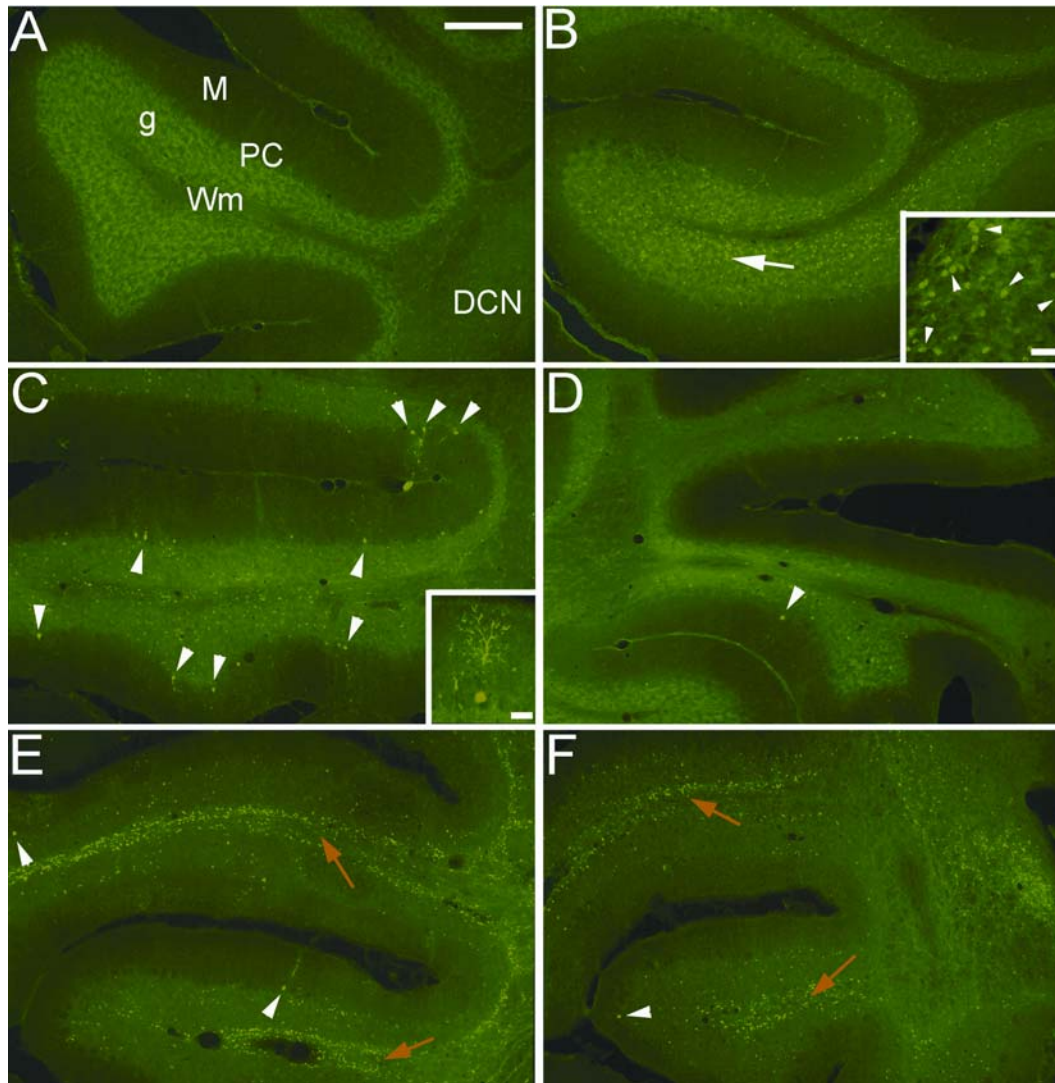
Figure II-4: Representative images from key time points in leaner cerebellar Purkinje cell death. Representative images of Fluoro-Jade staining in wild type (A) and leaner (B – F) cerebella. **A)** shows lobule III (rostral) from a wild type cerebellum at P40. M indicates molecular layer, PC indicates Purkinje cell layer, g indicates granule cell layer, Wm indicates white matter tracts and DCN indicates deep cerebellar nuclei. No positive staining is observed in the wild type cerebellum shown. **B)** shows lobule I/II (rostral) from a leaner cerebellum at P20. No positive Purkinje cells can be seen, but the arrow indicates numerous positive granule cells. The inset in **B** in a higher magnification image of the granule cell layer, the arrowheads indicate Fluoro-Jade positive granule cells. White arrowheads in C – F indicate positive Purkinje cells, and the orange arrows in E and F indicate white matter staining. C and D are taken from P40 leaner cerebella. **C)** shows lobule III (rostral), and **D)** shows lobules VIII and IX (caudal). Many fewer positive Purkinje cells were seen in the caudal lobules (VI – X) compared to the rostral lobules (I – V). Inset in **C** is a higher magnification image of a Fluoro-Jade positive Purkinje cell. The cell body in the Purkinje cell layer and the dendritic tree in the molecular layer are clearly visible. **E)** shows lobules III and VI/V (rostral) from a leaner cerebellum at P50. Fewer positive Purkinje cells were seen compared to P40, but white matter staining is quite prominent. **F)** shows lobules I/II and III (rostral) from a leaner cerebellum at P80. Numbers of positive Purkinje cells as well as white matter and deep cerebellar nuclei staining declined compared to earlier ages (P40 to P70). Scale bar in A indicates 100 μm for all images except insets in B and C. Scale bar in inset in B indicates 40 μm and the bar in inset in C indicates 50 μm. Images were adjusted for brightness and contrast using Adobe photoshop 5.0.

A comparison of Fluoro-Jade staining of cerebellar Purkinje cells in wild type and leaner cerebella is shown in Figure II-5A. Throughout the ages tested, wild type cerebella exhibited few Fluoro-Jade positive Purkinje cells. At P20 there were also no Fluoro-Jade positive Purkinje cells in the leaner cerebella, however, as expected and shown in Figure II-4B, large numbers of Fluoro-Jade positive granule cells could be detected. At P25, Purkinje cell death became evident in the leaner cerebellum. It is noteworthy that within this group, one leaner cerebellum had an estimated total of only 2 Fluoro-Jade positive Purkinje cells. This was followed by a rapid increase in Fluoro-Jade positive Purkinje cells until P40, then a steady decline, which continued past P80. In addition, white matter staining was detected beginning at P40 (Figure II-4C), becoming much more intense at P50 (Figures II-4E, II-6A and II-6B) and decreasing but still evident at P80 (Figure II-4F). Fluoro-Jade staining of axon fibers within the deep cerebellar nuclei was also detected between P50 and P80 (Figure II-6C and II-6D), but not in the inferior olivary nucleus (not shown). Trend analysis for comparison of wild type and leaner Purkinje cell death as determined by Fluoro-Jade staining indicates significant differences at P30, P40, P50, and P60 ($F_{1,69}$ = 17.02, 132.25, 82.43, and 23.81 respectively with $p < 0.0007$ in all cases). In order to facilitate the statistical analysis calculations, the P25 age group was excluded. Since the number of Fluoro-Jade positive Purkinje cells at P25 were less than those at P80 while its variance was similar, it is unlikely that significance could have been detected in this group. Tukey's HSD indicated a peak at or between P40 and P50.

Within the leaner cerebellum, the cerebellar vermis and pooled hemispheres had distinctly different patterns of Purkinje cell death (Figure II-5B). The leaner cerebellar hemispheres exhibited a slower increase in Purkinje cell death, with a broader peak and slower decline when compared to the leaner vermis. Trend analysis indicated that the leaner vermis and pooled hemispheres were significantly different from each other at P50 ($F_{1,69} = 40.64$, $p < 0.0007$). Trend analysis also indicated that the leaner vermis was only different from the wild type vermis at P40 ($F_{1,69} = 27.12$, $p < 0.0007$), while the leaner hemispheres were significantly different from wild type hemispheres at P40 ($F_{1,69} = 39.56$, $p < 0.0007$), P50 ($F_{1,69} = 54.51$, $p < 0.0007$), and P60 ($F_{1,69} = 14.85$, $p < 0.0007$). Tukey's HSD indicated a significant peak in Purkinje cell death as revealed by Fluoro-Jade staining at P30 and P40 in the leaner cerebellar vermis, and at P40 and P50 in the pooled hemispheres.

In addition, as shown in Figure II-5C, there is a distinct pattern of Purkinje cell death between the rostral (lobules I – V) and caudal (lobules VI – X) divisions of the leaner cerebellar vermis. Most of the Purkinje cell death in the leaner cerebellar vermis occurred rostrally, with only a low, steady level of Purkinje cell loss in the caudal lobules. Trend analysis indicated a significant difference at P40 between the leaner rostral and caudal cerebellar vermis ($F_{1,69} = 16.88$, $p < 0.0007$) and leaner and wild type rostral cerebellar vermis ($F_{1,69} = 19.72$, $p < 0.0007$). Tukey's HSD indicated a significant peak in Fluoro-Jade positive Purkinje cells in the leaner rostral cerebellar vermis at P40. In the leaner caudal cerebellar vermis, there is no significant difference when compared to wild type cerebella and no significant peak in Purkinje cell death.

Figure II-5: Quantitative evaluation of the Purkinje cell death pattern in the leaner cerebellum. Quantitative comparisons between leaner and wild type cerebella (A), between leaner vermis and pooled leaner hemispheres (B) and between rostral and caudal divisions of the leaner cerebellar vermis (C) over the time course P20 – P80. All age groups contain four leaner and four wild type mice except P25, P40 and P50, which contained six leaner mice and four wild type mice. For each individual the numbers of positive cerebellar Purkinje cells for half the cerebellum or region were used to estimate a total for the whole cerebellum or region, and the individuals for each age and genotype were averaged. Error bars represent the standard error of the mean. **A)** Comparison of whole cerebellum between wild type (black bars) and leaner mice (gray bars). Both wild type and leaner cerebella at P20 and the wild type cerebella at P40 have an average of zero. Wild type cerebella at P25, P30, and P70 had an average number of positive Purkinje cells of less than one. The wild type cerebella at P50 had an average positive Purkinje cell total of one, while wild type cerebella at P60 and P80 had an average of 1.5. The single asterisk (*) indicates significant differences in trend analysis, comparing the wild type Purkinje cell death trend to the leaner trend. The double asterisks (**) indicate significant peaks in leaner Purkinje cell death as indicated by Tukey's HSD. **B)** Comparison of vermis (gray bars) and pooled left and right hemispheres (black bars) in the leaner cerebellum. The single asterisk (*) indicates a significant difference in trend analysis comparing the leaner vermis and leaner hemispheres. The double asterisks (**) indicate significant peak in the leaner vermis and the triple asterisks (***) indicates significant peak in the leaner hemispheres as revealed by Tukey's HSD with each group. **C)** Comparison of rostral (lobules I – V, gray bars) and caudal (lobules VI – X, black bars) divisions of the leaner cerebellar vermis. The single asterisk (*) indicates a significant difference in trend analysis comparing the Purkinje cell death between the rostral and caudal leaner vermis. The double asterisks (**) indicate a significant peak in leaner Purkinje cell death in the rostral leaner vermis as revealed by Tukey's HSD. For all trend analyses in A – C, significance was indicated by $p < 0.0007$ as calculated for an $\alpha = 0.05$, and for the Tukey's HSD comparisons for determination of peaks in A - C, significance was calculated at $\alpha = 0.05$.
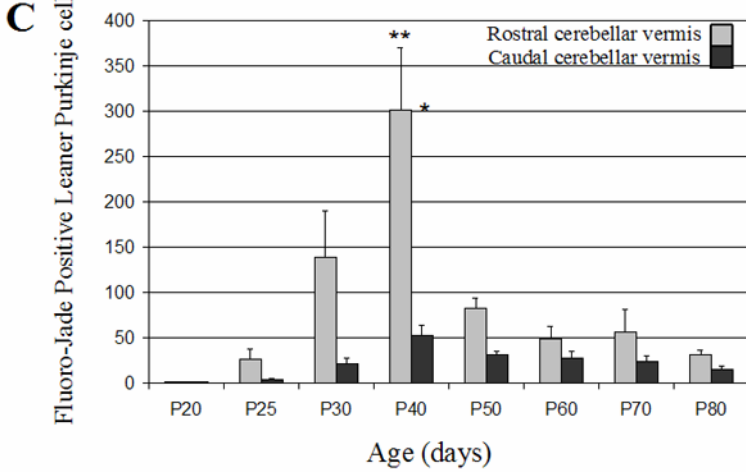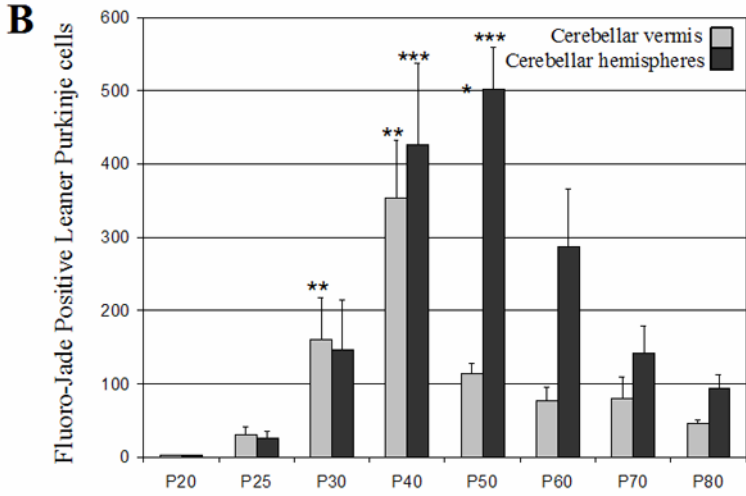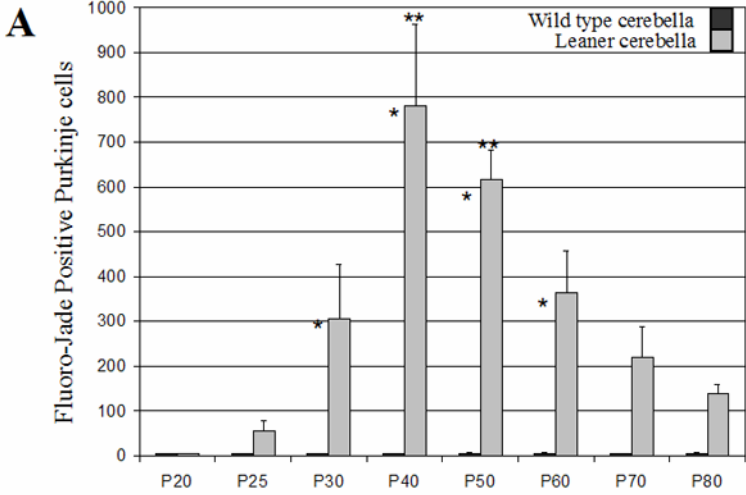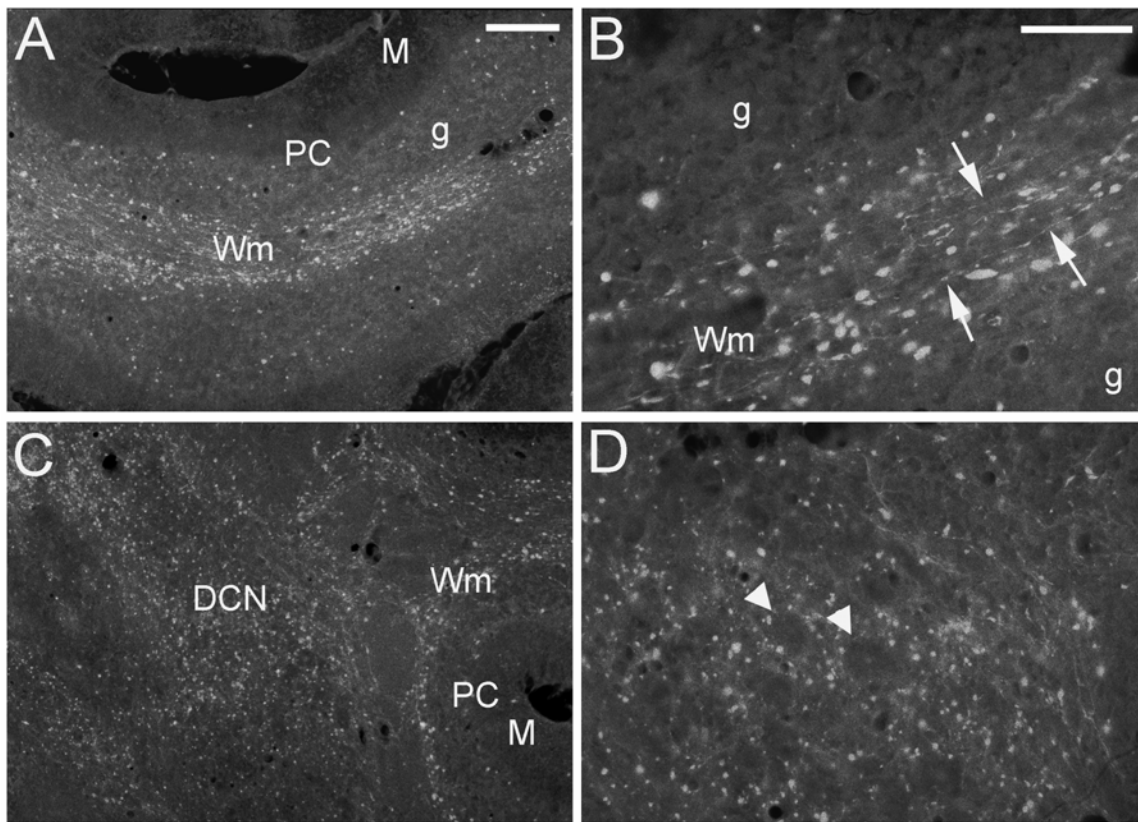
Figure II-6: Representative images of Fluoro-Jade staining in leaner white matter and deep cerebellar nuclei. Representative images of Fluoro-Jade staining of white matter and deep cerebellar nuclei at P50 in the leaner cerebellum. M indicates molecular layer, PC indicates Purkinje cell layer, g indicates granule cell layer, Wm indicates white matter tracts and DCN indicates deep cerebellar nuclei. A and B are images showing Fluoro-Jade positive white matter staining. B is a higher magnification image with some positive axons indicated by the arrows. C and D are images showing Fluoro-Jade positive staining in the deep cerebellar nuclei. D is a higher magnification image showing positive staining fibers surrounding unstained neurons, arrowheads indicate the deep cerebellar neurons. The scale bar in A indicates 50 μm for A and C, while the bar in B indicates 40 μm for B and D. Images were adjusted for brightness and contrast using Adobe photoshop 5.0.

DISCUSSION

Since its introduction in 1997, Fluoro-Jade has been used in a growing number of studies to identify or monitor neuronal cell death. These studies have focused primarily

on toxicity studies, cell culture systems or ischemia studies in the central nervous system (Noraberg, et al., 1999; Larsson, et al., 2001; Bishop and Robinson, 2001). The benefit of Fluoro-Jade is its nonspecific nature, identifying dying neurons regardless of the mechanism of cell death (Schmued, et al., 1997). It is this property of Fluoro-Jade that prompted its use in studies of the leaner mouse cerebellum.

Cerebellar granule cells that die secondary to expression of the leaner mutation are readily identified as typical apoptotic cells, by both morphology via cresyl violet staining (Herrup and Wilczynski, 1982) and fragmented DNA via TUNEL (Fletcher, et al., 1996; Lau, et al., 2004). Both of these methods have been used to establish the pattern of cerebellar granule cell death in the leaner mouse (Herrup and Wilczynski, 1982; Lau, et al., 2004). In addition, several studies clearly show that cerebellar Purkinje cells die during postnatal development in the leaner mouse (Herrup and Wilczynski, 1982; Heckroth and Abbott, 1994). Zebrin II staining (Hawkes and Herrup, 1995; Abbott, et al., 1996), aberrant tyrosine hydroxylase staining (Hess and Wilson, 1991; Austin, et al., 1992; Abbott, et al., 1996), and the known rostrocaudal (Herrup and Wilczynski, 1982) and mediolateral (Heckroth and Abbott, 1994) patterning of Purkinje cell death in the leaner mouse, indicate that it is a complex pattern with several factors involved in determining cell fate. A key, prerequisite step in determining the mechanism of leaner cerebellar Purkinje cell death is detailed knowledge of when and where Purkinje cells are dying. However, consistently and reliably identifying dying leaner cerebellar Purkinje cells has been difficult. The most detailed study on the timing of Purkinje cell death in the leaner mouse evaluated Purkinje cell survival and extrapolated

information concerning Purkinje cell death (Herrup and Wilczynski, 1982). Since Fluoro-Jade labels dying neurons in a way that is apparently nonspecific for the mechanism of cell death, it provides the opportunity to increase our knowledge about the timing of Purkinje cell death in the leaner mouse.

Fluoro-Jade identification of dying leaner cerebellar neurons

Since Fluoro-Jade had yet to be tested in a genetic model of cell death, our first objective was to evaluate Fluoro-Jade's ability to label neurons that were dying due to the leaner mutation. This was evaluated in cerebellar granule cells at their peak time of cell death (P20) by double labeling cerebellar sections with TUNEL and Fluoro-Jade, and in leaner cerebellar Purkinje cells based on their known pattern of survival and death.

We observed a significant number of dying cerebellar granule cells that were positive for both TUNEL and Fluoro-Jade, indicating that Fluoro-Jade will identify dying leaner granule cells. However, our results also showed that there was a significant difference between the populations of cerebellar granule cells, which were positive for one of the two stains. A likely explanation is that, since apoptosis is an orderly process by which a cell shuts down its functions in a sequential order, it takes time for the entire event to be completed (Raff, 1998; Sastry and Rao, 2000). TUNEL specifically identifies fragmented DNA associated with the end of the process of apoptosis (Raff, 1998; Sastry and Rao, 2000). While it has yet to be determined what compound or molecule Fluoro-Jade is labeling within neurons, it is not unreasonable to predict that it

is working at an earlier stage in the process of cell death than fragmentation of DNA. In addition, given the chemical nature of Fluoro-Jade, it has been postulated to bind basic compound such as biogenic polyamines (aminopropyl-butanediamine or spermidine, diaminobutane or putrescine, and diaminopentane or cadaverine), which are only produced in significantly increased amounts during cell death (Schmued and Hopkins, 2000).

The rostrocaudal striped pattern of leaner Purkinje cell survival and death is revealed by aberrant tyrosine hydroxylase (TH) expression in surviving leaner Purkinje cells (Hess and Wilson, 1991; Heckroth and Abbott, 1994; Abbott, et al., 1996). We used this pattern of TH expression to compare the pattern of Fluoro-Jade stained leaner Purkinje cells to that of surviving leaner Purkinje cells. Serially stained sections for tyrosine hydroxylase immunoreactivity or Fluoro-Jade showed almost no overlap (only one incidence in our data) between these two populations of Purkinje cells in the leaner cerebellum. A plausible explanation for the one region of overlap we did detect can be found in data presented for the wild type cerebella throughout the ages examined in this study. In some wild type cerebella, an occasional, apparently random dying Purkinje cell was detected with Fluoro-Jade. An occasional random dying Purkinje cell could also occur in the leaner cerebellum. If this were the case, these occasional random dying Purkinje cells in the leaner cerebellum would not necessarily follow the predicted pattern of cell death for the leaner cerebellum. Furthermore, it is clear from the wild type cerebella that there is no substantial normal developmental Purkinje cell death at the ages examined, making the difference between leaner and wild type cerebella striking,

both qualitatively and quantitatively. These results, when combined and viewed in light of previous studies, strongly support that Fluoro-Jade is indeed labeling dying leaner cerebellar Purkinje cells. Additionally, the granule cell data presented support that Fluoro-Jade also reliably identifies dying leaner cerebellar granule cells. Thus, leaner cerebellar granule cells and Purkinje cells, two types of neurons, which are dying as a result of a genetic mutation that profoundly affects the leaner mouse cerebellum can both be detected by Fluoro-Jade staining.

Leaner cerebellar Purkinje cell death pattern

Herrup and Wilczynski's (1982) study has provided the most detailed information about the timing of Purkinje cell death in the leaner cerebellum. While they noted substantial loss of cerebellar Purkinje cells that was greater rostrally than caudally, they were unable to confidently identify dying Purkinje cells throughout the ages of animals they examined (Herrup and Wilczynski, 1982). In order to provide a quantitative analysis, they evaluated surviving Purkinje cells that were compared to wild type cerebella. While no difference was seen at P26, they observed a peak in Purkinje cell death at P40 and a slow decline in Purkinje cell numbers through P359 (Herrup and Wilczynski, 1982). In addition, a later study demonstrated an additional complexity to cerebellar Purkinje cell loss in the leaner cerebellum in that Purkinje cells were lost from alternating sagittal zones (Heckroth and Abbott, 1994). By using Fluoro-Jade staining in the postnatal period between P20 and P80, this study clarifies several details in the developmental Purkinje cell death pattern in the leaner mouse.

Initiation of cerebellar Purkinje cell death in the leaner mouse, based on the results presented here is at or just prior to P25. This is earlier than reported by Herrup and Wliczynski (1982). They showed no difference between wild type and leaner cerebellar Purkinje cell death at P26. However, when one considers the methods employed in the two studies, it seems likely that the sensitivity of Fluoro-Jade in identifying dying Purkinje cells compared to the estimation of numbers of dying Purkinje cells from a count of surviving cells is greater, and thus allowed us to detect the increase in leaner Purkinje cell death with more precision. Data presented here confirm a peak in cerebellar Purkinje cell death at approximately P40 to P50 and a continued slow loss of Purkinje cells up to P80, which was the oldest age included in this study. While dying leaner cerebellar Purkinje cells were detected beginning at P25, axonal staining in the white matter of the cerebellum is not detected until P40. This staining could easily be followed into the deep cerebellar nuclei, beginning at P50, but none was detected in the inferior olivary nucleus at the ages examined. This strongly suggests that the majority of staining seen in the white matter was due to the axons of dying cerebellar Purkinje cells and not staining of climbing fiber afferents. However, contribution of dying climbing fibers to the white matter staining cannot be ruled out. Previous work has shown a minimal (Zanjani, et al., 2004), but patterned loss of neurons in the leaner inferior olive(Heckroth and Abbott, 1994), most likely due to a loss of their efferent targets. Given the delay seen between the beginning of Purkinje cell death and the appearance of white matter staining, the age range tested in this study may not be

sufficient to unequivocally identify degenerating climbing fibers and neuronal loss in the leaner inferior olive.

As expected, there are more complexities to the leaner Purkinje cell death pattern than initially seen when evaluating the pattern for the whole cerebellum. Not only is there a parasagittal pattern, demonstrated here by TH and Fluoro-Jade double labeling study as well as previous studies (Heckroth and Abbott, 1994; Abbott, et al., 1996), there are also patterns specific to the rostral and caudal divisions of the cerebellum as well as the cerebellar vermis and hemispheres. When compared to the wild type cerebellar vermis, the leaner cerebellar vermis only differs significantly at P40 and has a peak of Purkinje cell death between P30 and P40, while the pooled leaner hemispheres differ significantly between P40 to P60 and have a peak between P40 and P50. In addition, the leaner cerebellar vermis differs significantly from the pooled leaner cerebellar hemispheres at P50. When the cerebellar vermis is further divided into rostral and caudal subdivisions, the expected rostrocaudal division in leaner Purkinje cell death becomes clear. Purkinje cell death in the leaner rostral cerebellar vermis is significantly different from both the wild type and the leaner caudal cerebellar vermis at P40. In addition, the peak of leaner Purkinje cell death in the rostral vermis is narrowed to P40, compared to the range of P30 to P40 identified for the whole leaner vermis. In contrast, there was no significant peak in Purkinje cell death observed for the caudal leaner cerebellar vermis. While there is a notable trend towards more Purkinje cell death in the caudal leaner cerebellar vermis, it did not reach a level of significance for this study. This is probably due to individual variability rather than a real lack of difference

between wild type and leaner mice. In any case, it strengthens the argument that the pattern for leaner cerebellar Purkinje cell death is different in the rostral vermis when compared to the caudal vermis.

The pattern of cerebellar Purkinje cell death in the leaner mouse is indeed complex. As indicated by several previous studies, the cerebellum is comprised of several different compartments including the gross anatomical divisions, vermis, hemispheres, and flocculonodular lobes, as well as rostral and caudal compartments and mediolateral or parasagittal zones (Herrup and Kuemerle, 1997; Ozol, et al., 1999). These compartments are not only functionally distinct, they also represent barriers in developmental cell origin or migration and gene or protein expression (Herrup and Kuemerle, 1997). The mutated P/Q type voltage gated calcium ion channel subunit, α_{1A}, found in the adult leaner mouse, is uniformly expressed throughout the cerebellum at the same levels as those seen in wild type cerebella (Lau, et al., 1998). However, it is clear from this study and previous studies, that the same is not true for the consequences of this mutation.

The factors that determine death or survival for leaner cerebellar Purkinje cells are either components or consequences of the division of the various normal compartments of the cerebellum. Certainly, those cerebellar Purkinje cells that die in the leaner cerebellum either as a consequence of their location, synaptic afferents or efferents, or general molecular function are either less able to compensate for the alterations caused by the calcium ion channel mutation or simply respond differently from their counterparts in different compartments of the cerebellum to the same

circumstances. The dynamics of cerebellar structure and function are critical aspects of our understanding of not only normal development and function of the cerebellum, but also our understanding of the various disease states that affect its function. Now that we have a better understanding of the timing of Purkinje cell death in the various compartments of the cerebellum, further investigation into the mechanisms of cerebellar Purkinje cell death in the leaner mouse is likely to provide new key insights into general functions of the cerebellum and the complex interactions of neural circuitry and determinant factors in neuronal cell death and survival.

CHAPTER III

PURKINJE CELL DEATH IN THE α_{1A} CALCIUM ION CHANNEL MUTANT MOUSE, LEANER, IS PARTIALLY DEPENDENT ON CASPASE 3 ACTIVATION

SUMMARY

The leaner mouse carries a mutation (tg^{la}/tg^{la} or cacna1a^{tg-la}) in the α_{1A} subunit of P/Q-type voltage-gated calcium channels. One consequence of this mutation is a specific temporospatial loss of leaner cerebellar Purkinje cells that begins at postnatal day (P) 25 and peaks at P40 to P50. The molecular mechanism of this neuronal cell death remains unclear. Caspase protease cascades often have key roles in the major signaling pathways that direct neuronal cell death. We evaluated caspase 3 activation prior to the onset of leaner Purkinje cell death at P20 and at the peak of cell death P40 and P50. Prior to the onset of leaner Purkinje cell death there was no activation of caspase 3. However at the peak of leaner Purkinje cell death there was significant activation of caspase 3, which was confirmed with an activity assay. Using organotypic cerebellar cultures, we demonstrated that leaner Purkinje cell are significantly rescued by caspase 3 inhibition, they were still significantly decreased compared to wild type Purkinje cells. These studies demonstrated that while caspase activity and caspase cascades do have a key role in leaner Purkinje cell death, they may be acting in conjunction with other cell death signaling pathways or that blockade of caspase 3 increases cell death by caspase independent mechanisms.

INTRODUCTION

Neuronal cell death has key roles in both normal nervous system development and in the pathology of various neurodegenerative diseases. Neurologic disorders such as familial hemiplegic migraine (FHM), episodic ataxia type 2 (EA-2) and spinocerebellar ataxia type include a loss of cerebellar neurons as part of their pathology (Pietrobon, 2002). The leaner mouse (tg^{la} or cacna1a^{tg-la}), like FHM, EA-2 and SCA-6, carries a mutation in the α_{1A} or pore forming subunit of P/Q-type voltage-gated calcium ion channels that results in a specific loss of cerebellar neurons and has been used as a model to aid our understanding of these disorders (Herrup and Wilczynski, 1982; Fletcher, et al., 1996).

In the leaner mouse the P/Q-type voltage gated calcium channel mutation results in decreased calcium currents and altered calcium homeostasis of the affected neurons (Dove, et al., 2000; Murchison, et al., 2002). One consequence is an abnormal loss of granule cell and Purkinje cell neurons in the leaner cerebellum (Herrup and Wilczynski, 1982). Leaner cerebellar granule cells have been shown to die via an apoptotic pathway involving caspase 3 activation, nuclear condensation and DNA fragmentation (Lau, et al., 2004). The mechanism of leaner Purkinje cell death, however, still remains unclear. Ca^{2+} is a universal signaling molecule able to alter a wide variety of cellular processes including gene transcription, modulation of protein and enzyme functions and signaling at the mitochondria and the endoplasmic reticulum (Berridge, et al., 2000; Bootman, et al., 2001). In addition, previous gene array data in the leaner cerebellum and Purkinje cells have implicated several potential pathways in the mechanism of leaner Purkinje

cell death. There are increases in pro-cell death proteins Bad and Bak, which may increase mitochondrial sensitivity to apoptotic signals (Nahm, 2002). There is also an increase in the lysosomal enzyme, cathepsin D (Nahm, 2002). Lysosomes and lysosomal enzymes have been linked to cell death through direct activation of caspase 3 as well as macroautophagic mechanisms of cell death (Bursch, 2001; Hishita, et al., 2001; Wang and Klionsky, 2003; Klionsky, 2005). Alternately, calcium homeostasis and buffering is also disrupted in leaner cerebellar Purkinje cells (Dove, et al., 2000; Murchison, et al., 2002). Since mitochondria play an important role in buffering Ca^{2+}, these changes may place additional stresses mitochondria which result in cell death (Ichas and Mazat, 1998).

Mitochondria, macroautophagic mechanisms, and some receptor mediated mechanisms are able to trigger programmed cell death through the use of caspase cascades (Yuan, et al., 2003). Caspases are proteases synthesized as inactive zymogens which are cleaved and activated in many cell death pathways in order to carry out the breakdown of cellular components (Earnshaw, et al., 1999). Caspases can be divided into two main groups: initiator caspases and effector caspases. Initiator caspases, such as caspases 8, 9 and 12, are activated by various cellular signaling pathways to start a caspase cascade. Effector caspases, such as caspases 3, 6, and 7, are activated by upstream, initiator caspases to execute the breakdown of cellular components.

However, both mitochondria and macroautophagic mechanisms are also able to trigger programmed cell death independent of caspase activation (Susin, et al., 1999; Joza, et al., 2001; Bursch, 2001; Florez-McClure, et al., 2004). In order to elucidate the

mechanism of leaner cerebellar Purkinje cell death the role of caspases must be determined. Since caspase 3 is an effector caspase common to multiple cascade pathways, it can be used as general marker for presence of caspase proteases in programmed cell death. Our objective was to evaluate the role of caspase 3 activation in leaner cerebellar Purkinje cell death. The hypothesis that caspase 3 was specifically activated in dying leaner cerebellar Purkinje cells and its activation played a critical role in leaner Purkinje cell death was tested.

EXPERIMENTAL PROCEDURES

Animals

Wild type and homozygous leaner mice (tg^{la}/tg^{la} or Cacna1a^{tg-la}), on the C57BL/6J background at P10, P20, P40 and P50 were used. Animal handling and breeding procedures are described in Chapter II. All experimental procedures were carried out in accordance with National Institute of Health Guide for Care and Use of Laboratory Animals (NIH publication No. 85-23, revised, 1996). The minimum numbers of animals necessary for each experiment were used.

It was necessary in some experiments to determine the genotype of mutant mice prior to the onset of ataxia (P10). In order to distinguish genotypes of pre-ataxic pups, heterozygous mice leaner mice were also heterozygous for the dominant mutation oligosyndactyly. The gene for oligosyndactyly is closely linked to the *tg* locus resulting in very few crossover events (Isaacs and Abbott, 1992). Heterozygous oligosyndactyly causes a fusion of digits, while homozygous oligosyndactyly results in embryonic death.

Therefore, the presence or absence of fused digits on newborn pups allowed us to distinguish between homozygous leaner pups (normal number of digits) and heterozygous pups (fused digits). Starting at P20, homozygous leaner mice could easily be distinguished from their heterozygous littermates by their ataxic phenotype.

Tissue collection

For paraformaldehyde fixed and frozen brain tissue, mice were anesthetized intraperitoneally with 150 mg/kg ketamine and 15 mg/kg xylazine. Once anesthetized, the mice were perfused intracardially with 50 mL of Tyrode's Saline, followed by 400 to 500 mL of 4% paraformaldehyde in 0.12 M phosphate buffer (pH 7.4). The brains were removed from the skull, cryoprotected in 20% sucrose in 0.1M phosphate buffered saline, frozen with powdered dry ice and stored at -70°C until sectioning on a cryostat. Frozen cerebella were sectioned at 25 μm. For the experiments using fixed, frozen brains, the rostral cerebellum was defined as lobules I through V, and the caudal cerebellum was defined as lobules VI through X.

For cultured cerebellar slices, P10 mice were anesthetized with isoflurane and exsanguinated by cutting the heart. The brains were then removed using sterile surgical technique (Miranda, et al., 1996; McAlhany, et al., 1997; Cheema, et al., 2000) and the cerebella were sectioned coronally at 350 μm in ice cold dissection media containing 36mM glucose, 10mM $MgCl_2 \cdot 6H_2O$ in Gey's balanced salt solution (Sigma-Aldrich, St. Louis, MO, USA) on an Electron Microscopy Sciences (EMS) tissue slicer (OTS-4000, Hatfield, PA, USA). The whole cerebellum of each mouse was sectioned and cultured.

The cerebella were placed on Millicell organotypic inserts (PICM ORG 50, Millipore, Bedford, MA, USA) in sterile six well plates (Falcon, BD Biosciences, Franklin Lakes, NJ, USA). Culture media containing 50% Basal Media Eagle with Earle salts (Gibco, Carlsbad, CA, USA), 22.5% Hank's balanced salts (Gibco, Carlsbad, CA, USA), 25% heat inactivated horse serum (Sigma-Aldrich, St. Louis, MO, USA), 36mM glucose (Sigma), 1 mM glutamine (Sigma) and 50 μg/mL vitamin C (Sigma) was changed every 3 days for the duration of the culture. Slices were kept in a humid incubator at 37°C and 5% CO_2 for 31 days, the equivalent of approximately P40 *in vivo*.

For acute cerebellar slices, mice at P40 were anesthetized with isoflurane and decapitated. The brains were aseptically removed and the cerebella were coronally sectioned at 150 μm in ice cold dissection feed on an EMS tissue slicer.

Immunohistochemistry

Immunohistochemistry (IHC) was performed using a standard protocol described in Chapter II (Abbott and Jacobowitz, 1995). Cultured sections, however, were permeablized in 0.3% Triton X – 100 for 15 minutes instead of an hour and the quenching of endogenous peroxides was omitted.

Activated caspase 3 IHC used an affinity purified polyclonal rabbit antibody specific for the p17 cleavage product of caspase 3 at a 1:25,000 dilution (R&D Systems, Minneapolis, MN, USA). Tyrosine hydroxylase (TH) IHC used an affinity purified rabbit polyclonal antibody at a 1:2,500 dilution (Chemicon International, Temecula, CA, USA). Calbindin IHC used an affinity purified polyclonal rabbit antibody at 1:4,000

dilution (Chemicon International, Temecula, CA, USA). Neuronal nuclei (Neu N) IHC used a monoclonal mouse antibody at 1:2,000 dilution (Chemicon international, Temecula, CA, USA). For Neu N IHC blocking was done with horse serum and the secondary antibody was rat absorbed biotinylated horse antimouse (Vector, Burlingame, CA, USA).

Caspase 3 activity assay

Caspase 3 activity assay was performed using a carboxyfluorescein detection kit for live cells (Biocarta, San Diego, CA, USA). The carboxyfluorescein labeled caspase 3 inhibitor (FAM-DEVD-FMK, provided in kit) was mixed with dimethylsulfoxide (DMSO, Sigma-Aldrich, St. Louis, MO, USA) for a 150X stock solution, aliquoted and stored at -20°C. Working solution was made fresh for each use by diluting 4.0 μL 150X FAM-DEVD-FMK in 40.0 μL of autoclaved 0.1M phosphate buffered saline, then mixed with 1.5 mL dissection feed (acute slices) or culture feed (cultured slices) for a final dilution of 1:385. Acute cerebellar cultured cerebellar slices from each cerebellum were divided into two groups: negative control and FAM-DEVD-FMK treated.

Acute slices were incubated in depression slides with 200 μL of dissection media (negative control slices) or 200 μL working FAM-DEVD-FMK (treated slices) for one hour in a humid incubator at 37°C, 5% CO_2. Incubation was stopped with two, 10 minute washes in 1X wash buffer (provided in kit). Slices were fixed overnight at 4°C (fixative provided in kit). Slices were mounted on 0.3% gelatin coated slides and coverslipped with vectashield (Vector, Burlingame, CA, USA). Cerebellar slices were

tested and imaged in pairs of one wild type and one leaner mouse each. Slices were imaged, maintaining constant exposure for controls and treated slices within each cerebellar pair on a Zeiss Axioplan 2 research microscope (Plan-APOCHROMAT 10X, 0.45 numerical aperture objective) and a Zeiss color Axiocam HRC digitial camera (acquisition software Axiovision 4.2). FAM-DEVD-FMK fluorescence intensity was determined by calculating an integrated density value (IDV) using Alpha Innotech AlphaEase 3.1 software for each mouse, subtracting background fluorescence (negative control) from FAM-DEVD-FMK treated fluorescence of cerebellar Purkinje cell bodies. A minimum of three treated and two control slices were analyzed per cerebellum with 10 Purkinje cell bodies analyzed per slice.

Four cultured cerebellar slices from each cerebellum were evaluated: two negative controls and two FAM-DEVD-FMK treated. Slices were incubated with 1.0 mL of culture feed (negative control) or FAM-DEVD-FMK diluted in culture feed (treated) for one hour in a humid incubator at 37°C, 5% CO_2. Incubation was stopped with two, 10 minute washes in 1X wash buffer (provided in kit). Cultured slices were imaged as described for acute cerebellar slices, maintaining constant exposure for controls and treated slices from each cerebellum. A minimum of three treated and two control images were analyzed per cerebellum with 10 Purkinje cell bodies analyzed per slice. Following imaging, cultured slices were fixed in 4% paraformaldehyde in 0.12 M phosphate buffer (pH 7.4) overnight in the refrigerator, then washed in 0.1 M phosphate buffered saline. Fixed culture slices were further analyzed by immunohistochemistry.

Activation of caspase 3

Three age groups were examined: P20, prior to leaner Purkinje cell death and P40 and P50, at the peak of leaner Purkinje cell death. Six leaner and six wild type animals were examined at each age. Paraformaldehyde fixed frozen cerebella were collected and sectioned at 25 μm in serial pairs. Half the cerebellum of each animal, one slide from each serial pair, was immunostained for the cleaved or activated form of caspase 3 and the positive Purkinje cell bodies in each stained section were counted. A Genotypes within all age groups were compared using a 2-way analysis of variance (ANOVA) at significance level α = 0.05. Following a significant ANOVA, differences between genotypes at each age group were the compared using a linear contrast analysis with significance indicated by $p \leq 0.01$ for an experiment wise α = 0.05. The pattern of activation of caspase 3 in Purkinje cells was qualitatively compared to the Purkinje cell death pattern indicated by Fluoro-Jade at P20, P40 and P50, determined in Chapter II.

Leaner cerebellar Purkinje cells die in distinct rostrocaudal stripes or zones (Heckroth and Abbott, 1994). Surviving leaner Purkinje cells aberrantly express TH (Austin, et al., 1992; Heckroth and Abbott, 1994; Abbott, et al., 1996). We determined whether activated caspase 3 immunopositive leaner cerebellar Purkinje cells were restricted to dying or surviving zones of Purkinje cells using serial immunohistochemistry for TH and activated caspase 3. Paraformaldehyde fixed frozen cerebella were collected from four leaner mice (two males and 2 females). Cerebella were sectioned at 25 μm into serial pairs. Since the rostrocaudal zones of leaner Purkinje cell survival can be viewed in either coronal or frontal planes, two cerebella

were sectioned coronally and two were sectioned frontally. Eight pairs of slides evenly distributed throughout the cerebellum were evaluated with one slide in each pair immunostained for activated caspase 3 and the other for TH. All activated caspase immunopositive Purkinje cells were identified and imaged. An immediately adjacent TH immunostained section was then imaged to determine if the positive Purkinje cell was in a TH positive (surviving Purkinje cell) zone or a TH negative (dying Purkinje cell) zone.

Immunohistochemistry for the activated form of caspase 3 indicates the cleavage process required for caspase proteolytic activity. To confirm that caspase cleavage was associated with caspase proteolytic activity, a caspase 3 specific activity assay was used. Acute cerebellar slices were collected from four age matched wild type and leaner pairs at P40 and assayed for caspase 3 activity. A one-tail paired t test at $\alpha = 0.05$ was used to statistically determine if leaner cerebellar Purkinje cells had more caspase 3 activity than wild type.

Leaner Purkinje cell death dependence on caspase 3 activity

In vitro inhibition of caspase 3 was used to evaluate the dependence of leaner cerebellar Purkinje cell death on caspase activity. Nine wild type and nine leaner cerebella were cultured. Three cerebella from each genotype were maintained in culture for 31 days, to obtain the approximate *in vivo* age of P40. These cultures were paraformaldehyde fixed then immunostained for either calbindin or Neu N to evaluate cerebellar morphology. Based on this preliminary data, a Power Analysis at $\alpha = 0.05$

indicated an n = 6 would be necessary to evaluate differences between wild type and leaner cerebella. Six cerebellar cultures of each genotype were allowed to stabilize for 11 days, equivalent to approximately P20 *in vivo*. Beginning at this age, which is prior to the onset of leaner Purkinje cell death, slices were incubated with or without a caspase 3 specific inhibitor, z-DEVD-FMK (R&D Systems, Minneapolis, MN, USA). The caspase 3 inhibitor was added to the culture feed at 50 µM. Cultures were maintained with or without the caspase 3 inhibitor for an additional 20 days, equivalent to the peak of leaner Purkinje cell death, P40. Cultured slices were assayed for caspase 3 activity to confirm successful inhibition of caspase activity, then paraformaldehyde fixed. The entire cerebellum from each mouse was immunostained for calbindin. Immunopositive Purkinje cell bodies were counted in each section blind to individual animal, genotype and treatment group. Caspase activity assay data were collected on an individual basis rather than as paired groups. Since this introduced the possibility of some variation in labeling due to differences in staining on different days, the statistical evaluation of caspase inhibition was therefore limited to and analyzed nonparametrically using Kruskal-Wallis test at $\alpha = 0.05$. A 2-way ANOVA at $\alpha = 0.05$ and Tukey's HSD posthoc test were used to statistically determine the differences in Purkinje cell survival between genotypes and in response to caspase 3 inhibition.

RESULTS

Activation of caspase 3 corresponds with leaner Purkinje cell death

Caspase 3 is synthesized in an inactive form which must be cleaved in order to become proteolytically active (Earnshaw, et al., 1999; Hengartner, 2000). We used immunohistochemistry for activated caspase 3, which specifically recognizes the cleaved form of caspase 3, to determine if caspase 3 was specifically activated in dying leaner Purkinje cells. Representative examples of activated caspase 3 immunostaining are shown in Figure III-1 A and B. Counts of immunopositive cerebellar Purkinje cell bodies are shown in Figure III-2. The ANOVA indicated a significant activation of caspase 3 in leaner Purkinje cells ($F_{1,31} = 48.73$, $p < 0.05$) that is age dependent ($F_{2,31} = 30.65$, $p < 0.05$). At P20, prior to the onset of leaner Purkinje cell death, there was no activation of caspase 3 for either wild type or leaner Purkinje cells. However, at the peak of leaner Purkinje cell death, P40 and P50, activated caspase 3 Purkinje cells were significantly increased in leaner compared to wild type cerebella (For P40: $t_{10} = 6.83$, $p < 0.01$ and for P50: $t_{10} = -8.58$, $p < 0.01$).

The spatial pattern of caspase 3 activation in leaner cerebellar Purkinje cell at P40 and P50 was compared to that of cell death as determined by Fluoro-Jade labeling in Chapter II. Figure III-3 shows that the regional distribution of activated caspase 3 immunopositive leaner Purkinje cells mirrors that of cell death. A notable difference is seen in the magnitude of numbers of positive cells (see Figures III-2 and III-3). Many more positive Fluoro-Jade Purkinje cells were identified than activated caspase 3 positive Purkinje cells.
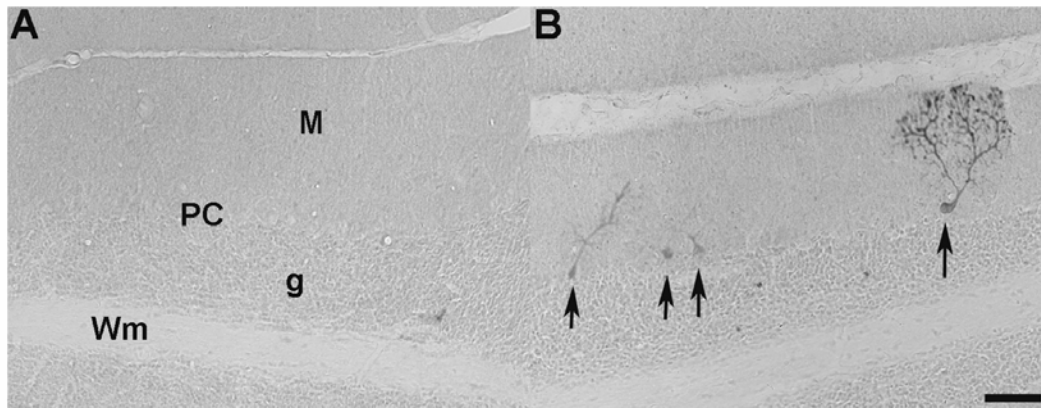
Figure III-1: Representative images of activated caspase 3 immunohistochemistry at P40. A is wild type and B is leaner. M is molecular layer, PC is Purkinje cell layer, g is granule cell layer and Wm is white matter. Arrows indicate immunopositive Purkinje cells. Scale bar in B is 100 μm.

To determine if leaner activated caspase 3 positive Purkinje cells were restricted to dying leaner Purkinje cells, serially paired coronal and frontal cerebellar sections were immunostained for activated caspase 3 or TH. TH immunostained sections were used to define parasagittal regions of surviving verses dying leaner Purkinje cells. Activated caspase 3 positive leaner Purkinje cells were identified and evaluated in reference to regions of TH labeling to determine if it was in a dying or surviving Purkinje cell parasagittal zone. Representative images of immunolabeling are shown in Figure III-4. With the exception of one Purkinje cell in each orientation, coronal and frontal, immunopositive activated caspase 3 positive Purkinje cells were restricted to the dying population of leaner Purkinje cells (Table III-1).

Activated Caspase 3
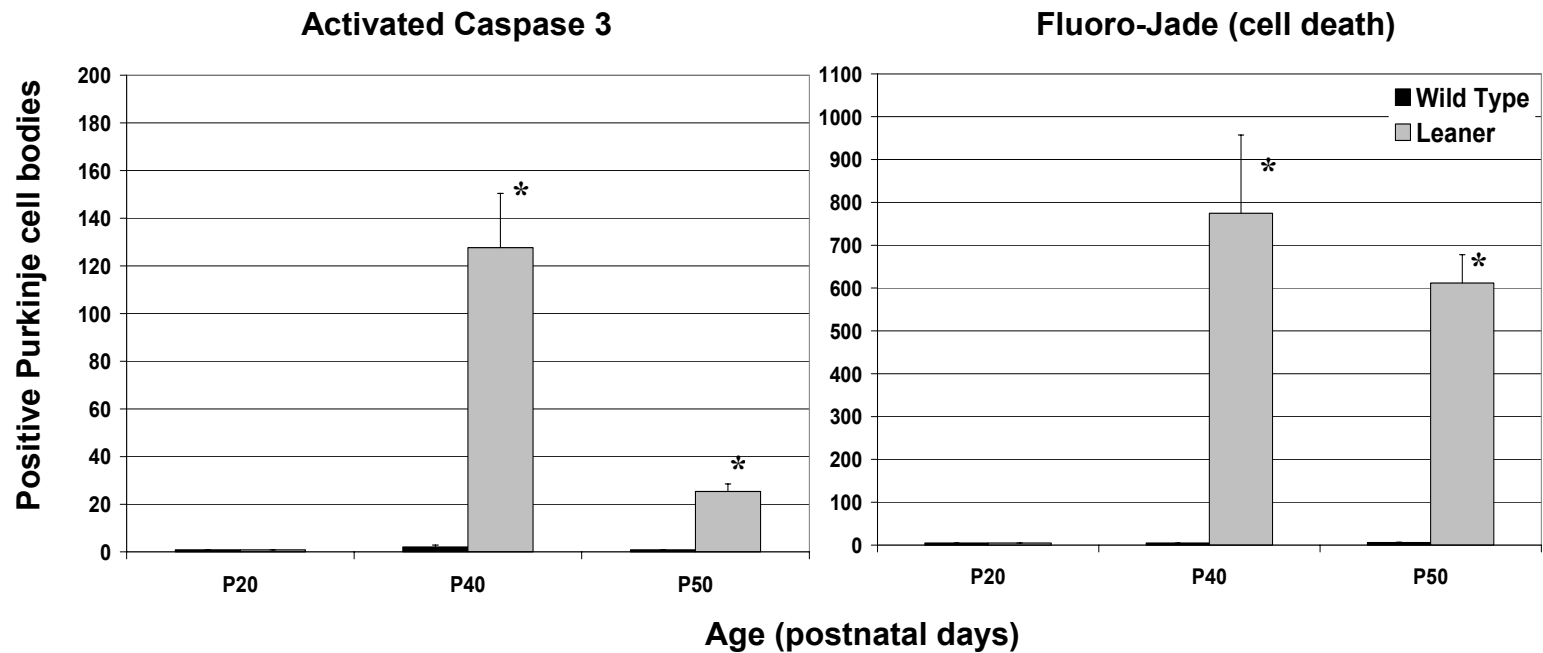
Fluoro-Jade (cell death)

Figure III-2: Quantitative evaluation of activation of caspase 3 in cerebellar Purkinje cell bodies compared to Fluoro-Jade labeled cell death in the whole cerebellum. Positive Purkinje cell bodies were counted in half the cerebellum to estimate total numbers of stained Purkinje cells per cerebellum. * represent statistically significant differences between wild type and leaner cerebella at each age group. Error bars are standard error of the mean.
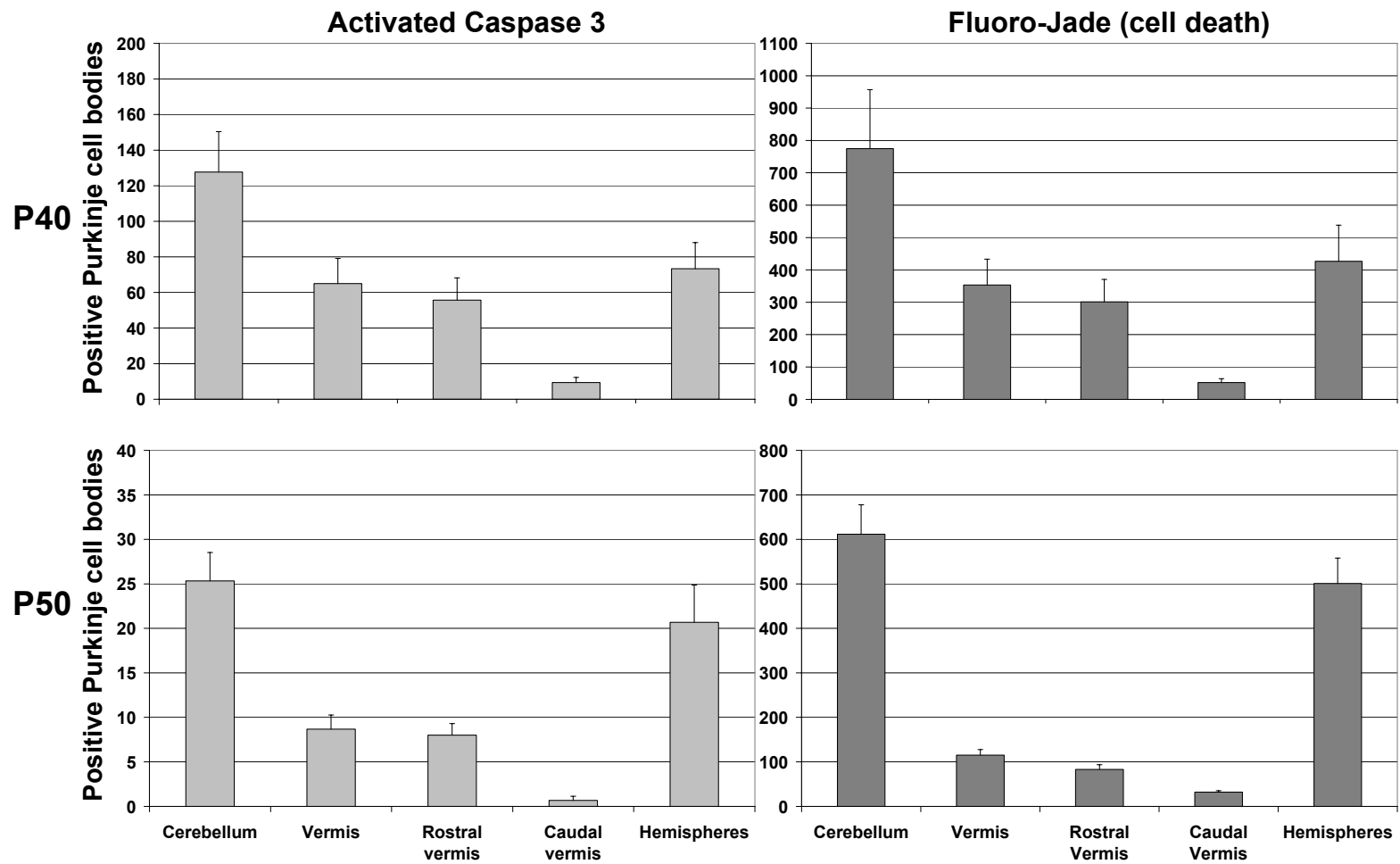
Figure III-3: Regional comparison of leaner caspase 3 activation to leaner cerebellar Purkinje cell death. The distribution of positive Purkinje cell bodies for each stain (activated caspase 3 or Fluoro-Jade) are compared by anatomical cerebellar region at P40 and P50. Error bars represent standard error of the mean.
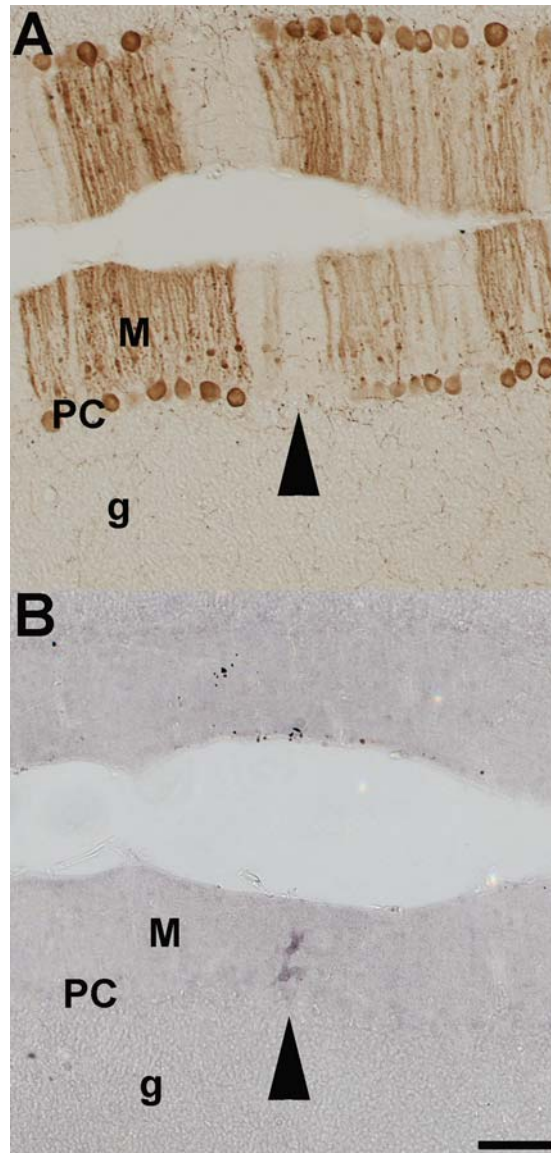
Figure III-4: Representative images of tyrosine hydroxylase (TH) and activated caspase 3 serial immunohistochemistry of leaner cerebella at P40. A is TH immunostaining and B is activated caspase 3 immunostaining. Arrow head indicates activated caspase 3 positive Purkinje cell (B) and its location within a TH negative or dying leaner Purkinje cell zone (A). M is molecular layer, PC is Purkinje cell layer, and g is granule cell layer. Scale bar in B is 100 μm.

Table III-1: Localization of activated caspase 3 positive leaner Purkinje cells relative to dying Purkinje cell zones.

Orientation (2 cerebella each)	Leaner Purkinje cell zone	
	Surviving (TH positive)	Dying (TH negative)
Coronal	1	20
Frontal	1	24

In addition to proteolytic cleavage of caspase 3, enzymatic activity of caspase 3 was confirmed with an activity assay for caspase 3 in acute slices from wild type and leaner cerebella at the peak of cell death and caspase 3 activation, P40. The activity assay used a fluorescently labeled caspase 3 specific substrate that irreversibly binds in active site of proteolytically active caspase 3. Representative images of activity assays are shown in Figure III-5. Densitometry analysis of the fluorescent intensity of Purkinje cell bodies (Figure III-6), indicated there was significantly more caspase 3 activity in leaner cerebellar Purkinje cells than wild type Purkinje cells ($t_3 = -2.92, p < 0.05$)
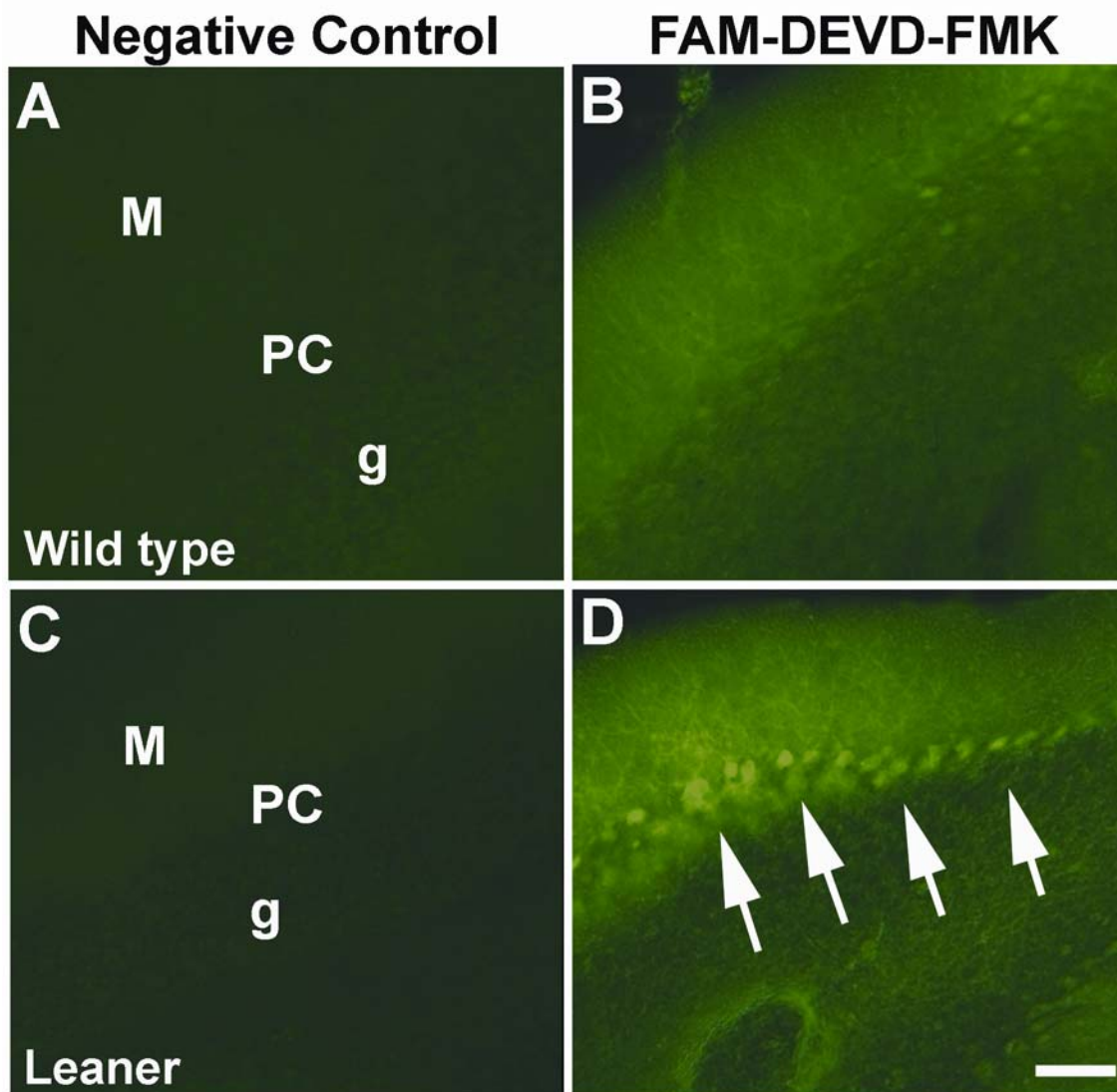
Figure III-5: Representative images of caspase 3 activity assay in acute cerebellar slices at P40. A and B are wild type slices from the same individual incubated with (FAM-DEVD-FMK) or without (negative control) fluorescently tagged irreversible caspase 3 inhibitor. C and D are leaner slices from the same individual incubated with or without the caspase 3 inhibitor. A and C are negative control slices. B and D are caspase 3 inhibitor treated slices. Arrows in D indicate labeled Purkinje cells. M is molecular layer, PC is Purkinje cell layer, and g is granule cell layer. Scale bar in D is 100 μm.
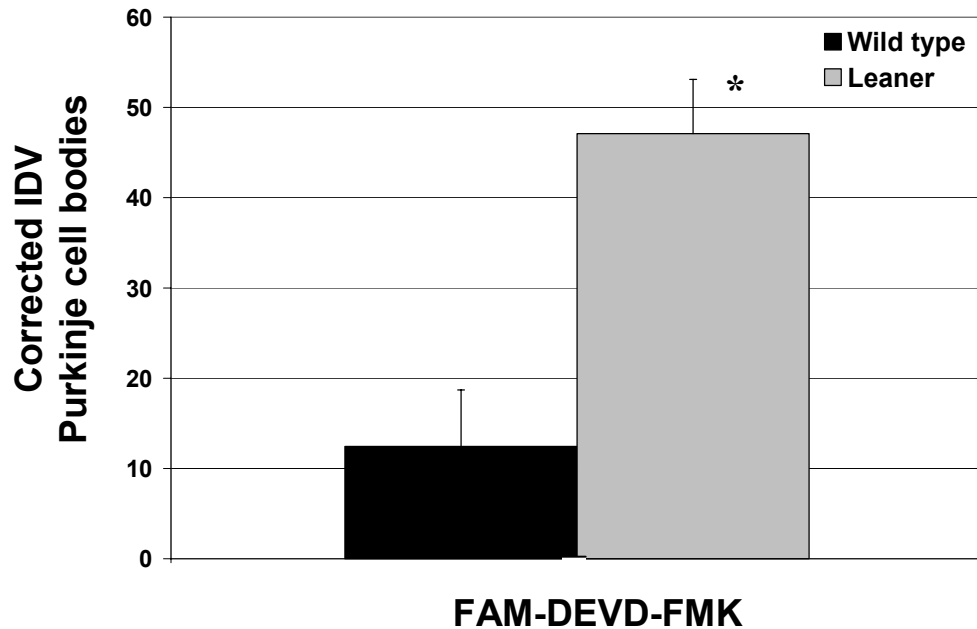
Figure III-6: Caspase 3 is active in leaner cerebellar Purkinje cells at P40. Fluorescence intensity of Purkinje cell bodies was determine by calculating an integrated density value (IDV) for fluorescence of FAM-DEVD-FMK treated slices and subtracting background or negative control fluorescence using Alpha Innotech software (corrected IDV). * indicates significant increase in leaner Purkinje caspase 3 activity. Error bars represent standard error of the mean.

Leaner Purkinje cell death partially dependent on caspase 3 activity

In vitro organotypic cerebellar cultures were used to determine the dependence of leaner cerebellar Purkinje cell death on caspase 3 activity. Cultures were established at P10 and maintained for 31 days until the peak of leaner Purkinje cell death and caspase 3 activation, equivalent of approximately P40 *in vivo*. Cerebellar morphology was evaluated with immunohistochemistry for Neu N and calbindin (Figure III-7). Calbindin

is a calcium binding protein found specifically in cerebellar Purkinje cells, while Neu N identifies the nuclei of neurons in the cerebellum excluding Purkinje cells. Together these demonstrate that basic cerebellar architecture in both leaner and wild type cerebella are maintained throughout the culture period.

Wild type and leaner organotypic cerebellar slices were placed in culture and allowed to stabilize for 10 days. Beginning on day 11, cultures were either incubated with or without a caspase 3 specific inhibitor (z-DEVD-FMK) until the approximate peak of leaner Purkinje cell death, an additional 20 days. This allowed cell death due to culture set up procedures to occur, and allowed caspase inhibition to begin prior to the onset of leaner Purkinje cell death. Sufficient inhibition of caspase 3 during the culture was confirmed using the caspase 3 activity assay (Figures III-8 and III-9). Densitometry analysis revealed, that as observed with *in vivo* acute cerebellar slices, caspase 3 activity was increased in leaner cerebellar Purkinje cells and this increase was prevented by caspase inhibition ($H_3 = 7.42$ $0.05 < p < 0.1$). While there is a noticeable decrease in fluorescence of caspase 3 inhibitor treated slices, it was not significantly different from wild type, untreated slices.
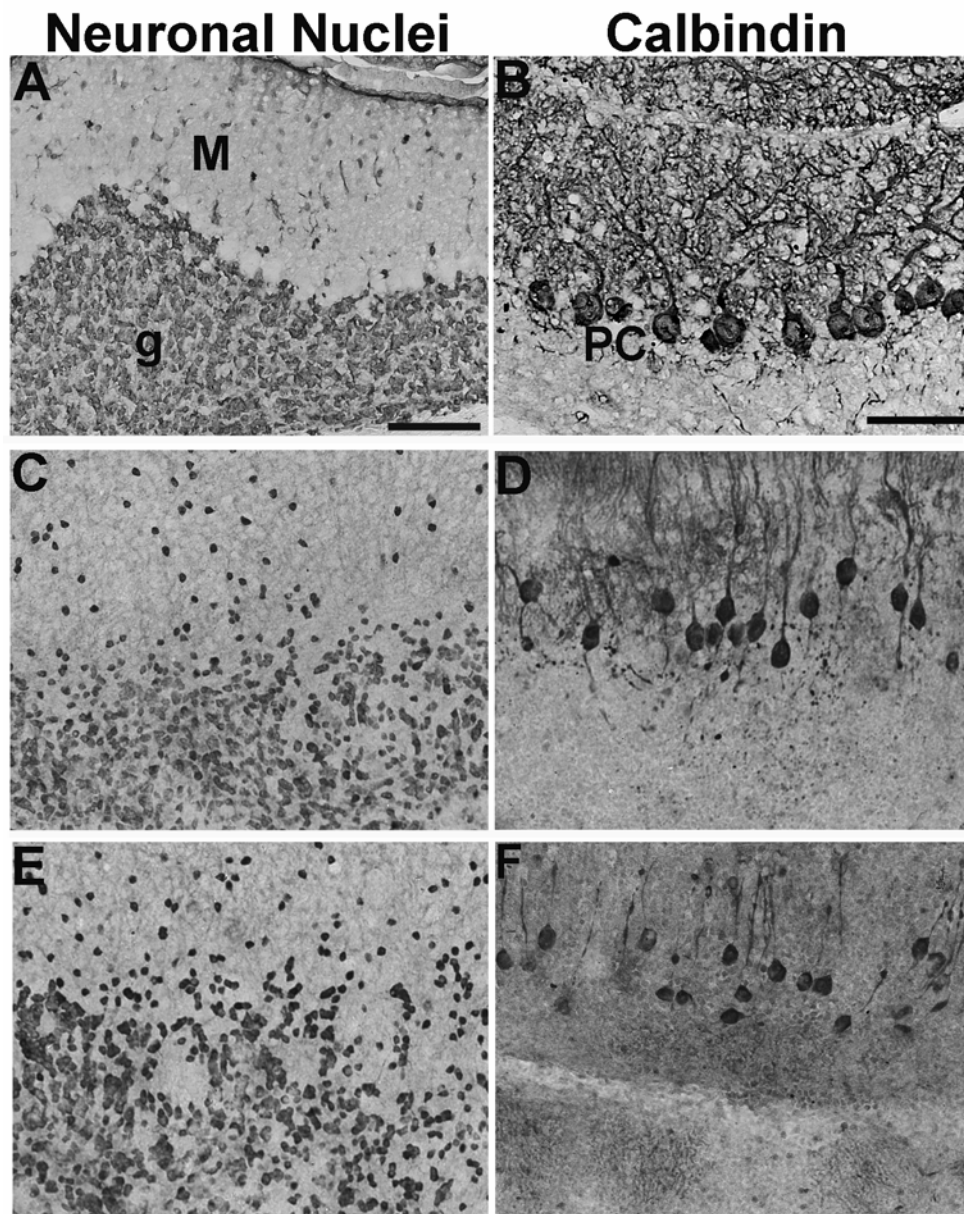
Figure III-7: Typical cerebellar morphology is maintained in long term organotypic cerebellar cultures. After 31 days in culture, slices were immunolabeled for neuronal nuclei (Neu N) to detect neurons excluding cerebellar Purkinje cells (A, C and E) or calbindin to detect Purkinje cells (B, D and F). A and B are paraformaldehyde fixed tissue positive controls. B and D are wild type cerebellar cultures. E and F are leaner cerebellar cultures. M is molecular layer, PC is Purkinje cell layer, g is granule cell layer. Scale bars in A and B are 100 μm.
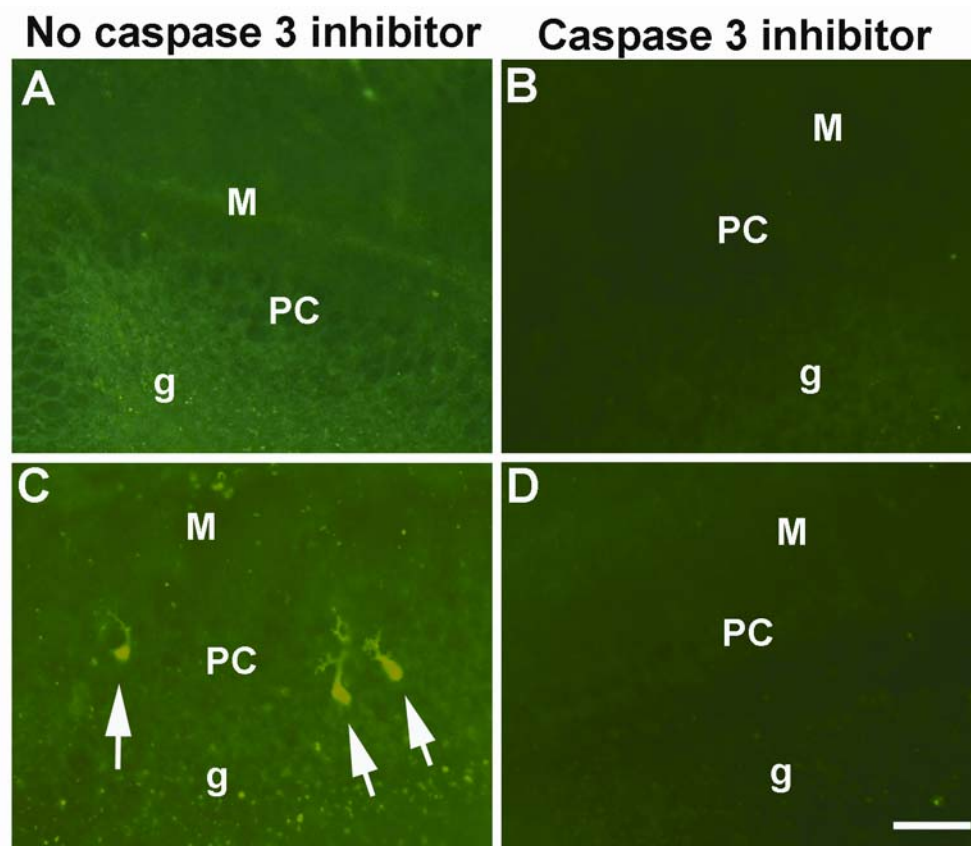
Figure III-8: Representative images of caspase activity assay in cerebellar slice cultures with and without caspase 3 inhibition. Cultured cerebellar slices were incubated with (B and D) or without (A and C) a caspase 3 specific inhibitor (z-DEVD-FMK at 50μM). A and B are wild type cerebellar slices. C and D are leaner cerebellar slices. M is molecular layer, PC is Purkinje cell layer and g is granule cell layer. Arrows in C indicated Purkinje cells with high amounts of caspase 3 activity. Scale bar in D is 100 μM.
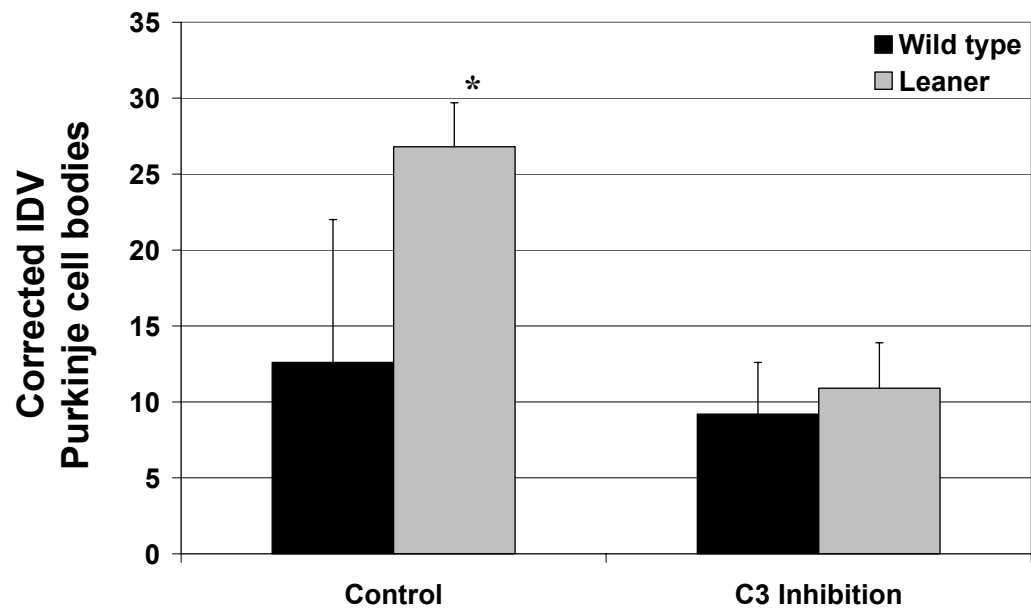
Figure III-9: Caspase 3 is active in cultured leaner cerebellar Purkinje cells and blocked by caspase 3 inhibition. Fluorescent intensity of Purkinje cell bodies was determine by calculating an integrated density value (IDV) for fluorescence of FAM-DEVD-FMK treated slices and subtracting background or negative control fluorescence using Alpha Innotech software (corrected IDV). * indicates significant increase in leaner Purkinje caspase 3 activity in untreated leaner Purkinje cells. Error bars represent standard error of the mean.

Following the activity assay, cerebellar culture were paraformaldehyde fixed and immunostained for calbindin. Calbindin positive Purkinje cell bodies were counted to evaluate Purkinje cell survival and are shown in Figure III-10. ANOVA analysis revealed a significant effect of both genotype ($F_{1,18}$ = 15.92, p < 0.05) and inhibition ($F_{1,18}$ = 11.27, p < 0.05). As expected from *in vivo* studies approximately half of cerebellar Purkinje cells were lost in the leaner cerebella compared to wild type cerebella in the absence of caspase 3 inhibitor (Tukey's HSD, p < 0.05). Inhibition of caspase 3 resulted in a significant increase in leaner Purkinje cells compared to leaner cerebella without inhibitor (Tukey's HSD, p < 0.05). In spite of caspase 3 inhibition, the number of leaner Purkinje cells was still decreased compared to wild type Purkinje cell counts in the presence of inhibitor (Tukey's HSD, p < 0.1). However, there was no significant difference between wild type cerebella without inhibitor and leaner cerebella with caspase 3 inhibition. While there was a tendency for an increase in Purkinje cell in wild type cerebella treated with the caspase 3 inhibitor, there was no significant difference in Purkinje cell survival in wild type cerebella either with or without caspase inhibitor.
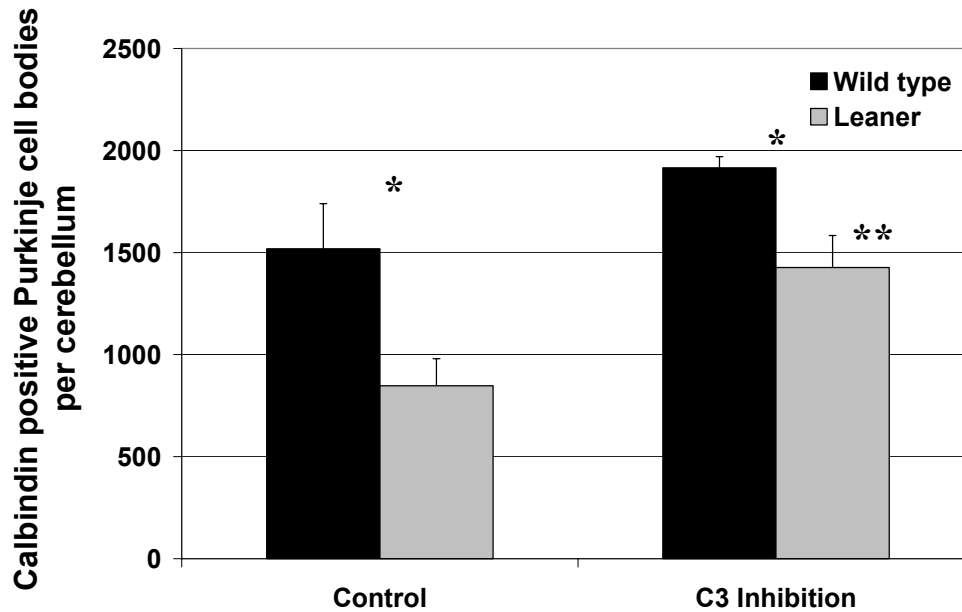
Figure III-10: Partial rescue of leaner cerebellar Purkinje cells in the presence of caspase 3 inhibition. Cultured cerebellar slices were treated with (C3 inhibition) or without (control) a caspase 3 specific inhibitor (z-DEVD-FMK). Purkinje cell survival was assessed using calbindin immunohistochemistry and counting positive Purkinje cell bodies. * indicates significant a difference between wild type and leaner cerebellar within the treatment group. ** indicates a significant increase in leaner Purkinje cells with C3 inhibition compared to untreated leaner controls. Error bars represent standard error of the mean.

DISCUSSION

This study has shown that caspase 3 is specifically cleaved and enzymatically active in leaner, but not wild type cerebellar Purkinje cells. Immunohistochemistry also showed that caspase 3 was activated in a pattern consistent with leaner Purkinje cell death. Furthermore, this activation of caspase 3 was restricted to dying parasagittal zones of leaner Purkinje cells. However, there were notably fewer activated caspase 3 positive Purkinje cells than dying Purkinje cells indicated by Fluoro-Jade.

While it is uncertain what Fluoro-Jade recognizes in dying neurons, it presumptively has a broad window of labeling activity during the process of cell death (Schmued and Hopkins, 2000). It is possible, since activation of caspase 3 is a specific point in the process of programmed cell death, that it is limited to a narrower window and would therefore identify fewer cells than Fluoro-Jade at any given time point.

Alternately, while caspase 3 is activated in at least some dying leaner Purkinje cells, it may not represent the only driving force or determining factor directing leaner Purkinje cell death. Inhibition of caspase 3 in cultured cerebellar slices supports this possibility since it was able to rescue a significant number of leaner Purkinje cells, but it was unable to completely prevent leaner Purkinje cell death. Another possibility is that cellular dysfunction of dying leaner Purkinje cells was so severe that blockade of cell death signaling pathway leads to activation of alternate pathways, which although at a decrease rate, continue to carry out the cell death program. Evidence for both possibilities exist in other cell death model systems. Knockouts (genetic deletion) of caspases does not prevent developmental normal programmed cell death during normal development of the brainstem and spinal cord (Oppenheim, et al., 2001). Oppenheim's study (2001) indicates that caspase independent mechanisms of programmed cell death exist and at least in some cases may be a cell preferred means of cell death. Studies of macroautophagic cell death have shown that while caspases activate macroautophagy in some circumstances (Canu, et al., 2005), in others they work downstream of macroautophagic induction where blockade of caspase activity does not prevent cell death (Xue, et al., 1999). In addition, the release of some mitochondrial proteins, such

as apoptosis inducing factor (AIF), are able to activate and use caspase cascades in executing cell death, yet caspase inhibition does not prevent DNA fragmentation or cell death associated with AIF release (Susin, et al., 1999; Joza, et al., 2001; Klein, et al., 2002).

The results of this study support the hypothesis that caspase 3 is specifically activated in dying leaner cerebellar Purkinje cells. The significant rescue of leaner cerebellar Purkinje cell by inhibition of caspase 3 indicates that caspases are an important factor in signaling leaner Purkinje cell death. However, caspase inhibition did not prevent all of the leaner Purkinje cell death, since there was still a significant decrease in Purkinje cell survival compared to wild type Purkinje cell counts. These results suggest the possibility that leaner cerebellar Purkinje cell death either uses, or in the face of caspase blockade, is capable of activating alternate cell death signaling pathways, which function independent of caspase activity.

CHAPTER IV

EVALUATION OF MACROAUTOPHAGY AND MITOCHONDRIA IN P/Q-TYPE VOLTAGE-GATED CALCIUM CHANNEL MUTANT MOUSE, LEANER

SUMMARY

The leaner mouse (tg^{la}/tg^{la} or cacna1a$^{\text{tg-la}}$) carries a mutation in the α_{1A} subunit of P/Q type voltage gated calcium channels. The mutation causes reduced Ca^{2+} entry into the cell and altered calcium homeostasis. One effect of the leaner mutation is an abnormal loss of cerebellar granule cells and Purkinje cells. While granule cells utilize a classic apoptotic pathway, the mechanism of leaner Purkinje cell death remains unclear. In Chapter III we demonstrated that caspase 3 is specifically activated in dying leaner Purkinje cells and the Purkinje cell death is at least partially dependent on the actions of caspase 3. In this study we have investigated macroautophagy and mitochondrial triggers of caspase activation. Monodansylcadaverine, which specifically labels autophagic vesicles, indicated there was significant increase in macroautophagy in leaner cerebellar Purkinje cells compared to wild type. There was also a significant decrease in mitochondrial membrane potential in leaner Purkinje cells compared to wild type. However, the loss of mitochondrial membrane potential did not lead to a corresponding release of cytochrome C. These finding suggests that macroautophagy may have a key role in leaner Purkinje cell death, which could activate caspase 3. While these findings do not support a mitochondrial-cytochrome C mediated activation of caspase 3 or leaner

Purkinje cell death, it does not rule out the possibility of other mitochondrial proteins contributing to either caspase 3 activation or caspase independent cell death.

INTRODUCTION

In Chapter III is was shown that caspase 3 was specifically activated in dying Purkinje cells and had a role in directing leaner cerebellar Purkinje cell death. Caspase 3 is an effector caspase responsible for proteolytic cleavage of cellular proteins during programmed cell death (Earnshaw, et al., 1999; Hengartner, 2000). There are numerous signaling pathways which are able to activate caspase 3.

Macroautophagy is able to utilize caspase activity during the process of programmed cell death (Xue, et al., 1999; Canu, et al., 2005). However, the inhibition of caspase activity in these circumstances often does not prevent programmed cell death (Xue, et al., 1999). Activated caspase 3 is also able to trigger macroautophagic cell death in a manner that can be sensitive to caspase inhibition (Canu, et al., 2005). Lysosomal proteases are associated with macroautophagy since the autophagosome must fuse with lysosomes in order to degrade its contents (Bursch, 2001; Klionsky, 2005). Increases in lysosomal proteases occur with some instances of macroautophagic cell death (Bursch, 2001; Klionsky, 2005). In addition, lysosomal proteases are able to cleave and activate caspase 3 with out triggering macroautophagic cell death (Stoka, et al., 2001; Hishita, et al., 2001). Gene array studies in the leaner mouse indicate that the lysosomal protease, cathepsin D, is increased (Nahm, 2002). The initial description of dying leaner cerebellar Purkinje cells includes many of hallmarks of macroautophagic

cell death: pyknotic nuclei were not detected, nuclear and cytoplasmic membranes become less distinct rather that blebbing or rupturing, and "the entire cell gives the impression of simply dissolving" (Herrup and Wilczynski, 1982). These findings suggest that caspase 3 activation may either be triggering macroautophagy or that macroautophagy with subsequent caspase 3 activation is responsible for leaner Purkinje cell death.

Caspase 3 can also be activated through mitochondrial mechanisms. The release of mitochondrial proteins such as cytochrome C and second mitochondrial activator or caspase (SMAC) both function through activation of caspase 3. Cytochrome C forms an apoptosome complex with caspase 9 and apoptosis associated factor (Apaf) 1, which then activates caspase 9 (Li, et al., 1997; Slee, et al., 1999). Once activated, caspase 9 then cleaves and activates caspases 3 and 7 (Li, et al., 1997; Slee, et al., 1999). Alternately SMAC acts by blocking the action of inhibitor of apoptosis protein (IAP) (Du, et al., 2000). IAPs sequester caspase 3, preventing its activation (Du, et al., 2000). Blocking IAP action increases the amount of caspase 3 available for activation during a given cell death signal. Gene array data indicate that Bcl-2 family pro-apoptotic proteins Bad and Bak are increased in the leaner cerebellum (Nahm, 2002). Other studies have shown that calcium homeostasis is disrupted in leaner Purkinje cells in a manner that likely places heavier burdens on mitochondria to buffer excess cytosolic Ca^{2+} (Dove, et al., 2000; Murchison, et al., 2002). Both increases in Bcl-2 family pro-apoptotic proteins and excessive Ca^{2+} have been shown to cause programmed cell death through the release of mitochondrial proteins (Ichas and Mazat, 1998; Berridge, et al.,

2000; Cory and Adams, 2002). These studies suggest that mitochondrial signaling may be an additional or alternate means of caspase 3 activation responsible for leaner Purkinje cell death.

The objective of this study was to investigate some of the potential triggers of caspase 3 activation. We evaluated the potential role of macroautophagy in leaner cerebellar Purkinje cells by assessing the production of autophagic vesicles. We also evaluated mitochondria in Purkinje cells to assess the likelihood of mitochondrial protein release in leaner mice.

EXPERIMENTAL PROCEDURES

Animals

Wild type and homozygous leaner mice (tg^{la}/tg^{la} or $Cacn1a^{tg-la}$), on the C57BL/6J background at P20, P40 and P50 were used. Animal breeding and handling procedures are described in Chapter II. All experimental procedures were carried out in accordance with National Institute of Health Guide for Care and Use of Laboratory Animals (NIH publication No. 85-23, revised, 1996). Minimal numbers of animals necessary for each experiment were used.

Tissue collection

For paraformaldehyde fixed and frozen brain tissue, mice were anesthetized intraperitoneally with 150 mg/kg ketamine and 15 mg/kg xylazine. Once anesthetized, the mice were perfused intracardially with 50 mL of Tyrode's Saline, followed by 400 to

500 mL of 4% paraformaldehyde in 0.12 M phosphate buffer (pH 7.4). The brains were collected, cryoprotected in 20% sucrose in 0.1M phosphate buffered saline, frozen with powdered dry ice and stored at -70°C until sectioned on a cryostat. Frozen cerebella were sectioned at 25 μm. For the experiments using fixed, frozen brains, the rostral cerebellum was defined as lobules I through V, and the caudal cerebellum was defined as lobules VI through X.

For acute cerebellar slices, mice at P40 were anesthetized with isoflurane and decapitated. The brains were aseptically removed and the cerebella were coronally sectioned at 150 μm in ice cold dissection feed containing 36mM glucose, 10mM MgCl$_2$·6H$_2$O in Gey's balanced salt solution (Sigma-Aldrich, St. Louis, MO, USA) on an Electron Microscopy Sciences (EMS) tissue slicer (OTS-4000, Hatfield, PA, USA).

Monodansylcadaverine

Acute cerebellar slices were collected from four age matched wild type and leaner pairs at P40 and assayed for macroautophagic vesicles. Recent studies have shown that monodansylcadaverine (MDC) specifically localizes to macroautophagic vesicles and has been used as a marker to evaluate the numbers of these vesicles produced during macroautophagic mediated programmed cell death (Biederbick, et al., 1995; Munafo and Colombo, 2001). Monodansylcadaverine (Sigma-Aldrich, St. Louis, MO, USA) was mixed with dissection feed for a working concentration of 25 μM and prewarmed in a 37°C water bath. Slices from each cerebellum were divided into two groups: negative control (feed without MDC) and MDC treated. Slices were incubated

in control or 25 μM MDC media for 30 minutes at 37°C, 5% CO_2 humid incubator. Incubation was terminated with two, 10 minutes washes in dissection feed at 37°C, 5% CO_2. Slices were fixed in 4% paraformaldehyde in 0.12 M phosphate buffer (pH 7.4) for 24 – 48 hours, washed in 0.1 M phosphate buffered saline, mounted on plain glass slides and coverslipped with anti-fade mounting medium (Molecular Probes, Eugene, OR, USA). Slices were imaged using a DAPI Filter (MDC excitation 340-380 nm, emission 508 nm) on a Zeiss Axioplan 2 research microscope (Plan-NEOFLUAR 16X, 0.50 numerical aperture oil objective) and a Zeiss color Axiocam HRC digitial camera (acquisition software Axiovision 4.2). The same exposure was maintained for controls and treated slices within each cerebellar pair. MDC fluorescence intensity was determined by calculating an integrated density value (IDV) using Alpha Innotech AlphaEase 3.1 software for each mouse, by subtracting background fluorescence (negative control) from MDC treated fluorescence of cerebellar Purkinje cell bodies using. A minimum of three treated and two control slices were imaged. A one-tail paired t test at $\alpha = 0.05$ was used to statistically determine if leaner cerebellar Purkinje cells had increased MDC uptake compared to wild type.

Mitochondrial membrane potential

Acute cerebellar slices were collected from four age matched wild type and leaner pairs at P40 and assayed for mitochondrial membrane potential ($\Delta\Psi_m$). MitoTracker Red CM-H_2XRos (Molecular Probes, Eugene, OR, USA) was used to measure $\Delta\Psi_m$. Mitochondrial uptake of MitoTracker Red is dependent on the $\Delta\Psi_m$, with

decreased fluorescence of MitoTracker Red associated with decreased $\Delta\Psi_m$. The product instructions for labeling adherent cells was adapted for labeling acute cerebellar slices. 50 µg of MitoTracker Red was dissolved in 100 µL of sterile DMSO (Sigma-Aldrich, St. Louis, MO, USA) for a 10 mM concentration. MitoTracker Red was then diluted to a working concentration of 25 nM in dissection feed. Slices from each cerebella were divided into two groups: negative control (feed without MitoTracker Red) and MitoTracker Red treated. Slices were incubated in control or 25 nM MitoTracker Red media for 30 minutes at 37°C, 5% CO_2 humid incubator. Incubation was terminated with two, 10 minutes washes in dissection feed at 37°C, 5% CO_2. Slices were fixed in 4% paraformaldehyde in 0.12 M phosphate buffer (pH 7.4) for 24 – 48 hours, washed in 0.1 M phosphate buffered saline, mounted on plain glass slides and coverslipped with anti-fade mounting medium (Molecular Probes, Eugene, OR, USA). Slices were imaged on a Zeiss Axioplan 2 research microscope (Plan-APOCHROMAT 10X, 0.45 numerical aperture objective) and a Zeiss color Axiocam HRC digitial camera (acquisition software Axiovision 4.2) using a Texas Red Filter (MitoTracker Red excitation 579 nm, emission 599 nm) and maintaining exposure for controls and treated slices within each cerebellar pair. MitoTracker Red fluorescent intensity was determined by calculating an integrated density value (IDV) using Alpha Innotech AlphaEase 3.1 software for each mouse, subtracting background fluorescence (negative control) from MitoTracker Red treated fluorescence of cerebellar Purkinje cell bodies. A minimum of three treated and two control sections with at least 10 Purkinje bodies per image were evaluated for each

cerebellum. A one-tail paired *t* test at $\alpha = 0.05$ was used to statistically determine if leaner cerebellar Purkinje cells had lower $\Delta\Psi_m$ than wild type Purkinje cell bodies.

Cytochrome C immunohistochemistry

Immunohistochemistry (IHC) was performed as described in Chapter II (Abbott and Jacobowitz, 1995). Cytochrome C IHC used an affinity purified monoclonal mouse antibody at 1:4,000 dilution (BD PharMingen, San Diego, CA, USA). For Cytochrome C IHC blocking was done with horse serum and the secondary antibody was rat absorbed biotinylated horse antimouse (Vector, Burlingame, CA, USA).

Four leaner and four wild type mice were used in each age group P20, P40 and P50. Whole cerebella were serially sectioned in a sagittal orientation. Every fifth section was immunostained for cytochrome C. Purkinje cell bodies in each stained section were evaluated blinded to genotype for cytochrome C localization. Mitochondrial cytochrome C produced a punctate staining pattern while cytosolic cytochrome C produces diffuse staining throughout the cell body. 2-way ANOVA was used to evaluate differences due to genotype and age.

RESULTS

Macroautophagy

Monodansylcadaverine (MDC) is specifically sequestered in autophagic vesicles. Previous studies have demonstrated its localization to autophagic vesicles through electron microscopy (Biederbick, et al., 1995; Munafo and Colombo, 2001). In addition,

it has been shown that MDC is not incorporated into nonautophagic vesicles or lysosomes (Biederbick, et al., 1995). Increased MDC uptake is associated with increase numbers of autophagic vesicles produced during macroautophagy (Biederbick, et al., 1995). Representative images of MDC labeling in acute cerebellar slices are shown in Figure IV-1. Densitometry of MDC fluorescence of cerebellar Purkinje cell bodies is shown in Figure IV-2. There was a significant increase in MDC uptake in leaner cerebellar Purkinje cell bodies ($t_3 = 4.01$, $p = 0.01$).
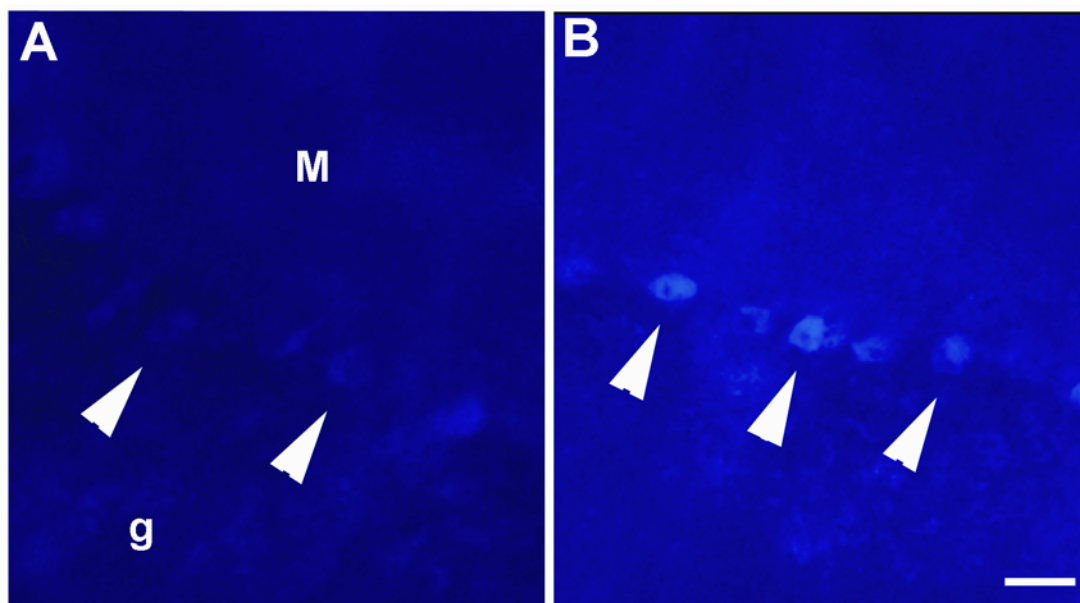

Figure IV-1: Representative images of monodansylcadaverine (MDC) labeling in acute cerebellar slices at P40. A is a wild type cerebellar slice. B is a leaner cerebellar slice. Arrows indicate Purkinje cell bodies. M is molecular layer and g is granule cell layer. Scale bar in B is 50 μm.
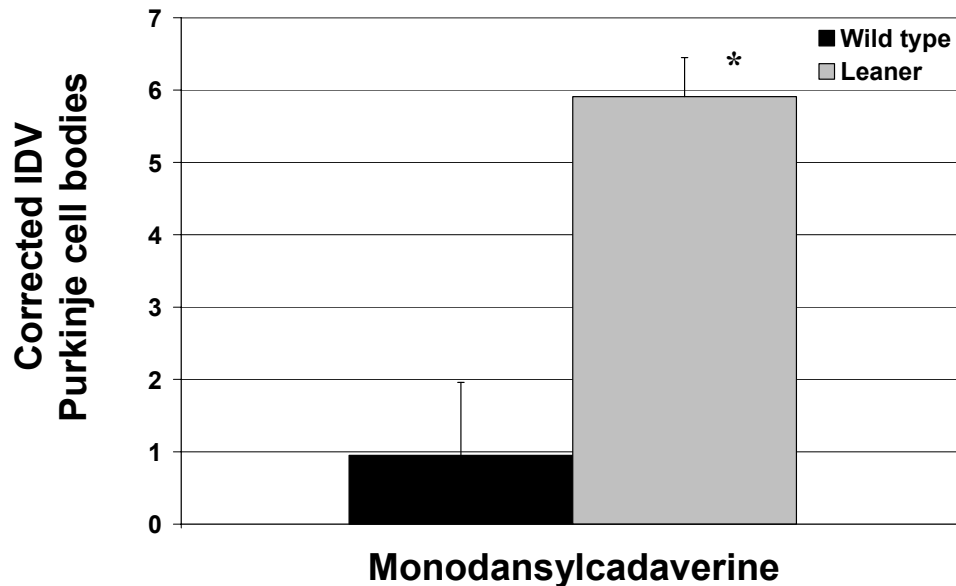
Figure IV-2: Monodansylcadaverine (MDC) labeling is increased in leaner cerebellar Purkinje cells at P40. Fluorescent intensity of Purkinje cell bodies was determine by calculating an integrated density value (IDV) for fluorescence of MDC in treated slices and subtracting background or negative control fluorescence using Alpha Innotech software (corrected IDV). Error bars are standard error of the mean. * indicates a significant increase in MDC staining in leaner Purkinje cell bodies compared to wild type.

Mitochondrial mediated activation of cell death

A common feature of mitochondrial mediated programmed cell death is a loss of mitochondrial membrane potential associated with the induction of the mitochondrial permeability transition pore or pore formation associated with oligomerization of Bcl-2 proteins Bax or Bak. MitoTracker Red CM-H_2XRos is a plasma membrane permeable, mitochondrial selective probe that is concentrated by actively respiring mitochondria and retained within the mitochondria following fixation (Deshmukh, et al., 2000;

Strahlendorf, et al., 2003). This mitochondrial probe was used to assess the mitochondrial membrane potential in leaner and wild type cerebellar Purkinje cell bodies from acute cerebellar slices (Figure IV-3). Densitometry analysis of fluorescent intensity of cerebellar Purkinje cell bodies is shown in Figure IV-4. There was a significant decrease in MitoTracker Red staining in leaner cerebellar Purkinje cell bodies compared to wild type Purkinje cell bodies ($t_3 = 2.89$, $p < 0.05$), indicating a decrease in mitochondrial membrane potential in leaner cerebellar Purkinje cells compared to wild type Purkinje cells.
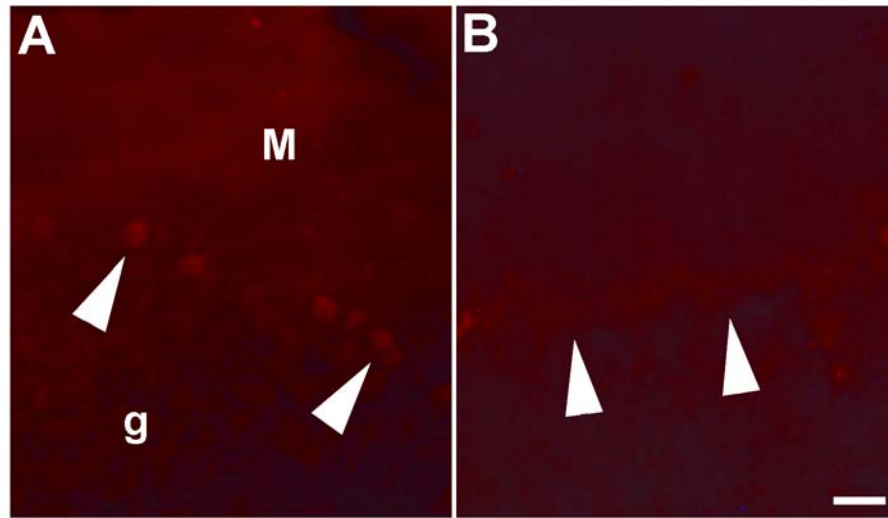

Figure IV-3: Representative images of MitoTracker Red staining of acute cerebellar slices at P40. Wild type (A) and leaner (B) acute cerebellar slices at P40 are labeled with MitoTracker Red. M is molecular layer and g is granule cell layer. Arrows indicate Purkinje cell bodies. Scale bar in B is 50 μm.
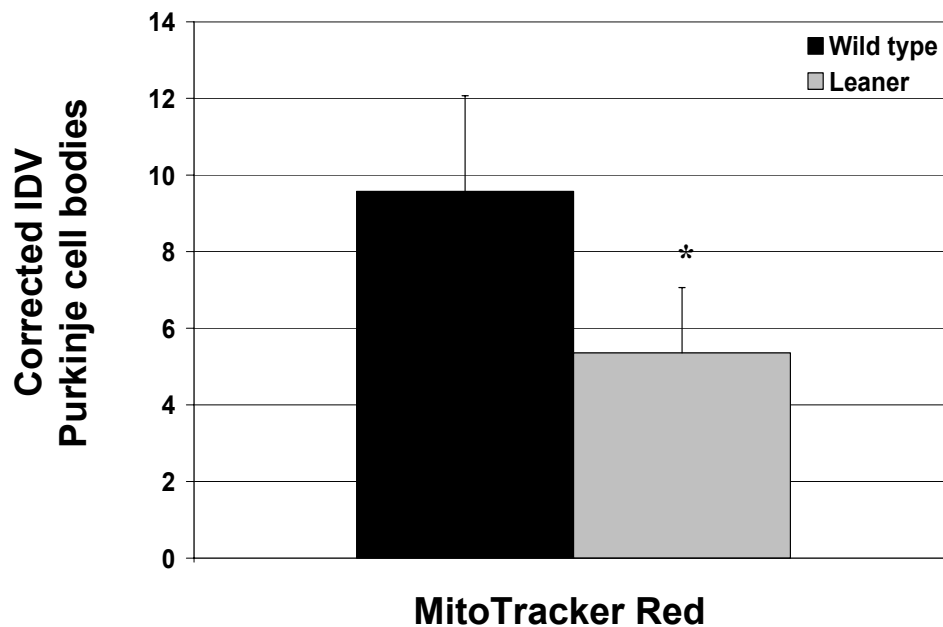
Figure IV-4: MitoTracker Red staining is decreased in leaner cerebellar Purkinje cell bodies at P40. Fluorescent intensity of Purkinje cell bodies was determine by calculating an integrated density value (IDV) for fluorescence of MitoTracker Red in treated slices and subtracting background or negative control fluorescence using Alpha Innotech software (corrected IDV). Error bars are standard error of the mean. * indicates a significant decrease in leaner Purkinje cell bodies compared to wild type.

Loss of mitochondrial membrane potential in mitochondrial mediated programmed cell death leads to a release of mitochondrial proteins, which then activate downstream cell death signaling pathways (Green and Reed, 1998; Green, 2005). Cytochrome C is a mitochondrial protein normally involved in oxidative phosphorylation, which is often released during apoptotic cell death (Liu, et al., 1996; Hao, et al., 2005). Following an appropriate signal, the mitochondria are able to release cytochrome C and subsequently trigger caspase 3 activation to induce programmed cell death. We used immunohistochemistry for cytochrome C at P20, P40 and P50 to

determine if the loss of mitochondrial membrane potential in leaner cerebellar Purkinje cells seen at P40 was associated with cytosolic cytochrome C release in a pattern consistent with caspase 3 activation and Purkinje cell death.

Cytosolic cytochrome C was defined as diffuse staining of cerebellar Purkinje cell bodies, while mitochondrial cytochrome C staining was restricted to a punctate pattern (Figure IV-5). Estimated numbers cerebellar Purkinje cells per whole cerebellum with cytosolic cytochrome C in comparison to activation of caspase 3 are shown in Figure IV-6. While cytosolic cytochrome C can be detected, cytochrome C release was not significantly different between wild type and leaner in cerebellar Purkinje cells. Furthermore, it did not correspond with the pattern of leaner Purkinje cell death or caspase 3 activation (Figure IV-7). The estimated numbers of leaner cerebellar Purkinje cells with cytosolic cytochrome C release were much lower than those observed for both Fluoro-Jade labeled cell death and for caspase 3 activation. In addition, at P20, prior to the onset of leaner Purkinje cell death and caspase 3 activation, several leaner Purkinje cells were observed with distinct cytosolic cytochrome C staining patterns. This age group also had more Purkinje cells with cytosolic cytochrome C staining pattern than were found at P40 and P50, which are the peak times of leaner Purkinje cell death and caspase 3 activation. It should also be noted that cytosolic cytochrome C release was not detected in two leaner cerebella and was found in less than an estimated 10 Purkinje cells in another two leaner cerebella at P50, which is one of the peak ages of Purkinje cell death. And lastly, it should be also be noted that in the leaner cerebella examined at P40, the peak of both caspase 3 activation and Purkinje cell death, one

leaner cerebellum had an estimated total of only 10 Purkinje cells with cytosolic cytochrome C detected.
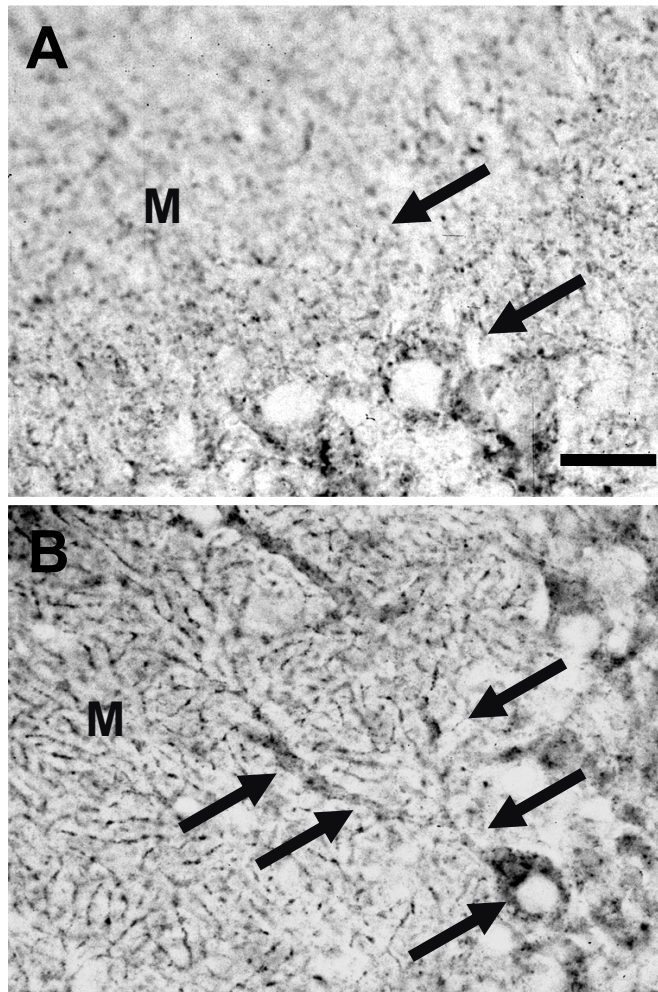
Figure IV-5: Representative examples of punctate verses diffuse staining for cytochrome C. Wild type (A) and leaner (B) cerebella at P40 immunostained for cytochrome C. Arrows indicate Purkinje cell body and dendrites. Staining in A is punctate indicating containment within mitochondria, while staining in B is diffuse indicating cytosolic release. M is molecular layer. Scale bar in A is 25 μm.
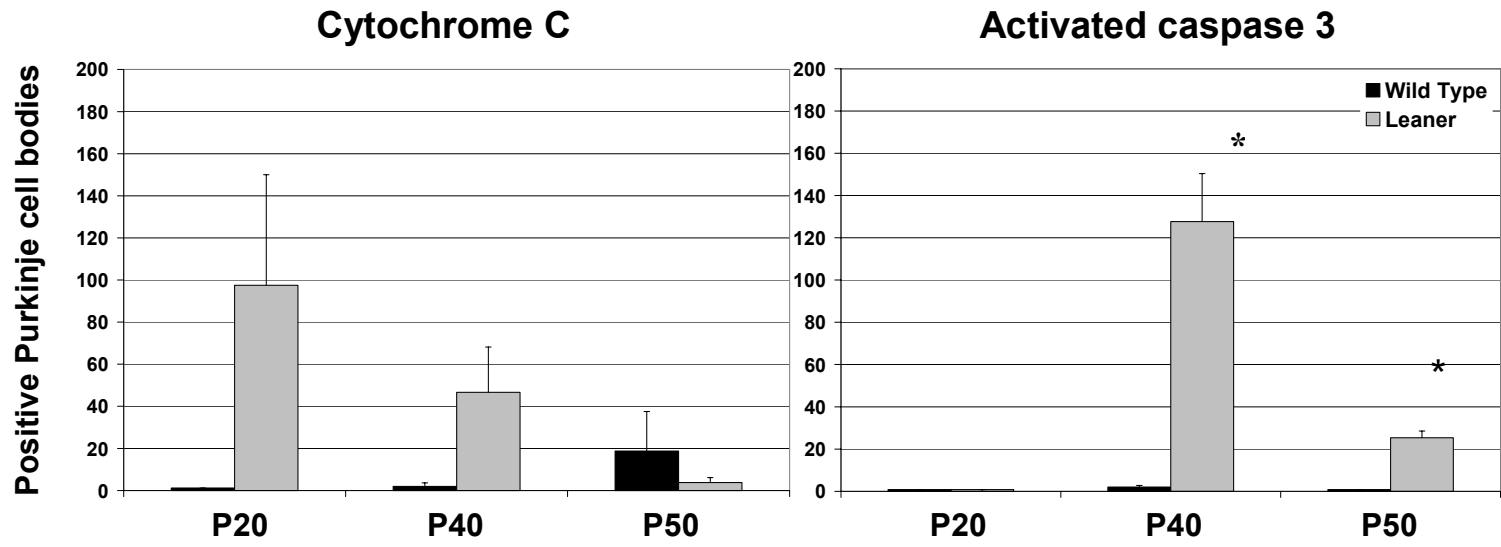
Figure IV-6: Quantitative evaluation of cytochrome C cytosolic release in cerebellar Purkinje cell bodies compared to activation of caspase 3 in the whole cerebellum. Positive Purkinje cell bodies were counted and estimated numbers per whole cerebellum were determined. * represents statistically significant differences. Error bars are standard error of the mean.
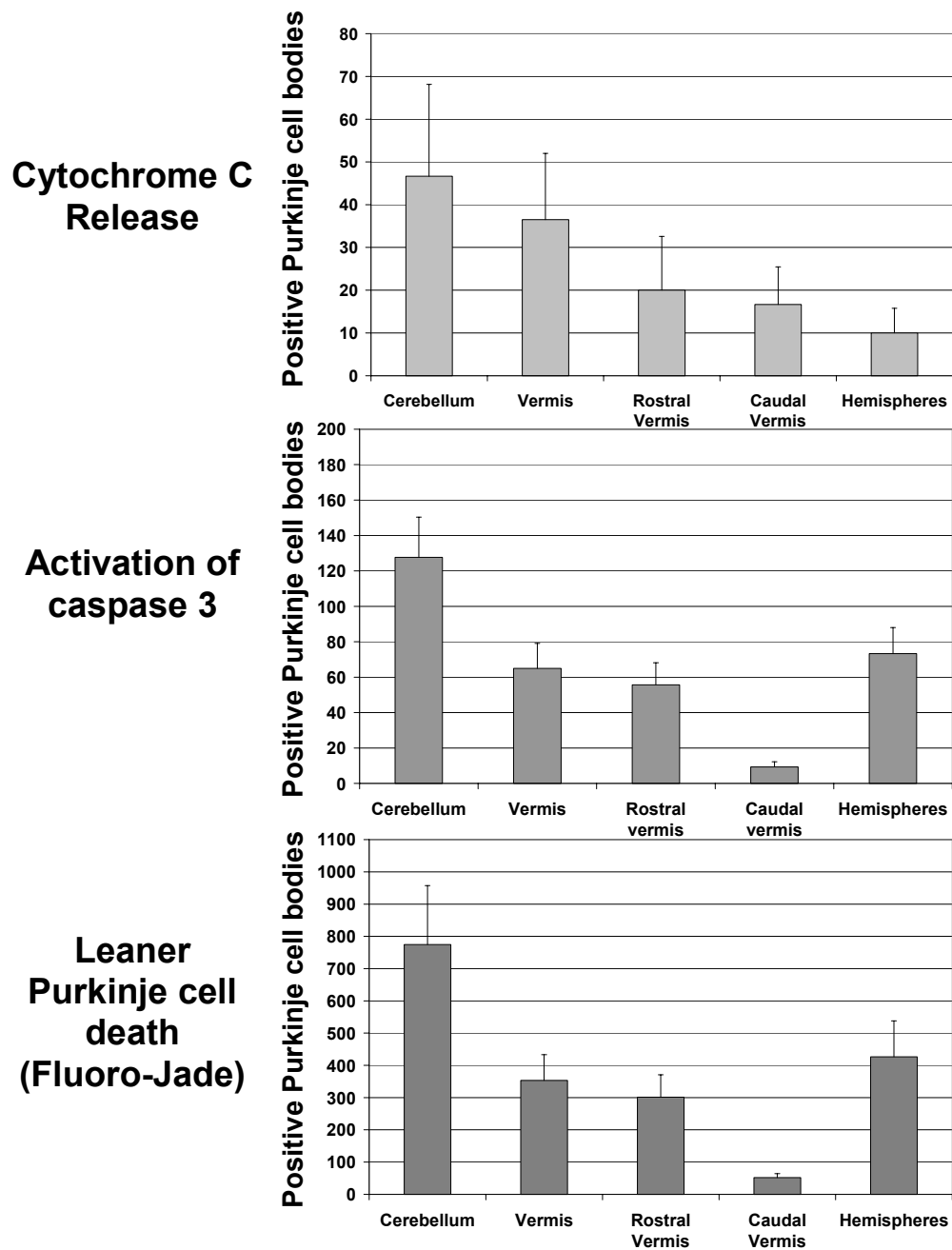
Figure IV-7: Regional comparison of leaner cytosolic release of cytochrome C to activated caspase 3 and Fluoro-Jade labeled cell death at P40. Estimated total numbers of positive Purkinje cell bodies per cerebellum for each stain by anatomical cerebellar region.

DISCUSSION

These results demonstrate that both mitochondrial mediated and macroautophagy mediated mechanisms could be responsible for leaner cerebellar Purkinje cell death and caspase 3 activation. The increase in MDC staining in leaner cerebellar Purkinje cells indicated a marked increase in autophagosome production, which is a hallmark of macroautophagic cell death. Alternately, the loss of $\Delta\Psi_m$ indicated that it is also possible that mitochondrial proteins responsible for activating programmed cell death could be released into the cytosol.

Morphologic descriptions of dying leaner Purkinje cells are more closely associated with macroautophagic cell death pathways than apoptotic pathways. Dying leaner Purkinje cells lack overt DNA fragmentation, pyknotic nuclei, cytoplasmic condensation and membrane blebbing typical of apoptosis (Herrup and Wilczynski, 1982). They instead lose cytoplasmic density, typical of macroautophagy (Herrup and Wilczynski, 1982). MDC is highly specific for labeling autophagosomes and it is excluded from lysosomes and other vesicles (Biederbick, et al., 1995; Munafo and Colombo, 2001). Its increase in leaner cerebellar Purkinje cells strongly supports the activation or induction of macroautophagy during leaner cerebellar Purkinje cell death.

A loss of $\Delta\Psi_m$ is indicative of opening of the permeability transition pore or oligomerization and pore formation induced by Bax or Bak, which can lead to cytosolic release of mitochondrial proteins and subsequent cell death (Desagher, et al., 1999; Eskes, et al., 2000; Letai, et al., 2002). The loss of $\Delta\Psi_m$ observed in leaner cerebellar Purkinje cells must be considered carefully. The method of analysis was densitometry

of whole Purkinje cell bodies. If macroautophagy is indeed the primary mechanism of leaner Purkinje cell death, then it is possible that mitochondrial numbers are decreased in leaner Purkinje cells compared to wild type Purkinje cells (Bursch, 2001). This could confound the measurement of $\Delta\Psi_m$, with our result actually reflecting a loss of mitochondria rather than a loss of $\Delta\Psi_m$ within mitochondria. Alternately, because of the profound changes in Ca^{2+} homeostasis and buffering the loss of $\Delta\Psi_m$ may reflect a lower resting membrane potential rather than pore opening or pore formation with a release of mitochondrial proteins (Duchen, 1999; Dove, et al., 2000; Murchison, et al., 2002). Both of these possibilities are supported by the cytochrome C IHC analysis which showed cytochrome C release in a pattern inconsistent with leaner cerebellar Purkinje cell death and not significantly different from wild type.

However, mitochondria are capable of being selective in protein release. It has been show that SMAC can be released without cytochrome C, resulting in caspase 3 activation (Deng, et al., 2003). Apoptosis inducing factor (AIF) can be also be specifically released from mitochondria (Wang, et al., 2004). AIF's primary function is to translocate to the nucleus and activate endonucleases (Yuan, et al., 2003). However, secondary and downstream of these events, AIF is also able to activate caspase 3 to perpetuate the programmed cell death cycle (Susin, et al., 1999; Joza, et al., 2001; Klein, et al., 2002). So, the possibility of mitochondrial proteins other than cytochrome C contributing to leaner cell death cannot be ruled out.

This study demonstrates that cytosolic release of the mitochondrial protein cytochrome C does not have a significant role in direct leaner Purkinje cell death. This

study does however, support the hypothesis that macroautophagy is activated leaner Purkinje cells. While we have shown a decrease in mitochondrial membrane potential in leaner cerebellar Purkinje cells, the significance of this finding remains to be determined.

CHAPTER V

CONCLUSIONS

SUMMARY AND CONCLUSIONS

The leaner mouse is a neurologic mutant mouse that carries a mutation in the pore forming (α_{1A}) subunit of P/Q-type voltage-gated calcium channels (Fletcher, et al., 1996; Doyle, et al., 1997). Phenotypically the leaner mouse exhibits a severe cerebellar ataxia, absence seizures and paroxysmal dyskinesia (Sidman, et al., 1965). Because P/Q-type VGCCs are highly expressed in the cerebellum (Stea, et al., 1994), many of the behavioral and morphological abnormalities due to the leaner mutation are also concentrated in the cerebellum or are associated with cerebellar function. The primary effect of the leaner mutation of P/Q-type calcium channels is decreased calcium current (Dove, et al., 1998; Lorenzon, et al., 1998; Wakamori, et al., 1998). In cerebellar Purkinje cells this is accompanied by compensatory responses including decreased concentrations of calcium binding proteins and altered calcium buffering at the ER and mitochondria that allow leaner Purkinje cells to maintain normal resting Ca^{2+} concentration (Dove, et al., 2000; Murchison, et al., 2002). However, because of these changes, upon depolarization and activation of P/Q-type VGCCs, the nature of Ca^{2+} signaling is altered due to a lack of Ca^{2+} buffering capacity. Changes in Ca^{2+} signaling affect many additional cellular functions, the most notable of which is patterned neurodegeneration of cerebellar Purkinje cells.

Cerebellar neurodegeneration is a common feature in human mutations of the P/Q-type VGCC, including Familial hemiplegic migraine, episodic ataxia type 2 and spinocerebellar ataxia type 6 (Pietrobon, 2002). Cerebellar atrophy in these human diseases occurs in a pattern that is similar to that of the leaner mouse, making the leaner mouse an important model to investigate the causes of neurodegeneration secondary to P/Q-type VGCC mutations (Pietrobon, 2002). In addition to helping us understand the functions of P/Q-type VGCCs in these diseases, the leaner mouse is also an important model for investigating the functions of compartmentalization in the cerebellum (Herrup and Kuemerle, 1997). The leaner mutation is uniformly expressed throughout the cerebellum (Wakamori, et al., 1998; Lau, et al., 1998). However, Purkinje cell death is restricted to known parasagittal divisions of the cerebellum (Heckroth and Abbott, 1994). As we begin to understand the complex signaling mechanisms involved in directing leaner Purkinje cell death the nature of the fundamental difference between surviving and dying leaner Purkinje cells will also be elucidated. This will provide input to a variety of cerebellar disorders, regardless of cause, that result in patterned neurodegeneration or dysfunction.

This dissertation focused on identifying which of the main components of cell death signal pathways were activated in leaner cerebellar Purkinje cells. In order to accomplish this, we expanded on previous work by Herrup and Wilczynski (1982) by more precisely defining the timing of leaner cerebellar Purkinje cell death (Chapter II). We then used this information to investigate potential cell death signaling pathways. Previous studies of the leaner cerebellum suggested multiple cell signaling pathways,

which could lead to programmed cell death. The second part of this dissertation was to investigate the fundamental question of the role of caspase proteases in leaner cerebellar Purkinje cell death (Chapter III). This was followed up by investigating two potential activators of caspase activity; mitochondrial signaling and macroautophagy (Chapter IV). The results are summarized in Figure V-1.
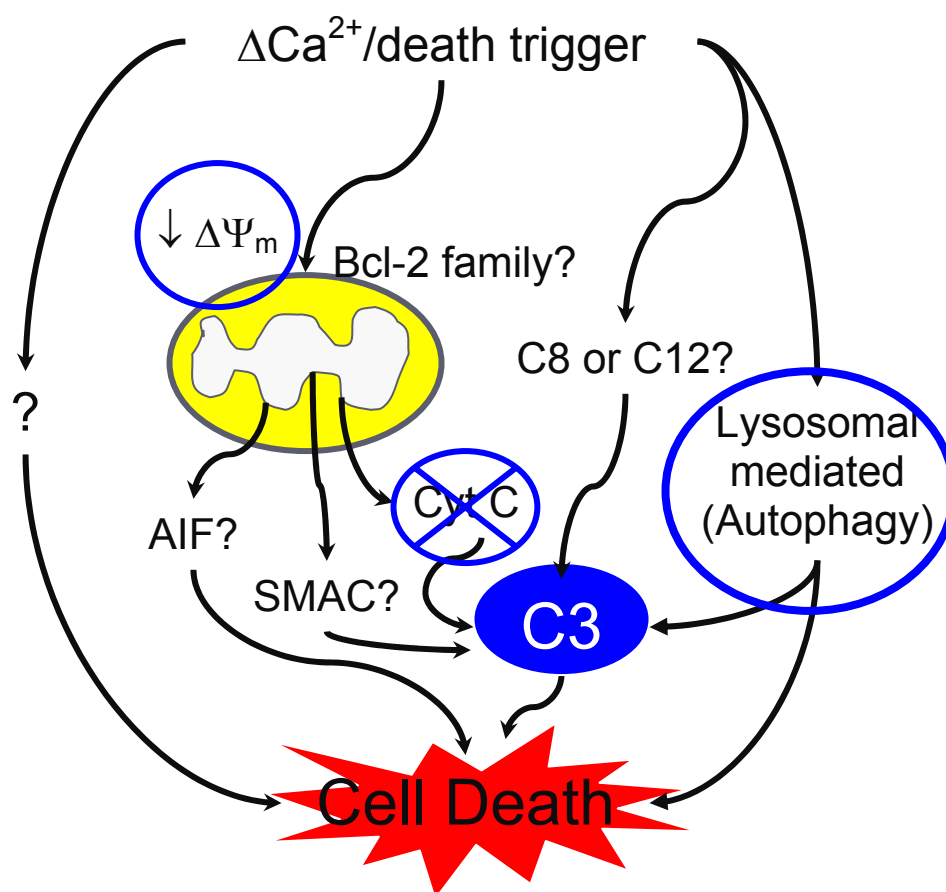

Figure V-1: Possible mechanism(s) of leaner cerebellar Purkinje cell death. Circle indicates possible mechanism. Filled circle indicated confirmed mechanism. Crossed circle indicates rejected mechanism. C is caspase, Cyt C is cytochrome C, and ΔCa^{2+} is change in Ca^{2+} due to the leaner mutation.

Using the mechanism-independent cell death stain Fluoro-Jade, we determined that leaner cerebellar Purkinje cell death was initiated at approximately P25 and peaked between P40 and P50. In addition it was shown that Purkinje cell death occurred earlier in the vermis than the hemispheres. Focusing on key time points, we investigated the activation of caspase 3. Our results showed that prior to leaner Purkinje cell death (P20) there was no activation of caspase 3, while at the peak of Purkinje cell death there was significant caspase 3 activation. Further examination showed this activation of caspase 3 was restricted to dying leaner Purkinje cell parasagittal zones, and that inhibition of caspase 3 could rescue a significant number of leaner cerebellar Purkinje cells. These finding suggest that while caspases are activated in leaner Purkinje cell death either they are working in conjunction with alternate cell death signaling pathways or their blockade results in cell death that uses other pathways.

Macroautophagy has been shown to utilize caspases in signaling programmed cell death and it is able to function independent of caspases (Xue, et al., 1999; Canu, et al., 2005). Using the autophagic vesicle specific marker, monodansylcadaverine (MDC), to assess macroautophagy induction we showed that there was a significant increase in autophagic vesicles in leaner cerebellar Purkinje cells. We also investigated mitochondrial membrane potential ($\Delta\Psi_m$), since the loss of $\Delta\Psi_m$ is a hallmark event preceding the cytosolic release of mitochondrial proteins which can subsequently trigger cell death. While our data demonstrated a significant decrease in $\Delta\Psi_m$ in leaner Purkinje cells, this did not correspond with cytosolic release of cytochrome C.

FUTURE DIRECTIONS

There are several questions about the main cell death signaling pathways directing leaner cerebellar Purkinje cell death that remain to be answered. While the activation of caspase 3 indicates that caspases are involved in leaner Purkinje cell death, it is still unclear how caspase 3 was activated. Caspase 3 has several potential activators not investigated in this study. These include proteins such as lysosomal proteases (Hishita, et al., 2001), the mitochondrial protein SMAC (Deng, et al., 2003), and the ER associated caspase, caspase 12, which can be activated by changes in ER Ca^{2+} load (Hitomi, et al., 2004). Furthermore, since caspase 3 inhibition failed to completely prevent leaner Purkinje cell death, caspase independent means of cell death should also be considered. Caspase independent pathways, such as cytosolic release of the mitochondrial protein AIF may be acting in conjunction with caspase mediated pathways or may be triggered in response to caspase blockade (Susin, et al., 1999; Joza, et al., 2001; Wang, et al., 2004).

We presented evidence of macroautophagy mediated programmed cell death in leaner Purkinje cells. This evidence should be corroborated with electron microscopic identification of autophagosomes in leaner cerebellar Purkinje cells. Once confirmed, future work can investigate the dependence of leaner Purkinje cell death on macroautophagy and how it relates to the activation of caspase 3 in dying leaner Purkinje cells.

Our studies also indicated a decrease in mitochondrial membrane potential at the peak of leaner Purkinje cell death and caspase activation, but which did not correspond

with cytosolic release of cytochrome C. There are several possibilities which should be investigated to clarify this finding. Macroautophagy is associated with a decrease in the number of mitochondria. And, if macroautophagy is activated in leaner Purkinje cells, it is possible that the decreased $\Delta\Psi_m$ actually reflects decreased numbers of normal mitochondria. It is also possible that the decreased $\Delta\Psi_m$ represents a decreased resting membrane potential related to altered Ca^{2+} buffering rather than a loss of $\Delta\Psi_m$ associated with mitochondrial protein release. Because of these possibilities, it will be important to reassess $\Delta\Psi_m$, either in the light of mitochondrial numbers or at the level of individual mitochondria. And lastly, even though there was not significant release of cytochrome C at the time of peak activation of leaner Purkinje cell death and caspase 3 activation, it does not rule out the release of other mitochondrial proteins, such as SMAC or AIF which may be contributing to leaner Purkinje cell death.

As research in this area progresses we will elucidate the mechanisms of leaner Purkinje cell death, understanding what is being triggered and how. We will then be able to apply that knowledge to investigate potential therapies aimed at preserving neuronal survival and cerebellar function.

REFERENCES

Abbott, LC, Isaacs, KR, Heckroth, JA (1996) Co-localization of tyrosine hydroxylase and zebrin II immunoreactivities in Purkinje cells of the mutant mice, tottering and tottering/leaner. Neuroscience 71: 461-475.

Abbott, LC, Jacobowitz, DM (1995) Development of calretinin-immunoreactive unipolar brush-like cells and an afferent pathway to the embryonic and early postnatal mouse cerebellum. Anat Embryol 191: 541-559.

Abbott, LC, Jacobowitz, DM (1999) Developmental expression of calretinin-immunoreactivity in the thalamic eminence of the fetal mouse. Int J Dev Neurosci 17: 331-345.

Adcock, KH, Metzger, F, Kapfhammer, JP (2004) Purkinje cell dendritic tree development in the absence of excitatory neurotransmission and of brain-derived neurotrophic factor in organotypic slice cultures. Neuroscience 127: 137-145.

Allen, GV, Gerami, D, Esser, MJ (2000) Conditioning effects of repetitive mild neurotrauma on motor function in an animal model of focal brain injury. Neuroscience 99: 93-105.

Altman, J, Bayer, SA (1978) Prenatal development of the cerebellar system in the rat. I. Cytogenesis and histogenesis of the deep nuclei and the cortex of the cerebellum. J Comp Neurol 179: 23-48.

Altman, J, Bayer, SA (1985a) Embryonic development of the rat cerebellum. I. Delineation of the cerebellar primordium and early cell movements. J Comp Neurol 231: 1-26.

Altman, J, Bayer, SA (1985b) Embryonic development of the rat cerebellum. II. Translocation and regional distribution of the deep neurons. J Comp Neurol 231: 27-41.

Altman, J, Bayer, SA (1997) Development of the Cerebellar System: In Relation to Its Evolution, Structure and Functions, CRC Press, New York, NY.

Arico, S, Petiot, A, Bauvy, C, Dubbelhuis, PF, Meijer, AJ, Codogno, P, Ogier-Denis, E (2001) The tumor suppressor PTEN positively regulates macroautophagy by inhibiting the phosphatidylinositol 3-kinase/protein kinase B pathway. J Biol Chem 276: 35243-35246.

Arsenio Nunes, ML, Sotelo, C (1985) Development of the spinocerebellar system in the postnatal rat. J Comp Neurol 237: 291-306.

Ashby, MC, Tepikin, AV (2001) ER calcium and the functions of intracellular organelles. Semin Cell Dev Biol 12: 11-17.

Ashkenazi, A, Dixit, VM (1998) Death receptors: signaling and modulation. Science 281: 1305-1308.

Austin, MC, Schultzberg, M, Abbott, LC, Montpied, P, Evers, JR, Paul, SM, Crawley, JN (1992) Expression of tyrosine hydroxylase in cerebellar Purkinje neurons of the mutant tottering and leaner mouse. Brain Res Mol Brain Res 15: 227-240.

Ayata, C, Shimizu-Sasamata, M, Lo, EH, Noebels, JL, Moskowitz, MA (2000) Impaired neurotransmitter release and elevated threshold for cortical spreading depression in mice with mutations in the alpha1A subunit of P/Q type calcium channels. Neuroscience 95: 639-645.

Bastianelli, E (2003) Distribution of calcium-binding proteins in the cerebellum. Cerebellum 2: 242-262.

Benn, SC, Woolf, CJ (2004) Adult neuron survival strategies--slamming on the brakes. Nat Rev Neurosci 5: 686-700.

Berridge, MJ, Lipp, P, Bootman, MD (2000) The versatility and university of calcium signalling. Nat Rev Mol Cell Biol 1: 11-21.

Biederbick, A, Kern, HF, Elsasser, HP (1995) Monodansylcadaverine (MDC) is a specific in vivo marker for autophagic vacuoles. Eur J Cell Biol 66: 3-14.

Billups, D, Liu, YB, Birnstiel, S, Slater, NT (2002) NMDA receptor-mediated currents in rat cerebellar granule and unipolar brush cells. J Neurophysiol 87: 1948-1959.

Bishop, GM, Robinson, SR (2001) Quantitative analysis of cell death and ferritin expression in response to cortical iron: implications for hypoxia-ischemia and stroke. Brain Res 907: 175-187.

Blackstone, C, Sheng, M (2002) Postsynaptic calcium signaling microdomains in neurons. Front Biosci 7: d872-d885.

Blommaart, EF, Krause, U, Schellens, JP, Vreeling-Sindelarova, H, Meijer, AJ (1997) The phosphatidylinositol 3-kinase inhibitors wortmannin and LY294002 inhibit autophagy in isolated rat hepatocytes. Eur J Biochem 243: 240-246.

Blommaart, EF, Luiken, JJ, Blommaart, PJ, van Woerkom, GM, Meijer, AJ (1995) Phosphorylation of ribosomal protein S6 is inhibitory for autophagy in isolated rat hepatocytes. J Biol Chem 270: 2320-2326.

Bootman, MD, Collins, TJ, Peppiatt, CM, Prothero, LS, MacKenzie, L, De Smet, P, Travers, M, Tovey, SC, Seo, JT, Berridge, MJ, Ciccolini, F, Lipp, P (2001) Calcium signalling--an overview. Semin Cell Dev Biol 12: 3-10.

Bowyer, JF, Peterson, SL, Rountree, RL, Tor-Agbidye, J, Wang, GJ (1998) Neuronal degeneration in rat forebrain resulting from D-amphetamine- induced convulsions is dependent on seizure severity and age. Brain Res 809: 77-90.

Bursch, W (2001) The autophagosomal-lysosomal compartment in programmed cell death. Cell Death Differ 8: 569-581.

Canu, N, Tufi, R, Serafino, AL, Amadoro, G, Ciotti, MT, Calissano, P (2005) Role of the autophagic-lysosomal system on low potassium-induced apoptosis in cultured cerebellar granule cells. J Neurochem 92: 1228-1242.

Catterall, WA (2000) Structure and regulation of voltage-gated Ca2+ channels. Annu Rev Cell Dev Biol 16: 521-555.

Chan-Palay, V, Palay, SL, Brown, JT, Van Itallie, C (1977) Sagittal organization of olivocerebellar and reticulocerebellar projections: autoradiographic studies with 35S-methionine. Exp Brain Res 30: 561-576.

Cheema, ZF, West, JR, Miranda, RC (2000) Ethanol induces Fas/Apo. Alcohol Clin Exp Res 24: 535-543.

Chi, S, Kitanaka, C, Noguchi, K, Mochizuki, T, Nagashima, Y, Shirouzu, M, Fujita, H, Yoshida, M, Chen, W, Asai, A, Himeno, M, Yokoyama, S, Kuchino, Y (1999) Oncogenic Ras triggers cell suicide through the activation of a caspase-independent cell death program in human cancer cells. Oncogene 18: 2281-2290.

Collin, T, Chat, M, Lucas, MG, Moreno, H, Racay, P, Schwaller, B, Marty, A, Llano, I (2005) Developmental changes in parvalbumin regulate presynaptic Ca2+ signaling. J Neurosci 25: 96-107.

Cory, S, Adams, JM (2002) The Bcl2 family: regulators of the cellular life-or-death switch. Nat Rev Cancer 2: 647-656.

De Maria, R, Lenti, L, Malisan, F, d'Agostino, F, Tomassini, B, Zeuner, A, Rippo, MR, Testi, R (1997) Requirement for GD3 ganglioside in CD95- and ceramide-induced apoptosis. Science 277: 1652-1655.

De Zeeuw, CI, Wylie, DR, DiGiorgi, PL, Simpson, JI (1994) Projections of individual Purkinje cells of identified zones in the flocculus to the vestibular and cerebellar nuclei in the rabbit. J Comp Neurol 349: 428-447.

Deng, Y, Ren, X, Yang, L, Lin, Y, Wu, X (2003) A JNK-dependent pathway is required for TNFα-induced apoptosis. Cell 115: 61-70.

Desagher, S, Osen-Sand, A, Nichols, A, Eskes, R, Montessuit, S, Lauper, S, Maundrell, K, Antonsson, B, Martinou, JC (1999) Bid-induced conformational change of Bax is responsible for mitochondrial cytochrome c release during apoptosis. J Cell Biol 144: 891-901.

Deshmukh, M, Kuida, K, Johnson, EM Jr (2000) Caspase inhibition extends the commitment to neuronal death beyond cytochrome c release to the point of mitochondrial depolarization. J Cell Biol 150: 131-143.

Dino, MR, Schuerger, RJ, Liu, Y, Slater, NT, Mugnaini, E (2000) Unipolar brush cell: a potential feedforward excitatory interneuron of the cerebellum. Neuroscience 98: 625-636.

Dove, LS, Abbott, LC, Griffith, WH (1998) Whole-cell and single-channel analysis of P-type calcium currents in cerebellar Purkinje cells of leaner mutant mice. J Neurosci 18: 7687-7699.

Dove, LS, Nahm, SS, Murchison, D, Abbott, LC, Griffith, WH (2000) Altered calcium homeostasis in cerebellar Purkinje cells of leaner mutant mice. J Neurophysiol 84: 513-524.

Doyle, J, Ren, X, Lennon, G, Stubbs, L (1997) Mutations in the Cacnl1a4 calcium channel gene are associated with seizures, cerebellar degeneration, and ataxia in tottering and leaner mutant mice. Mamm Genome 8: 113-120.

Du, C, Fang, M, Li, Y, Li, L, Wang, X (2000) Smac, a mitochondrial protein that promotes cytochrome c-dependent caspase activation by eliminating IAP inhibition. Cell 102: 33-42.

Duchen, MR (1999) Contributions of mitochondria to animal physiology: from homeostatic sensor to calcium signalling and cell death. J Physiol 516 : 1-17.

Ducros, A, Denier, C, Joutel, A, Vahedi, K, Michel, A, Darcel, F, Madigand, M, Guerouaou, D, Tison, F, Julien, J, Hirsch, E, Chedru, F, Bisgard, C, Lucotte, G, Despres, P, Billard, C, Barthez, MA, Ponsot, G, Bousser, MG, Tournier-Lasserve, E (1999) Recurrence of the T666M calcium channel CACNA1A gene mutation in familial hemiplegic migraine with progressive cerebellar ataxia. Am J Hum Genet 64: 89-98.

Earnshaw, WC, Martins, LM, Kaufmann, SH (1999) Mammalian caspases: structure, activation, substrates, and functions during apoptosis. Annu Rev Biochem 68: 383-424.

Eccles, JC, Sasaki, K, Strata, P (1967) A comparison of the inhibitory actions of Golgi cells and of basket cells. Exp Brain Res 3: 81-94.

Edwards, MA, Yamamoto, M, Caviness, VS Jr (1990) Organization of radial glia and related cells in the developing murine CNS. An analysis based upon a new monoclonal antibody marker. Neuroscience 36: 121-144.

Eskes, R, Desagher, S, Antonsson, B, Martinou, JC (2000) Bid induces the oligomerization and insertion of Bax into the outer mitochondrial membrane. Mol Cell Biol 20: 929-935.

Fletcher, CF, Lutz, CM, O'Sullivan, TN, Shaughnessy, JD Jr, Hawkes, R, Frankel, WN, Copeland, NG, Jenkins, NA (1996) Absence epilepsy in tottering mutant mice is associated with calcium channel defects. Cell 87: 607-617.

Fletcher, CF, Tottene, A, Lennon, VA, Wilson, SM, Dubel, SJ, Paylor, R, Hosford, DA, Tessarollo, L, McEnery, MW, Pietrobon, D, Copeland, NG, Jenkins, NA (2001) Dystonia and cerebellar atrophy in Cacna1a null mice lacking P/Q calcium channel activity. FASEB J 15: 1288-1290.

Florez-McClure, ML, Linseman, DA, Chu, CT, Barker, PA, Bouchard, RJ, Le, SS, Laessig, TA, Heidenreich, KA (2004) The p75 neurotrophin receptor can induce autophagy and death of cerebellar Purkinje neurons. J Neurosci 24: 4498-4509.

Freyaldenhoven, TE, Ali, SF, Schmued, LC (1997) Systemic administration of MPTP induces thalamic neuronal degeneration in mice. Brain Res 759: 9-17.

Fujita, S, Shimada, M, Nakamura, T (1966) H3-thymidine autoradiographic studies on the cell proliferation and differentiation in the external and the internal granular layers of the mouse cerebellum. J Comp Neurol 128: 191-208.

Fureman, BE, Campbell, DB, Hess, EJ (1999) L-type calcium channel regulation of abnormal tyrosine hydroxylase expression in cerebella of tottering mice. Ann N Y Acad Sci 868: 217-219.

Fureman, BE, Campbell, DB, Hess, EJ (2003) Regulation of tyrosine hydroxylase expression in tottering mouse Purkinje cells. Neurotox Res 5: 521-528.

Frank, TC, Nunley, MC, Sons, HD, Ramon, R, Abbott, LC (2003) Fluoro-Jade identification of cerebellar granule cell and Purkinje cell death in the α1A calcium channel mutant mouse, leaner. Neuroscience 118: 667-680.

Giehl, KM, Rohrig, S, Bonatz, H, Gutjahr, M, Leiner, B, Bartke, I, Yan, Q, Reichardt, LF, Backus, C, Welcher, AA, Dethleffsen, K, Mestres, P, Meyer, M (2001) Endogenous brain-derived neurotrophic factor and neurotrophin-3 antagonistically regulate survival of axotomized corticospinal neurons in vivo. J Neurosci 21: 3492-3502.

Gillard, SE, Volsen, SG, Smith, W, Beattie, RE, Bleakman, D, Lodge, D (1997) Identification of pore-forming subunit of P-type calcium channels: an antisense study on rat cerebellar Purkinje cells in culture. Neuropharmacology 36: 405-409.

Goldwitz, D, Hamre, K (1998) The cells and molecules that make a cerebellum. Trends Neurosci 21: 375-382.

Green, DR (2005) Apoptotic pathways: ten minutes to dead. Cell 121: 671-674.

Green, DR, Reed, JC (1998) Mitochondria and apoptosis. Science 281: 1309-13012.

Green, MC, Sidman, RL (1962) Tottering--a neuromuscular mutation in the mouse. J Hered 5: 233-237.

Grishkat, HL, Eisenman, LM (1995) Development of the spinocerebellar projection in the prenatal mouse. J Comp Neurol 363: 93-108.

Hallonet, ME, Le Douarin, NM (1993) Tracing neuroepithelial cells of the mesencephalic and metencephalic alar plates during cerebellar ontogeny in quail-chick chimaeras. Eur J Neurosci 5: 1145-1155.

Hallonet, ME, Teillet, MA, Le Douarin, NM (1990) A new approach to the development of the cerebellum provided by the quail-chick marker system. Development 108: 19-31.

Hao, Z, Duncan, GS, Chang, CC, Elia, A, Fang, M, Wakeham, A, Okada, H, Calzascia, T, Jang, Y, You-Ten, A, Yeh, WC, Ohashi, P, Wang, X, Mak, TW (2005) Specific ablation of the apoptotic functions of cytochrome C reveals a differential requirement for cytochrome C and Apaf-1 in apoptosis. Cell 121: 579-591.

Hawkes, R, Faulkner-Jones, B, Tam, P, Tan, SS (1998) Pattern formation in the cerebellum of murine embryonic stem cell chimeras. Eur J Neurosci 10: 790-793.

Hawkes, R, Herrup, K (1995) Aldolase C/zebrin II and the regionalization of the cerebellum. J Mol Neurosci 6: 147-158.

Heckroth, JA, Abbott, LC (1994) Purkinje cell loss from alternating sagittal zones in the cerebellum of leaner mutant mice. Brain Res 658: 93-104.

Hengartner, MO (2000) The biochemistry of apoptosis. Nature 407: 770-776.

Herlitze, S, Garcia, DE, Mackie, K, Hille, B, Scheuer, T, Catterall, WA (1996) Modulation of Ca2+ channels by G-protein beta gamma subunits. Nature 380: 258-262.

Herrup, K, Kuemerle, B (1997) The compartmentalization of the cerebellum. Annu Rev Neurosci 20: 61-90.

Herrup, K, Wilczynski, SL (1982) Cerebellar cell degeneration in the leaner mutant mouse. Neuroscience 7: 2185-2196.

Hess, EJ, Wilson, MC (1991) Tottering and leaner mutations perturb transient developmental expression of tyrosine hydroxylase in embryologically distinct Purkinje cells. Neuron 6: 123-132.

Hille, B (1994) Modulation of ion-channel function by G-protein-coupled receptors. Trends Neurosci 17: 531-536.

Hishita, T, Tada-Oikawa, S, Tohyama, K, Miura, Y, Nishihara, T, Tohyama, Y, Yoshida, Y, Uchiyama, T, Kawanishi, S (2001) Caspase-3 activation by lysosomal enzymes in cytochrome C-independent apoptosis in myelodysplastic syndrome-derived cell line P39. Cancer Res 61: 2878-2884.

Hitomi, J, Katayama, T, Taniguchi, M, Honda, A, Imaizumi, K, Tohyama, M (2004) Apoptosis induced by endoplasmic reticulum stress depends on activation of caspase-3 via caspase-12. Neurosci Lett 357: 127-130.

Hopkins, KJ, Wang, G, Schmued, LC (2000) Temporal progression of kainic acid induced neuronal and myelin degeneration in the rat forebrain. Brain Res 864: 69-80.

Hyun, BH, Kim, MS, Choi, YK, Yoon, WK, Suh, JG, Jeong, YG, Park, SK, Lee, CH (2001) Mapping of the pogo gene, a new ataxic mutant from Korean wild mice, on central mouse chromosome 8. Mamm Genome 12: 250-252.

Ichas, F, Mazat, JP (1998) From calcium signaling to cell death: two conformations for the mitochondrial permeability transition pore. Switching from low- to high-conductance state. Biochim Biophys Acta 1366: 33-50.

Ikeda, SR, Dunlap, K (1999) Voltage-dependent modulation of N-type calcium channels: role of G protein subunits. Adv Second Messenger Phosphoprotein Res 33: 131-151.

Isaacs, KR, Abbott, LC (1992) Development of the paramedian lobule of the cerebellum in wild-type and tottering mice. Dev Neurosci 14: 386-393.

Jeong, YG, Hyun, BH (2000) Abnormal synaptic organization between granule cells and Purkinje cells in the new ataxic mutant mouse, pogo. Neurosci Lett 294: 77-80.

Jeong, YG, Hyun, BH, Hawkes, R (2000) Abnormalities in cerebellar Purkinje cells in the novel ataxic mutant mouse, pogo. Brain Res Dev Brain Res 125: 61-67.

Jeong, YG, Kim, MK, Hawkes, R (2001) Ectopic expression of tyrosine hydroxylase in Zebrin II immunoreactive Purkinje cells in the cerebellum of the ataxic mutant mouse, pogo. Brain Res Dev Brain Res 129: 201-209.

Joza, N, Susin, SA, Daugas, E, Stanford, WL, Cho, SK, Li, CY, Sasaki, T, Elia, AJ, Cheng, HY, Ravagnan, L, Ferri, KF, Zamzami, N, Wakeham, A, Hakem, R, Yoshida, H, Kong, YY, Mak, TW, Zuniga-Pflucker, JC, Kroemer, G, Penninger, JM (2001) Essential role of the mitochondrial apoptosis-inducing factor in programmed cell death. Nature 410: 549-554.

Jun, K, Piedras-Renteria, ES, Smith, SM, Wheeler, DB, Lee, SB, Lee, TG, Chin, H, Adams, ME, Scheller, RH, Tsien, RW, Shin, HS (1999) Ablation of P/Q-type Ca(2+) channel currents, altered synaptic transmission, and progressive ataxia in mice lacking the α1A-subunit. Proc Natl Acad Sci USA 96: 15245-15250.

Kamada, Y, Funakoshi, T, Shintani, T, Nagano, K, Ohsumi, M, Ohsumi, Y (2000) Tor-mediated induction of autophagy via an Apg1 protein kinase complex. J Cell Biol 150: 1507-1513.

Kandel, ER, Siegelbaum, SA (2000) Principles of Neural Science: Synaptic Integration. McGraw-Hill: New York, NY 207-228.

Kerr, JF, Wyllie, AH, Currie, AR (1972) Apoptosis: a basic biological phenomenon with wide-ranging implications in tissue kinetics. Br J Cancer 26: 239-257.

Kharbanda, S, Saxena, S, Yoshida, K, Pandey, P, Kaneki, M, Wang, Q, Cheng, K, Chen, YN, Campbell, A, Sudha, T, Yuan, ZM, Narula, J, Weichselbaum, R, Nalin, C, Kufe, D (2000) Translocation of SAPK/JNK to mitochondria and interaction with Bcl-x(L) in response to DNA damage. J Biol Chem 275: 322-327.

Kihara, A, Kabeya, Y, Ohsumi, Y, Yoshimori, T (2001a) Beclin-phosphatidylinositol 3-kinase complex functions at the trans-Golgi network. EMBO Rep 2: 330-335.

Kihara, A, Noda, T, Ishihara, N, Ohsumi, Y (2001b) Two distinct Vps34 phosphatidylinositol 3-kinase complexes function in autophagy and carboxypeptidase Y sorting in Saccharomyces cerevisiae. J Cell Biol 152: 519-530.

Kish, L (1965) Survey Sampling, John Wiley & Sons, Inc: New York, NY.

Kitanaka, C, Kuchino, Y (1999) Caspase-independent programmed cell death with necrotic morphology. Cell Death Differ 6: 508-515.

Klein, JA, Longo-Guess, CM, Rossmann, MP, Seburn, KL, Hurd, RE, Frankel, WN, Bronson, RT, Ackerman, SL (2002) The harlequin mouse mutation downregulates apoptosis-inducing factor. Nature 419: 367-374.

Klionsky, DJ (2005) The molecular machinery of autophagy: unanswered questions. J Cell Sci 118: 7-18.

Klockgether, T, Evert, B (1998) Genes involved in hereditary ataxias. Trends Neurosci 21: 413-418.

Koester, J, Siegelbaum, SA (2000) Principles of Neural Science: Propagated signaling: The action potential, McGraw-Hill: New York, NY 150-174.

Kokaia, Z, Andsberg, G, Yan, Q, Lindvall, O (1998) Rapid alterations of BDNF protein levels in the rat brain after focal ischemia: evidence for increased synthesis and anterograde axonal transport. Exp Neurol 154: 289-301.

Krajewska, M, Mai, JK, Zapata, JM, Ashwell, KW, Schendel, SL, Reed, JC, Krajewski, S (2002) Dynamics of expression of apoptosis-regulatory proteins Bid, Bcl-2, Bcl- X, Bax and Bak during development of murine nervous system. Cell Death Differ 9: 145-157.

Kristensen, BW, Noraberg, J, Jakobsen, B, Gramsbergen, JB, Ebert, B, Zimmer, J (1999) Excitotoxic effects of non-NMDA receptor agonists in organotypic corticostriatal slice cultures. Brain Res 841: 143-159.

Kubova, H, Druga, R, Lukasiuk, K, Suchomelova, L, Haugvicova, R, Jirmanova, I, Pitkanen, A (2001) Status epilepticus causes necrotic damage in the mediodorsal nucleus of the thalamus in immature rats. J Neurosci 21: 3593-3599.

Larramendi, LMH, Victor, T (1967) Synapses on the Purkinje cell spines in the mouse an electron microscopic study. Brain Res 5: 15-30.

Larsson, E, Lindvall, O, Kokaia, Z (2001) Stereological assessment of vulnerability of immunocytochemically identified striatal and hippocampal neurons after global cerebral ischemia in rats. Brain Res 913: 117-132.

Lau, FC, Abbott, LC, Rhyu, IJ, Kim, DS, Chin, H (1998) Expression of calcium channel alpha1A mRNA and protein in the leaner mouse (tgla/tgla) cerebellum. Brain Res Mol Brain Res 59: 93-99.

Lau, FC, Frank, TC, Nahm, SS, Stoica, G, Abbott, LC (2004) Postnatal apoptosis in cerebellar granule cells of homozygous leaner (tg[1a]/tg[1a]) mice. Neurotox Res 6: 267-280.

Lau, FC (1999) Apoptosis, reduced intracellular free calcium level and altered gene expression in the cerebellum of the leaner mutant mouse. Dissertation. College Station, TX: Texas A&M University.

Leclerc, N, Gravel, C, Hawkes, R (1988) Development of parasagittal zonation in the rat cerebellar cortex: MabQ113 antigenic bands are created postnatally by the suppression of antigen expression in a subset of Purkinje cells. J Comp Neurol 273: 399-420.

Leclerc, N, Schwarting, GA, Herrup, K, Hawkes, R, Yamamoto, M (1992) Compartmentation in mammalian cerebellum: Zebrin II and P-path antibodies define three classes of sagittally organized bands of Purkinje cells. Proc Natl Acad Sci U S A 89: 5006-5010.

Lee, A, Wong, ST, Gallagher, D, Li, B, Storm, DR, Scheuer, T, Catterall, WA (1999) Ca2+/calmodulin binds to and modulates P/Q-type calcium channels. Nature 399: 155-159.

Leist, M, Single, B, Castoldi, AF, Kuhnle, S, Nicotera, P (1997) Intracellular adenosine triphosphate (ATP) concentration: a switch in the decision between apoptosis and necrosis. J Exp Med 185: 1481-1486.

Letai, A, Bassik, MC, Walensky, LD, Sorcinelli, MD, Weiler, S, Korsmeyer, SJ (2002) Distinct BH3 domains either sensitize or activate mitochondrial apoptosis, serving as prototype cancer therapeutics. Cancer Cell 2: 183-192.

Levitt, P (1988) Normal pharmacological and morphometric parameters in the noradrenergic hyperinnervated mutant mouse, "tottering". Cell Tissue Res 252: 175-180.

Li, D, Wang, F, Lai, M, Chen, Y, Zhang, JF (2005) A protein phosphatase 2cα-Ca2+ channel complex for dephosphorylation of neuronal Ca2+ channels phosphorylated by

protein kinase C. J Neurosci 25: 1914-1923.

Li, P, Nijhawan, D, Budihardjo, I, Srinivasula, SM, Ahmad, M, Alnemri, ES, Wang, X (1997) Cytochrome c and dATP-dependent formation of Apaf-1/caspase-9 complex initiates an apoptotic protease cascade. Cell 91: 479-489.

Liu, X, Kim, CN, Yang, J, Jemmerson, R, Wang, X (1996) Induction of apoptotic program in cell-free extracts: requirement for dATP and cytochrome c. Cell 86: 147-157.

Lorenzon, NM, Lutz, CM, Frankel, WN, Beam, KG (1998) Altered calcium channel currents in Purkinje cells of the neurological mutant mouse leaner. J Neurosci 18: 4482-4489.

Luo, X, Budihardjo, I, Zou, H, Slaughter, C, Wang, X (1998) Bid, a Bcl2 interacting protein, mediates cytochrome c release from mitochondria in response to activation of cell surface death receptors. Cell 94: 481-490.

Marani, E, Voogd, J (1979) The morphology of the mouse cerebellum. Acta Morphol Neerl Scand 17: 33-52.

Mason, CA, Christakos, S, Catalano, SM (1990) Early climbing fiber interactions with Purkinje cells in the postnatal mouse cerebellum. J Comp Neurol 297: 77-90.

Mason, CA, Gregory, E (1984) Postnatal maturation of cerebellar mossy and climbing fibers: transient expression of dual features on single axons. J Neurosci 4: 1715-1735.

McAlhany, REJ, West, JR, Miranda, RC (1997) Glial-derived neurotrophic factor rescues calbindin-D28k-immunoreactive neurons in alcohol-treated cerebellar explant cultures. J Neurobiol 33: 835-847.

McMahon, AP, Bradley, A (1990) The Wnt-1 (int-1) proto-oncogene is required for development of a large region of the mouse brain. Cell 62: 1073-1085.

Meier, P, Finch, A, Evan, G (2000) Apoptosis in development. Nature 407: 796-801.

Melendez, A, Talloczy, Z, Seaman, M, Eskelinen, EL, Hall, DH, Levine, B (2003) Autophagy genes are essential for dauer development and life-span extension in C. elegans. Science 301: 1387-1391.

Miale, IL, Sidman, RL (1961) An autoradiographic analysis of histogenesis in the mouse cerebellum. Exp Neurol 4: 277-296.

Miranda, R, Sohrabji, F, Singh, M, Toran-Allerand, D (1996) Nerve growth factor (NGF) regulation of estrogen receptors in explant cultures of the developing forebrain. J Neurobiol 31: 77-87.

Morin, F, Dino, MR, Mugnaini, E (2001) Postnatal differentiation of unipolar brush cells and mossy fiber-unipolar brush cell synapses in rat cerebellum. Neuroscience 104: 1127-1139.

Munafo, DB, Colombo, MI (2001) A novel assay to study autophagy: regulation of autophagosome vacuole size by amino acid deprivation. J Cell Sci 114: 3619-3629.

Murchison, D, Dove, LS, Abbott, LC, Griffith, WH (2002) Homeostatic compensation maintains Ca^{2+} signaling functions in Purkinje neurons in leaner mutant mouse. The Cerebellum 1: 119-127.

Nahm, SS, Jung, KY, Enger, MK, Griffith, WH, Abbott, LC (2005) Differential expression of T-type calcium channels in P/Q-type calcium channel mutant mice with ataxia and absence epilepsy. J Neurobiol 62: 352-360.

Nahm, SS, Tomlinson, DJ, Abbott, LC (2002) Decreased calretinin expression in cerebellar granule cells in the leaner mouse. J Neurobiol 51: 313-322.

Nahm, SS (2002) Analysis of gene and protein expression related cerebellar neurodegeneration in the calcium channel mutant mouse, leaner, Dissertation. College Station, TX: Texas A&M University.

Nitatori, T, Sato, N, Waguri, S, Karasawa, Y, Araki, H, Shibanai, K, Kominami, E, Uchiyama, Y (1995) Delayed neuronal death in the CA1 pyramidal cell layer of the gerbil hippocampus following transient ischemia is apoptosis. J Neurosci 15: 1001-1011.

Noda, T, Ohsumi, Y (1998) Tor, a phosphatidylinositol kinase homologue, controls autophagy in yeast. J Biol Chem 273: 3963-3966.

Noebels, JL (1984) Isolating single genes of the inherited epilepsies. Ann Neurol 16 Suppl: S18-S21.

Nolte, J (1999) The Human Brain: An Introductions to its Functional Anatomy, Mosby: New York, NY 469-493.

Noraberg, J, Kristensen, BW, Zimmer, J (1999) Markers for neuronal degeneration in organotypic slice cultures. Brain Res Brain Res Protoc 3: 278-290.

O'Leary, JL, Smith, JM, Inukai, J, O'Leary, M (1970) The inferior olive as a source of climbing fibers in the rat. Bibl Psychiatr 143: 128-137.

Oberdick, J, Baader, SL, Schilling, K (1998) From zebra stripes to postal zones: deciphering patterns of gene expression in the cerebellum. Trends Neurosci 21: 383-390.

Oda, S (1981) A new allele of the tottering locus, rolling mouse Nagoya, on chromosome no. 8 in the mouse. Jpn J Genet 56: 295-299.

Olschowka, JA, Vijayan, VK (1980) Postnatal development of cholinergic neurotransmitter enzymes in the mouse cerebellum. Biochemical, light microscopic and electron microscopic cytochemical investigations. J Comp Neurol 191: 77-101.

Ophoff, RA, Terwindt, GM, Vergouwe, MN, van Eijk, R, Oefner, PJ, Hoffman, SM, Lamerdin, JE, Mohrenweiser, HW, Bulman, DE, Ferrari, M, Haan, J, Lindhout, D, van Ommen, GJ, Hofker, MH, Ferrari, MD, Frants, RR (1996) Familial hemiplegic migraine and episodic ataxia type-2 are caused by mutations in the Ca2+ channel gene CACNL1A4. Cell 87: 543-552.

Oppenheim, RW, Flavell, RA, Vinsant, S, Prevette, D, Kuan, CY, Rakic, P (2001) Programmed cell death of developing mammalian neurons after genetic deletion of caspases. J Neurosci 21: 4752-4760.

Ozol, K, Hayden, JM, Oberdick, J, Hawkes, R (1999) Transverse zones in the vermis of the mouse cerebellum. J Comp Neurol 412: 95-111.

Palkovits, M, Magyar, P, Szentagothai, J (1971) Quantitative histological analysis of the cerebellar cortex in the cat. 3. Structural organization of the molecular layer. Brain Res 34: 1-18.

Pennypacker, KR, Eidizadeh, S, Kassed, CA, O'Callaghan, JP, Sanberg, PR, Willing, AE (2000) Expression of fos-related antigen-2 in rat hippocampus after middle cerebral arterial occlusion. Neurosci Lett 289: 1-4.

Petiot, A, Ogier-Denis, E, Blommaart, EF, Meijer, AJ, Codogno, P (2000) Distinct classes of phosphatidylinositol 3'-kinases are involved in signaling pathways that control macroautophagy in HT-29 cells. J Biol Chem 275: 992-998.

Pietrobon, D (2002) Calcium channels and channelopathies of the central nervous system. Mol Neurobiol 25: 31-50.

Poirier, JL, Capek, R, De Koninck, Y (2000) Differential progression of dark neuron and Fluoro-Jade labelling in the rat hippocampus following pilocarpine-induced status epilepticus. Neuroscience 97: 59-68.

Qian, J, Noebels, JL (2001) Presynaptic Ca2+ channels and neurotransmitter release at the terminal of a mouse cortical neuron. J Neurosci 21: 3721-3728.

Qin, N, Platano, D, Olcese, R, Stefani, E, Birnbaumer, L (1997) Direct interaction of gbetagamma with a C-terminal Gβγ-binding domain of the Ca2+ channel α1 subunit is responsible for channel inhibition by G protein-coupled receptors. Proc Natl Acad Sci U S A 94: 8866-8871.

Raff, M (1998) Cell suicide for beginners. Nature 396: 119-122.

Rhyu, IJ, Abbott, LC, Walker, DB, Sotelo, C (1999) An ultrastructural study of granule cell/Purkinje cell synapses in tottering (tg/tg), leaner (tg^{la}/tg^{la}) and compound heterozygous tottering/leaner (tg/tg^{la}) mice. Neuroscience 90: 717-728.

Sastry, PS, Rao, KS (2000) Apoptosis and the nervous system. J Neurochem 74: 1-20.

Savaskan, NE, Eyupoglu, IY, Brauer, AU, Plaschke, M, Ninnemann, O, Nitsch, R, Skutella, T (2000) Entorhinal cortex lesion studied with the novel dye Fluoro-jade. Brain Res 864: 44-51.

Schmued, LC, Albertson, C, Slikker, W Jr (1997) Fluoro-Jade: a novel fluorochrome for the sensitive and reliable histochemical localization of neuronal degeneration. Brain Res 751: 37-46.

Schmued, LC, Hopkins, KJ (2000) Fluoro-Jade B: a high affinity fluorescent marker for the localization of neuronal degeneration. Brain Res 874: 123-130.

Schrenk, K, Kapfhammer, JP, Metzger, F (2002) Altered dendritic development of cerebellar Purkinje cells in slice cultures from protein kinase Cgamma-deficient mice. Neuroscience 110: 675-689.

Schweichel, JU, Merker, HJ (1973) The morphology of various types of cell death in prenatal tissues. Teratology 7: 253-266.

Sgaier, SK, Millet, S, Villanueva, MP, Berenshteyn, F, Song, C, Joyner, AL (2005) Morphogenetic and cellular movements that shape the mouse cerebellum; insights from genetic fate mapping. Neuron 45: 27-40.

Shintani, T, Klionsky, DJ (2004) Autophagy in health and disease: a double-edged sword. Science 306: 990-995.

Sidman, RL, Green, MC, Appel, SH (1965) Catalog of the Neurological Mutants of the Mouse. Harvard University Press: Cambridge, MA.

Slee, EA, Harte, MT, Kluck, RM, Wolf, BB, Casiano, CA, Newmeyer, DD, Wang, HG, Reed, JC, Nicholson, DW, Alnemri, ES, Green, DR, Martin, SJ (1999) Ordering the cytochrome c-initiated caspase cascade: hierarchical activation of caspases-2, -3, -6, -7, -8, and -10 in a caspase-9-dependent manner. J Cell Biol 144: 281-292.

Stea, A, Tomlinson, WJ, Soong, TW, Bourinet, E, Dubel, SJ, Vincent, SR, Snutch, TP (1994) Localization and functional properties of a rat brain alpha 1A calcium channel reflect similarities to neuronal Q- and P-type channels. Proc Natl Acad Sci U S A 91: 10576-10580.

Stoka, V, Turk, B, Schendel, SL, Kim, TH, Cirman, T, Snipas, SJ, Ellerby, LM, Bredesen, D, Freeze, H, Abrahamson, M, Bromme, D, Krajewski, S, Reed, JC, Yin, XM, Turk, V, Salvesen, GS (2001) Lysosomal protease pathways to apoptosis. Cleavage of bid, not pro- caspases, is the most likely route. J Biol Chem 276: 3149-3157.

Strahlendorf, J, Box, C, Attridge, J, Diertien, J, Finckbone, V, Henne, WM, Medina, MS, Miles, R, Oomman, S, Schneider, M, Singh, H, Veliyaparambil, M, Strahlendorf, H (2003) AMPA-induced dark cell degeneration of cerebellar Purkinje neurons involves activation of caspases and apparent mitochondrial dysfunction. Brain Res 994: 146-159.

Suh, YS, Oda, S, Kang, YH, Kim, H, Rhyu, IJ (2002) Apoptotic cell death of cerebellar granule cells in rolling mouse Nagoya. Neurosci Lett 325: 1-4.

Susin, SA, Lorenzo, HK, Zamzami, N, Marzo, I, Snow, BE, Brothers, GM, Mangion, J, Jacotot, E, Costantini, P, Loeffler, M, Larochette, N, Goodlett, DR, Aebersold, R, Siderovski, DP, Penninger, JM, Kroemer, G (1999) Molecular characterization of mitochondrial apoptosis-inducing factor. Nature 397: 441-446.

Thayer, SA, Usachev, YM, Pottorf, WJ (2002) Modulating Ca2+ clearance from neurons. Front Biosci 7: d1255-d1279.

Thornberry, NA, Rano, TA, Peterson, EP, Rasper, DM, Timkey, T, Garcia-Calvo, M, Houtzager, VM, Nordstrom, PA, Roy, S, Vaillancourt, JP, Chapman, KT, Nicholson, DW (1997) A combinatorial approach defines specificities of members of the caspase family and granzyme B. Functional relationships established for key mediators of apoptosis. J Biol Chem 272: 17907-17911.

Vercammen, D, Brouckaert, G, Denecker, G, Van de Craen, M, Declercq, W, Fiers, W, Vandenabeele, P (1998) Dual signaling of the Fas receptor: initiation of both apoptotic and necrotic cell death pathways. J Exp Med 188: 919-930.

Voogd, J, Glickstein, M (1998) The anatomy of the cerebellum. Trends Neurosci 21: 370-375.

Wakamori, M, Yamazaki, K, Matsunodaira, H, Teramoto, T, Tanaka, I, Niidome, T, Sawada, K, Nishizawa, Y, Sekiguchi, N, Mori, E, Mori, Y, Imoto, K (1998) Single tottering mutations responsible for the neuropathic phenotype of the P-type calcium channel. J Biol Chem 273: 34857-34867.

Wang, CW, Klionsky, DJ (2003) The molecular mechanism of autophagy. Mol Med 9: 65-76.

Wang, H, Yu, SW, Koh, DW, Lew, J, Coombs, C, Bowers, W, Federoff, HJ, Poirier, GG, Dawson, TM, Dawson, VL (2004) Apoptosis-inducing factor substitutes for caspase executioners in NMDA-triggered excitotoxic neuronal death. J Neurosci 24: 10963-10973.

Werner, AB, de Vries, E, Tait, SW, Bontjer, I, Borst, J (2002) TRAIL receptor and CD95 signal to mitochondria via FADD, caspase-8/10, Bid, and Bax but differentially regulate events downstream from truncated Bid. J Biol Chem 277: 40760-40767.

Westenbroek, RE, Sakurai, T, Elliott, EM, Hell, JW, Starr, TV, Snutch, TP, Catterall, WA (1995) Immunochemical identification and subcellular distribution of the alpha 1A subunits of brain calcium channels. J Neurosci 15: 6403-6418.

Xue, L, Fletcher, GC, Tolkovsky, AM (1999) Autophagy is activated by apoptotic signalling in sympathetic neurons: an alternative mechanism of death execution. Mol Cell Neurosci 14: 180-198.

Ye, X, Carp, RI, Schmued, LC, Scallet, AC (2001) Fluoro-Jade and silver methods: application to the neuropathology of scrapie, a transmissible spongiform encephalopathy. Brain Res Brain Res Protoc 8: 104-112.

Yuan, J, Lipinski, M, Degterev, A (2003) Diversity in the mechanisms of neuronal cell death. Neuron 40: 401-413.

Yuan, J, Yankner, BA (2000) Apoptosis in the nervous system. Nature 407: 802-809.

Zanjani, H, Herrup, K, Mariani, J (2004) Cell number in the inferior olive of nervous and leaner mutant mice. J Neurogenet 18: 327-339.

Zhang, L, Goldman, JE (1996) Generation of cerebellar interneurons from dividing progenitors in white matter. Neuron 16: 47-54.

Zhou, YD, Turner, TJ, Dunlap, K (2003) Enhanced G protein-dependent modulation of excitatory synaptic transmission in the cerebellum of the Ca2+ channel-mutant mouse, tottering. J Physiol 547: 497-507.

Zwienenberg, M, Gong, QZ, Berman, RF, Muizelaar, JP, Lyeth, BG (2001) The effect of groups II and III metabotropic glutamate receptor activation on neuronal injury in a rodent model of traumatic brain injury. Neurosurgery 48: 1119-1127.

Zwingman, TA, Neumann, PE, Noebels, JL, Herrup, K (2001) Rocker is a new variant of the voltage-dependent calcium channel gene Cacna1a. J Neurosci 21: 1169-1178.

VITA

Name: Tamy Catherine Frank-Cannon

Address: Veterinary Integrative Biosciences, Texas A&M University, 4458
               TAMU, College Station, TX 77843

Email Address: tfrank@cvm.tamu.edu

Education: B.S. Zoology, Texas A&M University, 1992
               B.S. Veterinary Science, Texas A&M University, 1993
               D.V.M. Texas A&M University, 1996

Professional experience: Companion animal clinical practice, 1996 – 2000

Publications:

1. Lau, FC, Frank, TC, Nahm, SS, Stocia, G, Abbott, LC (2004) Postnatal apoptosis in cerebellar granule cells of homozygous leaner (tg^{la}/tg^{la}) mice. Neurotox Res 9: 267-280.

2. Frank, TC, Nunley, MC, Sons, HD, Ramon, R, Abbott, LC (2003) Fluoro-Jade identification of cerebellar granule cell and Purkinje cell death in the α1A calcium channel mutant mouse, leaner. Neuroscience 118: 667-680.

3. Rhyu, IJ, Nahm, SS, Hwang, SJ, Kim, H, Suh, YS, Oda, SI, Frank, TC, Abbott, LC (2003) Altered neuronal nitric oxide synthase expression in the cerebellum of calcium channel mutant mice, α1A. Brain Res 997: 129-140.

4. Nahm SS, Frank, TC, Browning, M, Sepulvado, J, Hiney, JK, Abbott, LC (2003) Insulin – like growth factor I improves cerebellar dysfunction, but does not prevent cerebellar neurodegeneration in the calcium channel mutant mouse, leaner. J Neurobiol 14: 157-165.